ผลกระทบของกรดไขมันปาล์มต่อปฏิกิริยาไฮโดรดีซัลเฟอไรเซชัน และปฏิกิริยาไฮโดรดีออกซิจีเนชัน
ในการป้อนร่วมกับน้ำมันปิโตรเลียมแก๊สออยล์ ในหน่วยไฮโดรทรีตติ้ง

นายสัญญา บุญญาสุวัฒน์

วิทยานิพนธ์นี้เป็นส่วนหนึ่งของการศึกษาตามหลักสูตรปริญญาวิศวกรรมศาสตรดุษฎีบัณฑิต
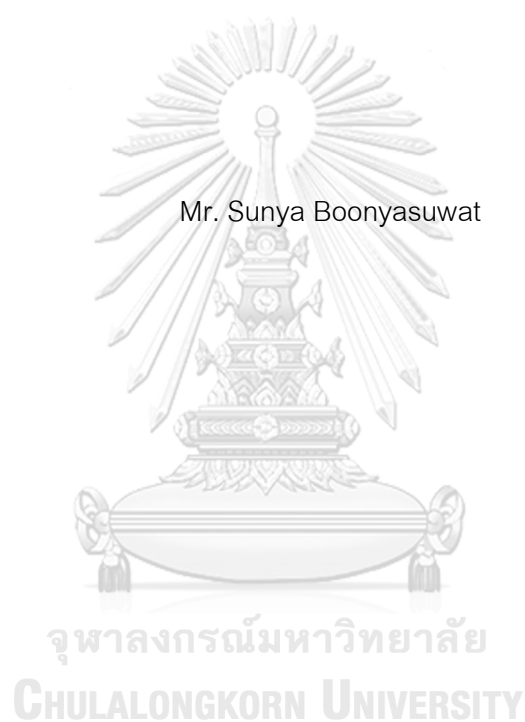สาขาวิชาวิศวกรรมเคมี ภาควิชาวิศวกรรมเคมี
คณะวิศวกรรมศาสตร์ จุฬาลงกรณ์มหาวิทยาลัย
ปีการศึกษา 2560

Effect of Palm Fatty Acid Distillate on Hydrodesulfurization and Hydrodeoxygenation in Co-processing with Petroleum Gas Oil in Hydrotreating Unit

Mr. Sunya Boonyasuwat

จุฬาลงกรณ์มหาวิทยาลัย
CHULALONGKORN UNIVERSITY

A Dissertation Submitted in Partial Fulfillment of the Requirements

for the Degree of Doctor of Engineering Program in Chemical Engineering

Department of Chemical Engineering

Faculty of Engineering

Chulalongkorn University

Academic Year 2017

Thesis Title	Effect of Palm Fatty Acid Distillate on Hydrodesulfurization and Hydrodeoxygenation in Co-processing with Petroleum Gas Oil in Hydrotreating Unit
By	Mr. Sunya Boonyasuwat
Field of Study	Chemical Engineering
Thesis Advisor	Dr.Jirdsak Tscheikuna

Accepted by the Faculty of Engineering, Chulalongkorn University in Partial Fulfillment of the Requirements for the Doctoral Degree

--- Dean of the Faculty of Engineering

(Supot Teachavorasinskun)

THESIS COMMITTEE

--- Chairman

(Associate Professor Varong Pavarajarn)

--- Thesis Advisor

(Dr.Jirdsak Tscheikuna)

--- Examiner

(Associate Professor Seeroong Prichanont)

--- Examiner

(Dr.Chalida Klaysom)

--- External Examiner

(Dr.Narisara Intrachadra)

สัญญา บุญญาสุวัฒน์ : ผลกระทบของกรดไขมันปาล์มต่อปฏิกิริยาไฮโดรดีซัลเฟอไรเซ ชัน และปฏิกิริยาไฮโดรดีออกซิจีเนชันในการป้อนร่วมกับน้ำมันปิโตรเลียมแก๊สออยล์ ใน หน่วยไฮโดรทรีตติ้ง (Effect of Palm Fatty Acid Distillate on Hydrodesulfurization and Hydrodeoxygenation in Co-processing with Petroleum Gas Oil in Hydrotreating Unit) อ.ที่ปรึกษาวิทยานิพนธ์หลัก: ดร.เจิดศักดิ์ ไชยคุนา, 107 หน้า.

ปฏิกิริยาไฮโดรดีออกซิจีเนชันของกรดไขมันปาล์มเพื่อผลิตน้ำมันดีเซลชีวภาพสังเคราะห์ ถูกศึกษาในการป้อนร่วมกับน้ำมันปิโตรเลียมแก๊สออยล์ในเครื่องปฏิกรณ์แบบวิวิธพันธุ์ลักษณะ ฟิกซ์เบดขนาดจำลองทางอุตสาหกรรม ปฏิกิริยาเกิดขึ้นบนตัวเร่งปฏิกิริยาโคบอลท์โมลิบดีนัมบน อะลูมินา การทดลองพบว่าปฏิกิริยาไฮโดรดีออกซิจิเนชันและปฏิกิริยาไฮโดรดีซัลเฟอไรเซชันเกิด อย่างสมบูรณ์แม้ว่าจะมีปริมาณกรดไขมันสูงถึงร้อยละ 25 โดยน้ำหนัก นอกจากนี้ยังได้น้ำมันที่มี คุณภาพเป็นไปตามมาตรฐานคุณภาพน้ำมันดีเซล (EN 590) กรดไขมันที่ป้อนร่วมส่งผลให้ค่าซีเท นสูงขึ้น ในขณะที่ความหนาแน่นของน้ำมันลดลง เครื่องปฏิกรณ์จำลองมีอุณหภูมิสูงขึ้นมาก เนื่องจากปฏิกิริยาโดยรวมเป็นปฏิกิริยาคายความร้อน ปริมาณไฮโดรเจนที่ใช้ได้ถูกคำนวณและ บันทึกผลเพื่อการวิเคราะห์เชิงเศรษฐศาสตร์ ต่อมาได้ทำการทดลองขนาดเล็กในสภาวะและตัวเร่ง ปฏิกิริยาเดียวกับแบบจำลองเพื่อศึกษาผลกระทบของกรดไขมันปาล์มที่มีต่อการเปลี่ยนแปลงของ ปฏิกิริยาไฮโดรดีออกซิจิเนชันและปฏิกิริยาไฮโดรดีซัลเฟอไรเซชันในระยะยาวโดยใช้กรดปาล์ม มิติกและสารจำลองน้ำมันปิโตรเลียมแก๊สออยล์ การทดลองพบว่าสารประกอบซัลเฟอร์ในรูปของ 4,6-DMDBT ทำให้ปฏิกิริยาไฮโดรดีออกซิจิเนชันเกิดได้ดี ในทางกลับกันกรดปาล์มมิติกส่งผล ให้ปฏิกิริยาไฮโดรดีซัลเฟอไรเซชันลดลงแต่สามารถผันกลับได้ นอกจากนี้การปรับปรุงปฏิกรณ์พบว่า ส่วนให้ความร้อนของสารก่อนป้อนเข้าส่วนเกิดปฏิกิริยานั้นเกิดพอลิเมอไรเซชันของพันธะคู่ซึ่งเป็น สาเหตุของการลดลงของทั้งสองปฏิกิริยาเนื่องจากอุดตันรูพรุนของตัวเร่งปฏิกิริยา เมื่อทดลองนำ สารตั้งต้นจำลองมาเติมไฮโดรเจนที่พันธะคู่โดยปฏิกิริยาไฮโดรจิเนชันพบว่าให้ผลดีต่อปฏิกิริยา และลดความดันตกคร่อมที่ส่วนให้ความร้อน และยังพบว่าการกระตุ้นให้ตัวเร่งปฏิกิริยามี ประสิทธิภาพสูงขึ้นสามารถทำได้โดยการป้อนไดเมทิลไดซัลไฟด์ (DMDS) 2 เปอร์เซนต์โดย น้ำหนักที่อุณหภูมิ 320 องศาเซลเซียส ข้อมูลที่ได้จากการทดลองนี้สามารถนำไปใช้เป็นแนวทาง สำหรับปรับปรุงหน่วยไฮโดรทรีตติ้งเพื่อนำกรดไขมันป้อนร่วมกับน้ำมันดีเซลในหน่วยไฮโดรทรีตติ้ง

ภาควิชา	วิศวกรรมเคมี	ลายมือชื่อนิสิต	_____
สาขาวิชา	วิศวกรรมเคมี	ลายมือชื่อ อ.ที่ปรึกษาหลัก	_____
ปีการศึกษา	2560		

5571437121 : MAJOR CHEMICAL ENGINEERING

KEYWORDS: HYDRODEOXYGENATION / HYDROTREATING / RENEWABLE DIESEL / PALM FATTY ACID DISTILLATE / DEOXYGENATION / DESULFURIZATION

SUNYA BOONYASUWAT: Effect of Palm Fatty Acid Distillate on Hydrodesulfurization and Hydrodeoxygenation in Co-processing with Petroleum Gas Oil in Hydrotreating Unit. ADVISOR: DR.JIRDSAK TSCHEIKUNA, 107 pp.

Deoxygenation of palm fatty acid distillate (PFAD) to produce renewable diesel had been experimented in co-processing with petroleum light gas oil (LGO) in a pilot-scale reactor. The reaction was achieved in the fixed-bed hydrotreating reactor, over commercial $CoMo/Al_2O_3$ under 280–350 $^{\circ}C$, 25 barg, H2/feed of 630 Nm^3/m^3 and 0.75 h^{-1} of LHSV. High conversion were achieved when varied PFAD up to 25 wt%. The presence of PFAD in LGO improved cetane index of the liquid products. Heat effect due to overall exothermic reactions was observed. Hydrogen consumption was then theoretically calculated and extrapolated for hydrotreating of pure PFAD. Further study by laboratory scale reactor with model component was to study the effects of PFAD on actvities over prolonging time at the similar conditions and catalyst by using palmitic acid, and model LGO. The presence of 4,6-DMDBT resulted in high deoxygenation conversions, while the palmitic acid decreased the desulfurization activity as a reversible effect. The modification of the reactor depicted the polymerization of unsaturated feed at heating section. Additional pretreatment by double-bond hydrogenation was benefited to both activities since the major cause of the deactivation was from the polymerized product that blocked the catalyst pore and lowered activity. The deactivated catalyst could be efficiently reactivated by 2 wt% of dimethyl-disulfide (DMDS) in n-C18 at 320 $^{\circ}C$. These results could be valuable as foreseeing information to an improvement of an existing hydrotreating unit for co-processing PFAD with LGO.

Department: Chemical Engineering   Student's Signature ....

Field of Study: Chemical Engineering   Advisor's Signature ....

Academic Year: 2017

ACKNOWLEDGEMENTS

CONTENTS

x

LIST OF TABLES AND FIGURES

CHAPTER ONE

INTRODUCTION

1.1   Overviews and significance

Due to the diminishing petroleum sources and increasing in concerns about world environment, there have been many contributions to the substitution of current fuel sources with renewable sources [1]. (e.g. natural oils, sugars, biomass, starches, lignin, and cellulosic, etc.) as shown in **Figure 1.1**. This concern has been widely spreading throughout many countries. For a few decades, the European Renewable Energy Council (EREC) has set the legislative framework to double the portion of biofuels up to 20% in 2020 and target to 10% biofuel in transportation sector [2, 3]. At the beginning, the first generation biofuels that has been produced is fatty acid methyl esters (FAME) so called bio-diesel via trans-esterification of natural fats and oils. The first generation has been widely commercialized especially in many South-East-Asia countries, e.g. Thailand. Although biodiesel has been widely substituted to petroleum diesel, it has been limited their applicability in various issues [4, 5]. Due to oxygen containing in alkyl esters group, An instability especially at elevated temperature, cold flow properties, and corrosiveness in engine and fuel storage tank by higher acid number compared to conventional diesel fuel were all main disadvantages [6].

A more attractive and promising technology existing in the form of hydroprocessing of vegetable oils has overcome the biodiesel disadvantages. The converted hydrocarbon products are then diesel-fuel-like molecules, oxygen-free, saturated at double bonds, resulting in better storability and possibility to higher blending fraction with diesel. The hydroprocessing of vegetable oils shares conditions, catalysts, hydrogen, and technologies similar to conventional hydrotreating unit in

complex oil refineries. This is a second generation biofuel for substituting diesel as it is so called Green Diesel [5, 6].
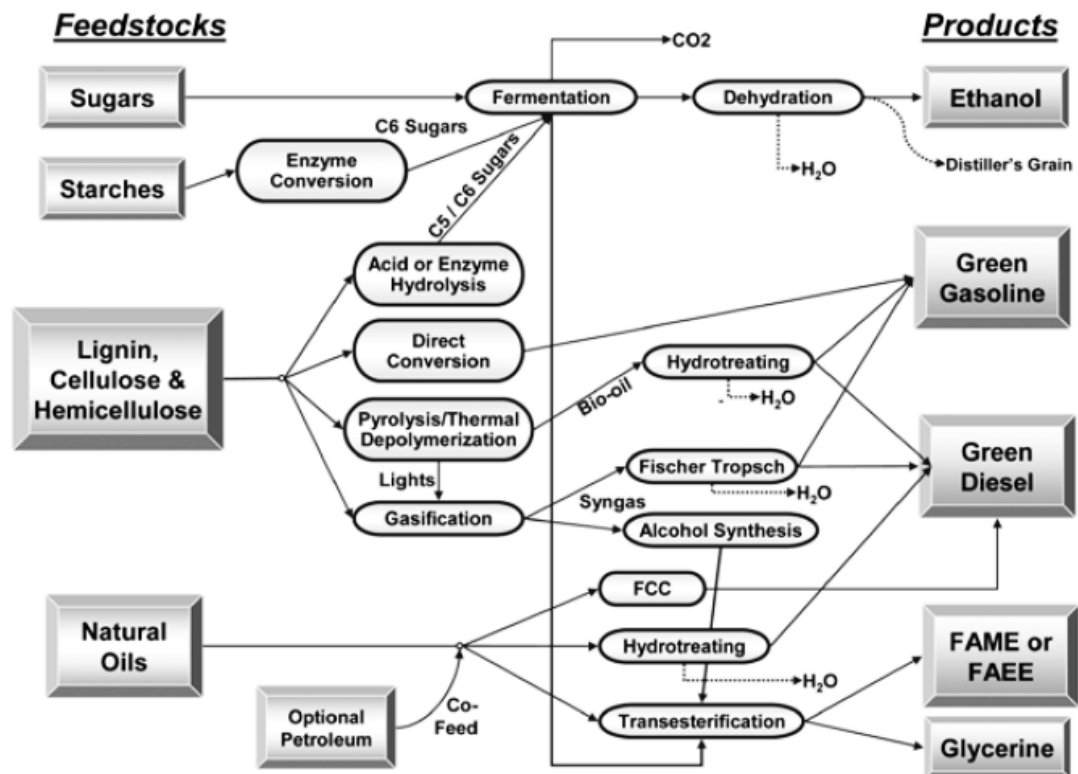
Figure 1.1   An overview of biofuel production [7].

Moreover, the hydrocarbon product from either pure or mixed hydrotreated vegetable oil is classified as a premium diesel that containing less sulfur than conventional diesel, higher energy containing than FAME, and higher cetane number up to 90 due to a mixture of ideal n-paraffinic molecules [8]. The advantages of green diesel properties compared to conventional biodiesel are shown in **Table 1.1**, and the quality of different diesel fuel are listed in **Table 1.2**. For each parameter, the properties of green diesel overcomes other types of diesel, except lower specific gravity due to the unconventional synthesis from vegetable oil as enriching normal alkane than naphthenic and aromatic hydrocarbons in petroleum diesel.

Table 1.1   Comparison of green diesel with biodiesel [9, 10].

Green Diesel	Bio-diesel
Compatible with existing engine with high blending ratio (Up to 20%)	Less compatible (Max 7%)
High Cetane number (70-90)	CN 50-65 (based on Palm Oil)
Similar energy density per volume compared to petroleum diesel	Lower energy density per volume
Excellent Storability due to • Low iodine value • Oxygen-free molecules	Poor storability especially subjecting to heat • High iodine value (45-60 mg/g) • Ester functional molecules
Reduce GHGs at tail pipe	Increase NO_x emissions
No treatment of by-product	Require treatment of by-product (Glycerol)
Better performance in cold weather	Poor performance in cold weather

Table 1.2   Comparison of diesel in fuel quality[11].

Parameter	Diesel (ULSD)	Biodiesel (FAME)	Green diesel	Fisher-Tropsch diesel
Oxygen, %	0	11	0	0
Specific gravity	0.84	0.88	0.78	0.77
Sulphur, ppm	<10	<1	<1	<1
Heating value, MJ/kg	43	38	44	44
Cloud point, ^{o}C	-5	-5 to 15	-20 to 20	Not available
Cetane	40	50-65	70-90	>75
Stability	Good	Marginal	Good	Good

1.2   Objective of the research

1. To evaluate the product quality and process parameters during co-processing of palm fatty acid distillate (PFAD) with light gas oil (LGO) in a commercial existing hydrotreating unit claimed as pilot-scale unit.

2. To study on the effect of PFAD on hydrodesulfurization and hydrodeoxygenation over different fraction of PFAD and prolonging time on stream up to 10 days in the laboratory scale reactor by using model components.

3. To investigate the cause of gradual deactivation of the catalyst, reactivation techniques, as well as pretreated feed for improving of the catalyst deactivation

1.3   Scope of work

All experiment must use the same catalyst, sulfidation technique, temperature range, pressure, and hydrogen to oil ratio. The steps of experiment with objectives are as follows.

1. Preliminary study hydrogenation of PFAD in laboratory-scale unit

    a. Evaluate the end-result product for blending with hydrotreated LGO as fuel purpose

2. Co-processing PFAD at 5, 8, 12 and 25 wt% with non-hydrotreated LGO <u>in pilot-scale unit</u>

    a. Evaluate product and feed composition before and after hydroprocessing

    b. Investigate cause of heat effect from PFAD

    c. Evaluate performance of the catalyst for both desulfurization and deoxygenation

    d.   Analysis of product quality in fuel using purpose as cetane index

    e.   Calculate hydrogen consumption based on PFAD

3. Co-processing palmitic acid in a mixture of 4,6-DMDBT in n-C18 at 5, 10, and 20 wt% <u>in laboratory-scale unit</u>

    a.   Evaluate the amount of palmitic acid on desulfurization of 4,6-DMDBT.

    b.   Evaluate the presence of 4,6-DMDBT on deoxygenation of palmitic acid.

    c.   Perform and suggest reactivation of deactivated catalyst

    d.   Study the cause of the deactivation by using model feed containing low impurities.

    e.   Study the pretreatment by hydrogenation to eliminate double bond to improve catalyst activity and deactivation
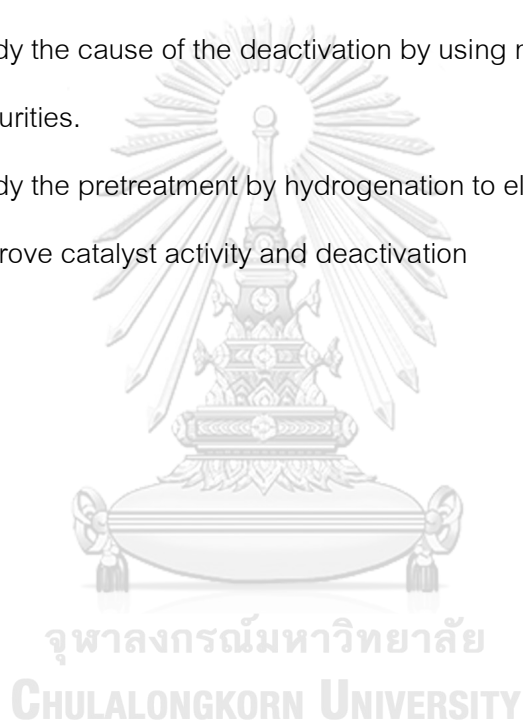
CHAPTER TWO

THEORY

2.1   Hydrotreating unit

Hydrotreating or hydroprocessing refers to a variety of catalytic hydrogenation process which saturates unsaturated hydrocarbons and remove unwanted element other than hydrocarbons, e.g. sulfur, nitrogen, oxygen, and transition metals from different petroleum streams in an oil refinery [12].

Currently, hydrotreating is used extensively in almost all complex refineries for both cracking heavy feedstocks and improving the quality of final products. At the first generation, the hydrotreating reaction has been introduced to eliminate much of sulfur from various fuel fractions to avoid poisoning noble metal in many catalytic units. For example, a hydrotreater of naphtha is aim to decrease sulfur in various form so as not to poison platinum in reformer unit. Consequently, hydrotreating catalysts are commonly referred to as hydrodesulfurization (HDS) catalysts. Various application of hydrotreating in a modern refinery is linked to the desired distribution of different refinery products and specification requirement [13]. The schematic of the application of hydrotreatment is shown in **Figure 2.1,** and the scheme of a typical hydrotreating for gas oil is shown in **Figure 2.2**.
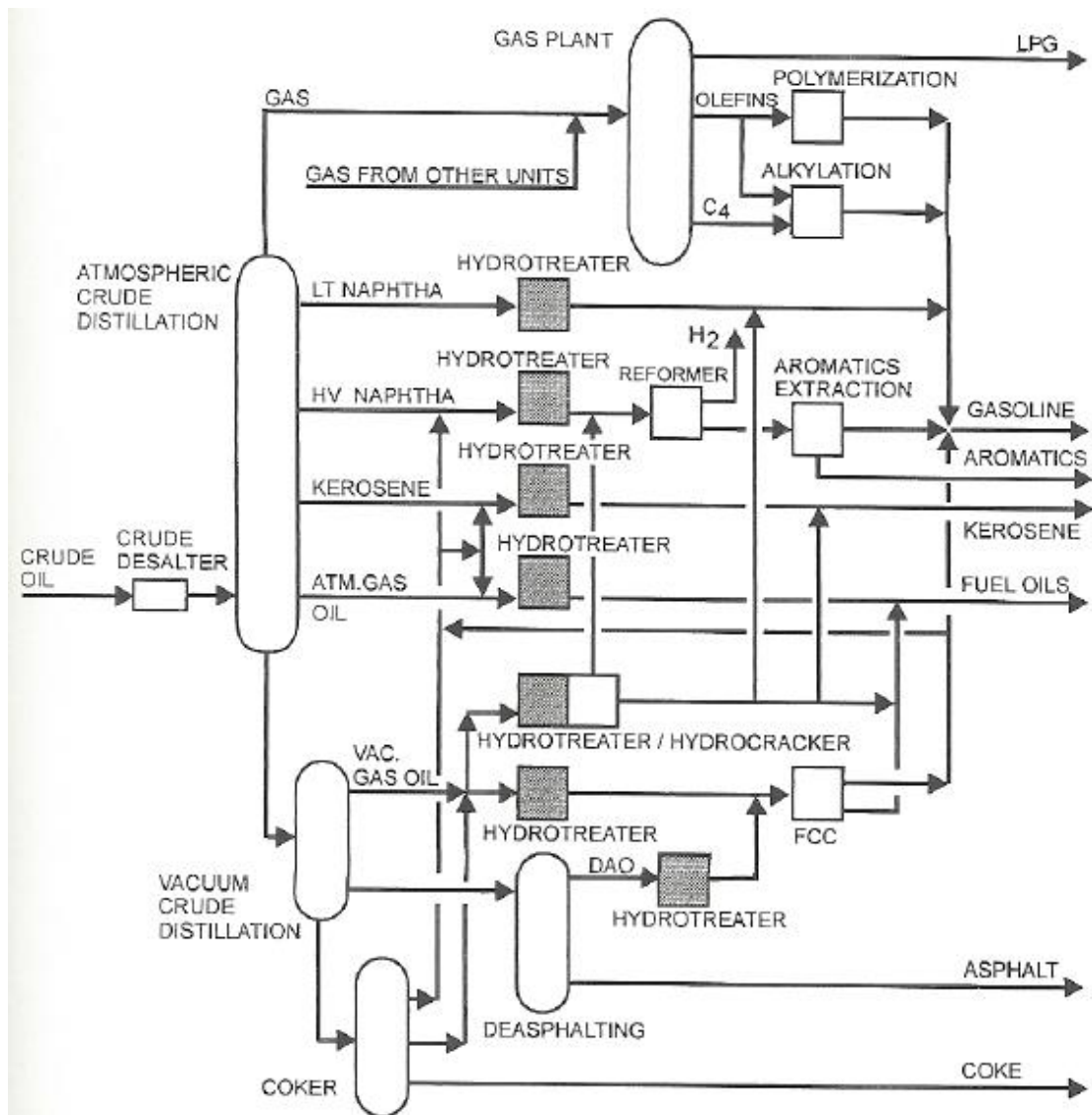
Figure 2.1   Schematics of a hypothetical refinery illustrating the applications of the

hydrotreatment [13].
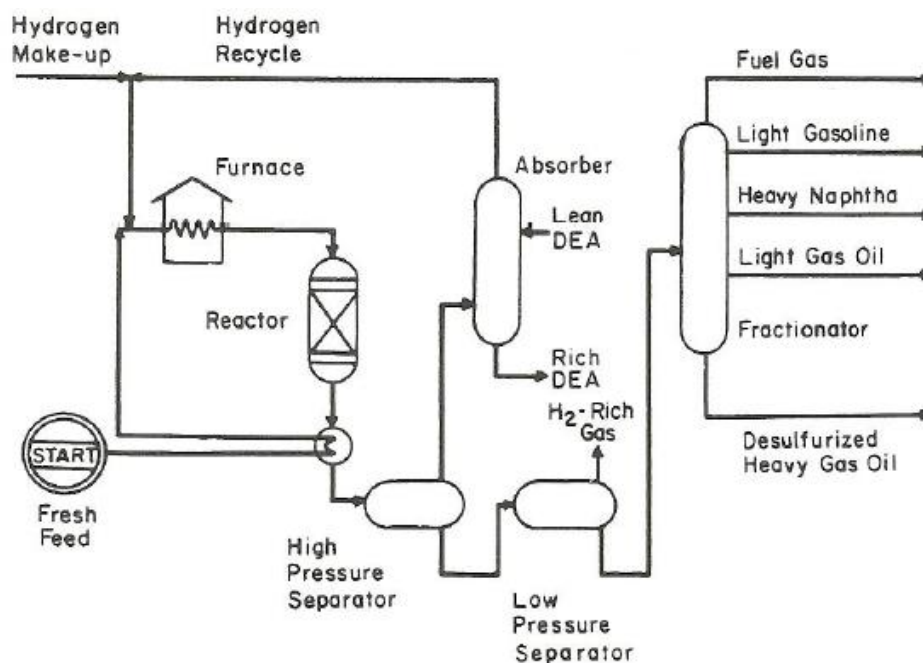
Figure 2.2   Scheme of a typical heavy gas-oil desulfurizer unit [13].

2.2   Chemistry of the hydrodesulfurization

Sulfur in petroleum is naturally occurred from decaying of organic matters for centuries. Sulfur-containing compounds are invariably ranging from hydrogen sulfide, thiophene, dibenzothiophene, and various heteroatom types. The amount of sulfur in petroleum is greatly impact on cost of refining finished petroleum products and fuels. Depending on type of compound, many desulfurization reaction routes have been proposed as both direct and indirect step of the cleavage of C-S bond. For example, as shown in **Figure 2.3**, partial hydrogenation of thiophene was proposed to be involved prior to the rupture of C-S bond, while the other route (a) is not required any ring hydrogenation. Some claimed that a variation of hydrogen partial pressure is the main key for the selective pathway [13]. Also, different substituent group adjacent to the S atom can affect the order in desulfurization rates. Methyl group at distant from S atoms increase HDS activity due to the higher electro density at S atoms, compared to those

adjacent to S which also create steric effect. The summary of the effect of substituent group on HDS activity is shown in **Table 2.1**.
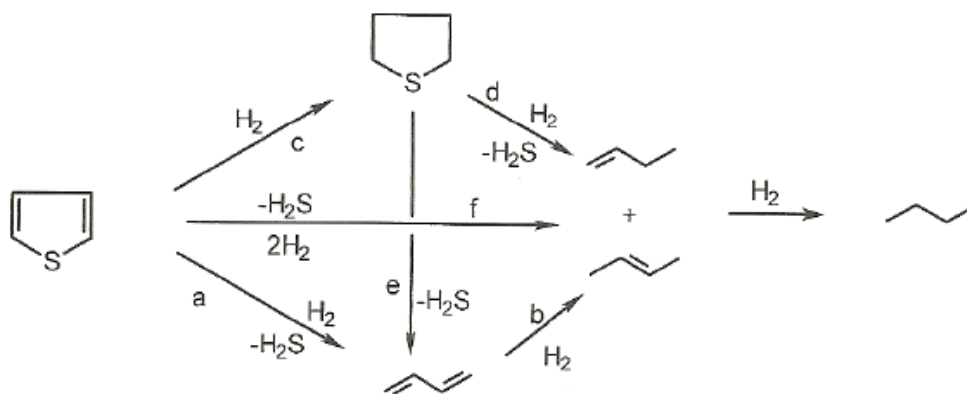
Figure 2.3   Proposed reaction pathway for thiophene HDS [13].

Table 2.1 Effects of substituent group on HDS activity [14].

Compound[a]	Relative activity[b]
TP	2,5-diMe < 2-Me < none
TP	2-Me < none < 3-Me
BTP	3-Me < 2-Me = none
	3,7-diMe < 3-Me = 2-Me = 7-Me < none
DBTP	4,6-diMe < 4-Me < none < 3,7-diMe < 2,8-diMe
	4,6-diMe < 4-Me < none < 2,8-diMe
	4,6-diMe < 4-Me < 3,7-diMe < 2,8-diMe < none
	4,6-diMe < 4-Me < none

[a] Compounds:

TP   BTP   DBTP

[b] Me = methyl; none = no substituents

Thus, it is important when considering the real feeds as it has been found that the overall activities of hydrodesulfurization depending not only on the amount of initial sulfur-containing compounds, but also on the type and amount of each organo-sulfur as well as the catalyst design on specific conditions. For instance, sweet petroleum

product might contain mainly difficult removing sulfur compounds, while sour one might has only light and easy-removal sulfur-containing compounds.

Dibenzothiophene (DBT) and 4,6-di-methyl dibenzothiophene (4,6-DMDBT) are selected as a representative compound for sulfur-containing hydrocarbon that intrinsically high refractory for desulfurization. The difficulty of sulfur-removing activity was considered so as to probe the efficiency of the hydrodesulfurization activity. In addition, current hydrotreating catalyst has been technologically-advanced designed to be able to ultra-deep desulfurization as low as 5 ppmw [14, 15]. The route to desulfurize DBT and 4,6-DMDBT are shown in **Figure 2.4** and **Figure 2.5**.
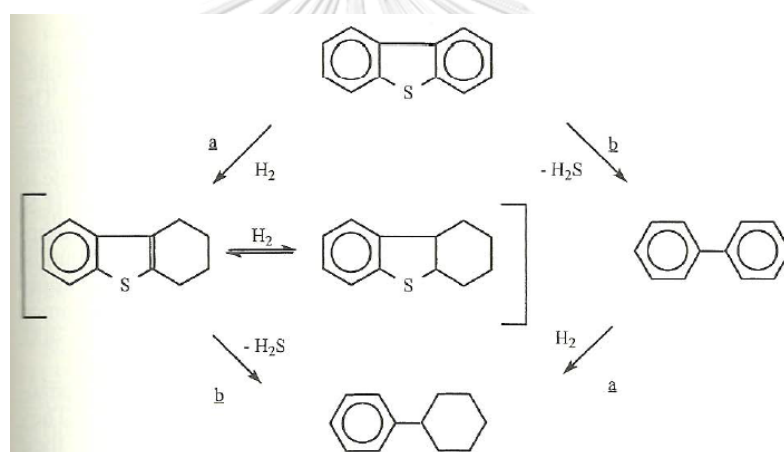
Figure 2.4   Proposed reaction network for the HDS reaction of DBT. (a) hydrogenation step, (b) C-S bond breaking step [13].
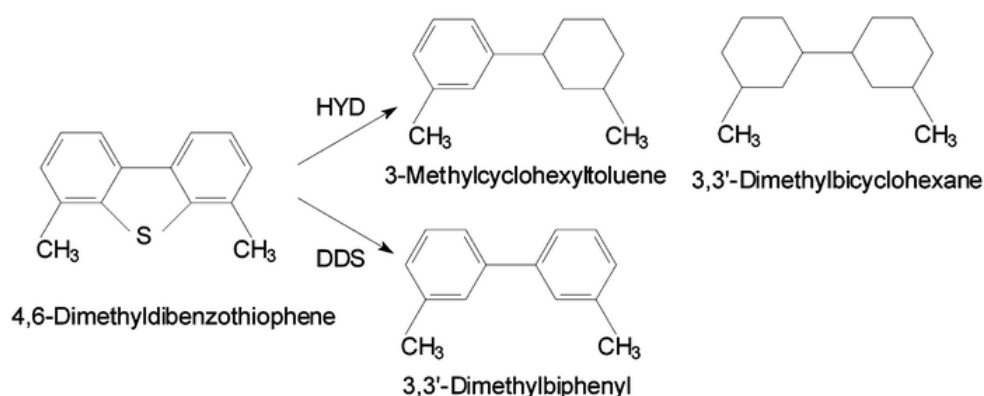
Figure 2.5   Proposed reaction network for the HDS reaction of 4,6-DMDBT.

DDS – Direct desulfurization, HYD – hydrogenation [16].

Typical conditions for hydrotreating reaction are given in **Table 2.2**. The variation in temperature, pressure and LHSV are accommodated variations in the reactivity of the feed and the desirable degree of desulfurization. In the case of gas oil, where the temperature is shown as in average, operating temperature is generally ranging from start-of-run (SOR) at 280 $^{\circ}$C to end-of-run (EOR) at 410 $^{\circ}$C. Gradual catalyst deactivation usually undergoes necessitating continuous elevation of the reactor temperature to maintain satisfied conversion so as to meet the specification of sulfur compound in diesel. Hydrogen partial pressure is also targeted on to the conversion, while hydrogen consumption is depending on the amount of unsaturated hydrocarbons and aromatics content. The reactor is generally downward flow scheme and fixed-bed reactor. The catalyst can be arranged in several beds with or without either feed or hydrogen gas quenching in order to reduce temperature rise caused by exothermic reaction mainly from hydrogenation of unsaturated HCs and aromatics.

Table 2.2   Typical process conditions and hydrogen consumption for various

hydrotreating reactions [13].

Hydrotreating process	Temperature (°C)	Hydrogen partial pressure (atm)	LHSV	Hydrogen consumption (Nm^3 m^{-3})
Naphtha	320	10– 20	3–8	2– 10
Kerosine	330	20– 30	2–5	5– 15
Atm. GO	340	25– 40	1.5–4	20– 40
VGO	360	50– 90	1–2	50– 80
ARDS[a]	370–410	80–130	0.2–0.5	100–175
VGO HCR	380–410	90–140	1–2	150–300
Residue HCR	400–440	100–150	0.2–0.5	150–300

[a] ARDS: atm residue desulfrization.

2.3   Chemistry of hydrodeoxygenation of vegetable oil

In the same fashion, so as to remove oxygen atoms in triglyceride molecules, hydrotreating of triglyceride shares a similar pathway on oxygen removal [17]. The triglycerides are suitably converted into hydrocarbons at the temperatures between 300 and 450 °C and hydrogen pressures above 3 MPa. The products are majority on n-paraffin and leaving CO, CO_2 and water as by-products. The catalytic hydrotreatment of triglycerides occurs through consecutive reactions. By analytical examination on products, the main reactions are the saturation of double bonds of triglycerides, the propane cleavage to generate carboxylic acids and esters, and the following oxygen-removal reactions, hydrodeoxygenation, decarboxylation, and decarbonylation [18]. Other reactions can be possible to undergo at more severe condition or on different catalyst, e.g. aromatization, hydrocracking, and isomerization. Different number of carbon of n-paraffinic hydrocarbons are final product that undergoing the complex and consecutive reaction steps. The number of carbon atoms is determined by the feedstock and process conditions [9]. These can be described by the diagram shown in Figure 2.6.

Figure 2.6   Possible reaction pathways of triglyceride over hydrotreating catalyst [19].

2.3.1   Hydrogenation of unsaturated bond of triglyceride

Since hydrogenation of carbon-carbon double bond of triglyceride requires such small activation energy (13-47 kJ/mol) [20], this functional group is susceptible to be hydrogenated to saturated bond via active reduced metal by single atom of hydrogen available on the active site and under hydrogen pressure. Hydrogenation of olefinic double bonds occurred rapidly and independent on the different catalysts tested, e.g. CoMo, NiMo, and NiW over alumina support. As a result, the first step under hydrotreating conditions results in saturated triglyceride molecules [18].

At this step, the amount of hydrogen consumed can be calculated by determining the amount double position by iodine value following ASTM D1959-9. As an option, triglyceride can be converted to fatty acid methyl esters (FAME), and it is analyzed the composition by gas chromatography. In addition, the latter one is also suitable for determining the genre of fatty acids comprised of triglyceride [21, 22].

2.3.2   Thermal decomposition of triglyceride

Decomposition of triglyceride can be readily occurred with or without hydrogen at high temperature. The decomposition could forms a large number of radical compounds containing acids, aldehydes, ketones, aliphatic and aromatic hydrocarbon groups. Lighter fraction of hydrocarbon is also produced mostly naphthenic group, while heavy fraction contains straight chain paraffinic hydrocarbons, and other polymerized substance. At elevated temperature above 300 $^{\circ}$C, alkyl radical from thermolysis was also found to be an initiator of cyclic formation [23]. Guzman et al found that at 15 barg under hydrogen pressure during hydroprocessing of crude palm oil, the product from triglyceride decomposition to free fatty acid could be defined as intermediate which will then be involved in the following reaction pathways, hydrodeoxygenation, decarboxylation, decarbonylation, and hydrocracking [24].

2.3.3   Hydrodeoxygenation

The use and modification of vegetable oil as a part of renewable-based resources are interested for decades. It has been involved in various applications, especially on renewable fuel processing and hydrocarbon synthesis to neat chemicals. Being composed primarily of triglycerides, esters of glycerol and fatty acids, they consist of hydrocarbon chain with C=C double bonds and carboxylic/esters functions that could be converted to hydrocarbons products over designated catalysts.

Hydrodeoxygenation of stearic acid

$$C_{17}H_{35}COOH \ + \ 3H_2 \ \rightarrow \ C_{18}H_{38} \ + \ 2H_2O$$
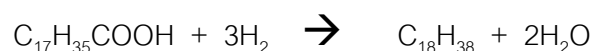
Hydrodeoxygenation is the desired pathway for oxygen removal in vegetable oil and derivatives by forming water molecules as by-product. The product from this pathway is a long-chain hydrocarbon containing the same number of carbon as corresponding to fatty acid derivatives. Compared to other oxygen removal reactions,

hydrodeoxygenation consumes the highest amount of hydrogen per mole of fatty acid chain so as to remove two of oxygen atoms of carboxylic group as one water molecules [18]. The selectivity on hydrodeoxygenation step is controlled by the nature of catalysts, reaction temperature, reaction pressure, and etc. Hydrodeoxygenation is preferred under comparatively low temperatures and high pressures [25]. NiMo based catalysts were much more favorable for hydrodeoxygenation than CoMo based one. Also, hydrogenation catalyst with high availability of hydrogen radical on the surface leads to selective hydrodeoxygenation and the other deoxygenations.

2.3.4   Decarbonylation

The alkanes produced by decarbonylation contain odd numbers of carbons together with carbon monoxide as a light gaseous compound and water. Less hydrogen is required compared to hydrodeoxygenation step, but one carbon atom is removes as CO. Huber et al. indicated that the rate of decarbonylation increases with increasing temperature determining from the yield of the relative ratio of n-C17 to n-C18 [26].

2.3.5   Decarboxylation

Decarboxylation is only an oxygen removal step that does not consume hydrogen to produce the straight chain alkane. Two oxygen atoms from carboxylic group are converted to carbon dioxide, resulting in odd number of hydrocarbon products. In parallel, the rate of decarboxylation increases with temperature but decreases with hydrogen partial pressure. The ratio of odd to even number of carbon atoms can only be served as an indication for evaluating decarbonylation and decarboxylation over hydrodeoxygenation reaction. It is impossible to precisely discriminate decarbonylation from decarboxylation with the light gaseous product (CO/CO_2), since there are undesirable reactions under hydrotreating conditions, water gas shift and reversed water gas shift [19].

2.3.6 Hydroisomerization and Hydrocracking

Both reactions involve destructive hydrogenation, and they can be characterized by the conversion of the higher molecular weight components to lighter and isomer products. From catalytic viewpoint, acid support is required to carry out hydrocracking, i.e., amorphous alumino-silicate, silica-alumino phosphate (SAPO), zeolites. The rearranging of carbenium ion on acidic support can from different isomer, so called isomerization. This step is generally occurred in common hydrotreating unit of oil refineries especially hydrocracking, and dewaxing unit so as to lower cloud point and cold flow plugging point of petroleum distillate and gasoil [9]. The reactions are favorable at lower LHSV (longer contact time to catalyst) and higher temperature (above $400 \, ^{\circ}C$) [18].

2.3.7 Side reactions

Other than liquid hydrocarbons, the light gaseous compounds such as carbon monoxide, carbon dioxide, methane, and water are generated by the main reactions and side reactions simultaneously [19]. The following reactions are inevitably occurred under reaction condition and the presence of hydrogen which is co-processed excessively.

Methanation of CO_2 : $\quad CO_2 + 4H_2 \quad \Leftrightarrow CH_4 + 2H_2O$

Methanation of CO : $\quad CO + 3H_2 \quad \Leftrightarrow CH_4 + H_2O$

Water Gas Shift : $\quad CO_2 + H_2 \quad \Leftrightarrow CO + H_2O$

Reverse Water Gas Shift: $\quad CO + H_2O \quad \Leftrightarrow CO_2 + H_2$
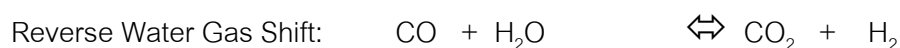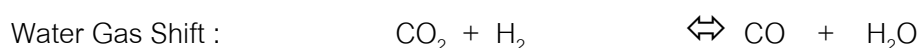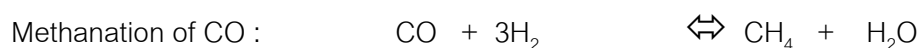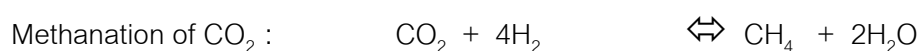
It should be noted that without both methanation reactions and water gas shift, the hydrogen consumption can be calculated by hydrodeoxygenation, decarbonylation, and decarboxylation. The consumption of hydrogen decreases in the order of

hydrodeoxygenation > decarbonylation > decarboxylation [24]. Also, the ratio of CO over CO_2 could be an indication of decarbonylation over decarboxylation. However, two methanation reactions and water gas shift reaction are in equilibrium under certain hydrogen partial pressure and temperature. These undesired reactions also play an important role on hydrogen consumption in triglyceride hydrotreatment and result in complication for determination of deoxygenation pathway [27].

2.4   Palm oil and current uses

The major products from palm oil are to various business sectors in the order of usage amount, cooking oil, bio-diesel, animal feedstocks, and as a raw material for detergents. In the food industry, palm oil is not only used as cooking oil but also manufacture of magarine, non-dairy creamers, and shortening [28]. Palm oil shares about 30-35 % of vegetable oil in the World's market, and 33% of palm oil is used as cooking oil among other vegetable oil in Thailand. Almost one-third of palm oil production in Thailand has been converted to bio-diesel which is currently mandatory at 7% of biodiesel in petroleum diesel to be used as automotive diesel selling in nationwide gas stations [29, 30].

Current palm oil uses in Thailand is to produce bio-diesel following the standard by department of energy business, Ministry of Energy, Thailand. According to the specification of bio-diesel and large availability of palm oil, the processing of biodiesel is mostly from crude palm oil. A number of palm oil refinery plants had been invested for the last decade to support many biodiesel refineries and the new-coming biodiesel refiners. However, there are a few refineries that use such waste product or by-products from palm oil refinery. It has long been known that one of the promising by-products was palm fatty acid distillate (PFAD). The diagram depicting the origin of PFAD from the refining process of crude palm oil was shown in **Figure 2.7**.
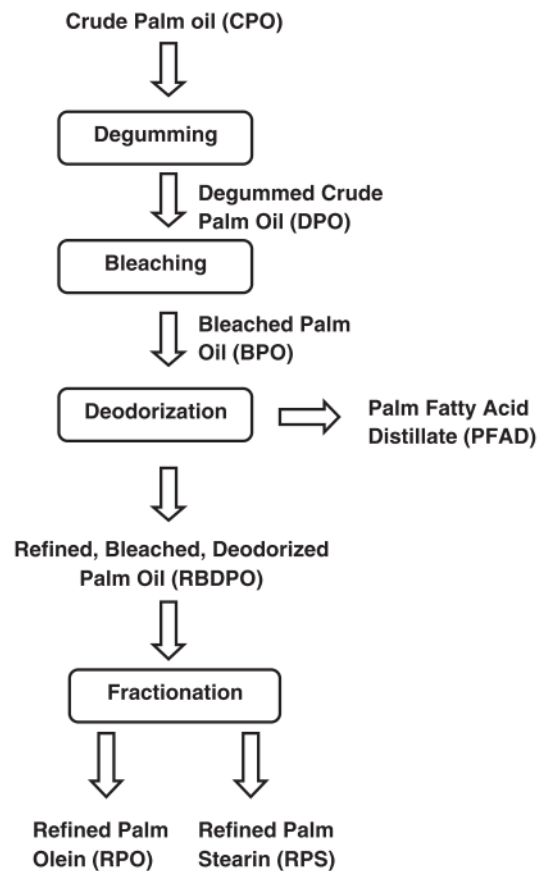
Figure 2.7   Physical refining process of crude palm oil [31].

2.5   Palm fatty acid distillate (PFAD)

According to **Figure 2.7**, palm fatty acid distillate (PFAD) is a by-product from commercial palm oil process at during stripping of palm oil which is already refined and bleached to reduce amount of free fatty acid by using super-saturated steam to reduce partial pressure at ultimate vacuum (< 10 mbar). Free fatty acid composition of PFAD follows that of palm oil as shown in **Table 2.3**. General specification of commercial PFAD was also followed palm oil. High fatty acid content in PFAD was about 75 wt%, and all of impurities was low compared to crude palm oil and used cooking oil.

Table 2.3   Typical composition of fatty acids present in some vegetable oils and
animal fats [32].

Vegetable oils	Compositions of fatty acids (% w/w)										
	12:0	14:0	16:0	18:0	18:1	18:2	18:3	20:0	22:0	22:1	24:0
Cotton		0.6-1.5	22-26	2.1-5	14-21	47-58					
Peanut		0-0.5	6.0-14.0	1.9-6	36-67	13-43		1.32	2.52	1.0	1.23
Babassu	44-45	15-17	5.8-9.0	2.5-6	12-16	1.4-3					
Canola			1.2-6.0	1-2.5	52-67	16-31	6-14			1-2	
Coconut	44-51	13-21	7.5-10	1-3.5	5-8.2	1-2.6	0-0.2				
Rapeseed		0-1.5	1.0-6.0	0.5-3.5	8-60	9-23	1-13			5-56	
Sesame			7.2-9.2	5.8-7.7	35-46	35-48					
Sunflower			3.5-7.6	1.3-6.5	14-43	44-74					
Linseed			6.0	3.2-4	13-37	5-23	26-60				
Corn		0-0.3	7.0-16.5	1-3.3	20-43	39-62	1-13	0.24			
Olive		0-1.3	7.0-20	0.5-5	55-85	4-21					
Palm		0.6-2.4	32-46.3	4-6.3	36-53	6-12					
Poppy			12.6	4.0	22.3	60.2					
Jatropha Curcas		0-0.1	14-15.3	3.7-9.8	34-46	29-44	0.3				
Soybean			2.3-13.3	2.4-6	18-31	49-57	2-10			0.3	
Jatropha		0.5-1.4	12-17	5.0-9.5	37-63	19-41				0.3	
Fats											
Lard	0.1	1.4	23.6	14.2	44.2	10.7	0.4				
Tallow	0.1	3.0-6.0	25-37	14-29	26-50	1-2.5	0.9				

PFAD was introduced into this study due to the price and availability. It has been claimed that PFAD is a potentially valuable, low cost material for bio-diesel production. Moreover, the major market of PFAD is generally sold as industrial fatty acid in non-food sector for soap industries, fuel for power plant, and industrial boiler fuel. Thus, it can be claimed as a non-food source. Consequently, the competition between biofuel feedstock over food resource strongly supports PFAD for biofuel resource [33].

Moreover, since most of the natural fats and oils are amenable to deoxygenate, and to avoid food supply detriment and land shifting to fuel crop, Santillan-Jimenez et al. proposed the use of non-edible, waste, and ultra-high yield feedstock such as tallow oil,

yellow grease, and brown grease. They gained an additional advantage of these feed in the hydrogen consumption issue [27]. According to the chemistry of deoxygenation of fats and oils derivatives in (2.2), the reaction of free fatty acids (FFA) to hydrocarbon products was apparently shorter than that of triglyceride. Moreover, FFA has been considered as reactive intermediate during the triglyceride transformation [34]. To avoid this cleavage step, free fatty acid molecule will be directly saturated and deoxygenated to hydrocarbon products. PFAD was then proposed as one of the promising feedstock that can be used as an alternative biofuel feedstock. The advantages of PFAD are listed as following.

- Availability in South East Asian Countries as much as palm oil
- Cheaper than crude palm oil, cooking palm oil, and palm stearin (as by-product)
- Non-edible feedstock
- Waste/by-product from palm oil refining process
- Less impurities (phosphorus, phospholipid, gums, salt, and sodium) since it was already refined and bleached
- Commercial PFAD contains minimum 75 wt% of free fatty acids, 25 wt% of palm oil as mono-, di-, and tri-glyceride. (In this study, PFAD contained 84.5 wt% of of free fatty acids)
- Consume lower hydrogen due to lower amount of glyceride (mono-, di-,tri-glyceride) that consume hydrogen during thermal decomposition to free fatty acids.
- Cost saving on propane separation or hydrogen purging rate

2.6   Properties of automotive diesel and renewable diesel

The production of renewable diesel has now been interested nationwide during the last decade. Neste oil in Europe and UOP Honeywell in the US were only two technology licensor for the plant. However, the standard of such drop-in fuel was not implemented internationally. Thus, in order to accomplish with quality standards to be used along with current fossil fuels, the specification of renewable diesel in only the most important properties was controlled as listed in **Table 2.4**.

Table 2.4   Accordance of renewable diesel to diesel fuel specification.

Property	Value range	ASTM	EN
Flash Point, $^{\circ}$C	38 min	D93	2719
Kinematic Viscosity, mm^2/s	1.9 min, 4.1 max	D445	3104
Ash, wt%	0.01 max	D482	6245
Cetane number	40 min.	D613	5165
Cloud Point, $^{\circ}$C	Climate spec.	D2500	ISO 3015

Note: Some properties of green diesel specified in test methods (Adapted from test methods ASTM D-975-11b, ASTM D-7566-11a).

It should be noted that density of renewable diesel was such lower than that of conventional diesel since deoxygenation of fats and oils mainly produces normal alkane and paraffinic hydrocarbon rather than cyclic aromatics and polycyclic aromatic hydrocarbons which are intrinsically heavier.

CHAPTER THREE

LITERATURE REVIEW

3.1   Green diesel processing and current technologies

According to the National Renewable Energy Laboratory (NREL), Green diesel is defined as a renewable diesel produced from hydroprocessing of triglyceride-containing oils. This type of renewable diesel is free of oxygen resulting in higher compatibility to petroleum diesel. The processing of green diesel could be derived from either standalone processing or co-processing with petroleum gas oil in hydrotreating unit in petroleum refineries.

The world's leading producers of green diesel are Neste Oil (NeXBTL®) and UOP (Eni Ecofining™, Honeywell Green Diesel™). Currently, Nestle oil has already been processing 2 metric tonnes per year in three plants, located in Finland, Holland, and Singapore since 2008. Whereas UOP Honeywell, profession in refining technology experience, has been providing services mainly on consulting, engineering and design, and training on Eni Ecofining™ process develop by the company to handle hydrotreatment of vegetable oil [35]. Both companies have been developed their technology mainly processing and designing the catalysts. Proprietary of the catalyst and process technology was not disclosed to public. A drop-in diesel fuel from the current processes was claimed as high quality and capable for blending with existing diesel in any percentages [11]. List of renewable producers are shown in **Table 3.1**.

Table 3.1   List of renewable diesel producer using hydroprocessing technology

[36].

Producer	Company size	Annual Production (gal)	Plant Locations	Remarks
Neste	Large	380 Million	Porvoo, Finland Rotterdam, The Netherlands Singapore	Finnish Petroleum Refiner, NeXBTL®
Eni S.p.A.	Medium	120-150 Million in 2016	Italy	UOP process Eni EcofiningTM
REG	Medium	75 Million	Geismer, LA	
Diamond Green	Medium	160 Million – expanding to 275 million	Norco, LA	UOP Process
Alt Air Paramount	Medium	45 Million (Jet and diesel)	Los Angeles, CA	UOP Process

The overall hydrotreatment diagram of triglyceride was shown in **Figure 3.1**. This is an ideal achievement to produce green diesel. The diagram also includes a separation of the products from undesired reaction, and unexpected reaction due to the conditions and catalysts.
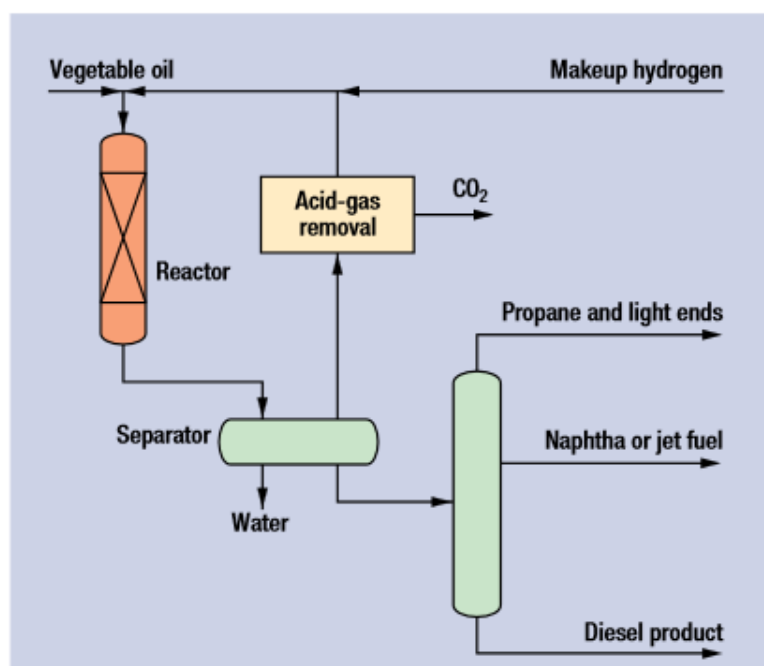
Figure 3.1   The new green diesel process converts vegetable oil into fuels [10].

Although green diesel are able to be processed by standalone hydrotreating unit with specific catalyst and process design, oil refiners are also interesting to co-process the renewable feedstocks to their existing hydrotreating unit. The purpose of co-processing is to minimize the cost, and the process investment. In this study, an introduction of renewable feedstocks will be studied in the existing hydrotreating unit together with laboratory-scale testing with both real and model compounds.

3.2   Catalysts and catalyst selection

The choice of catalyst requires a detailed study of specific situation, type of sulfur-containing compound, aromatic content, pressure drop, lifetime, and etc. Most of the commercial catalysts for hydrotreating of petroleum gas oil are mainly CoMo, NiMo, and NiW over stable catalyst supports. In general, the key of hydrotreating catalysts mainly dealt with molybdenum or tungsten as active metal impregnated on alumina support together with cobalt or nickel as a promoter. Many studies suggested that sulfur atoms replace oxygen molecules in the structures of active metal to form MoS_2 or WS_2,

which are then proven that those state are the active surface for removal of sulfur components. The addition of promoter was also proven to improve other supportive reactions to desulfurization on active metal (e.g. Co-Mo-S), e.g. hydrogenation of aromatic rings, and C-C hydrogenolysis. **Figure 3.2** shows the schematic view of the different phases of CoMo catalysts on the catalyst support. Other transition metals, rare earth metals, and basic elements are also researched for mainly catalyst development and some specific purposes, e.g. denitrogenation, decarbonylation, and hydrogen spill over on catalyst surface [13]. Nobel metals on alumina and modified support were also studied with various feed and conditions. However, due to the expensiveness of the catalyst and limited availability, the use of noble metal catalyst in commercial scale was not yet considered [37].
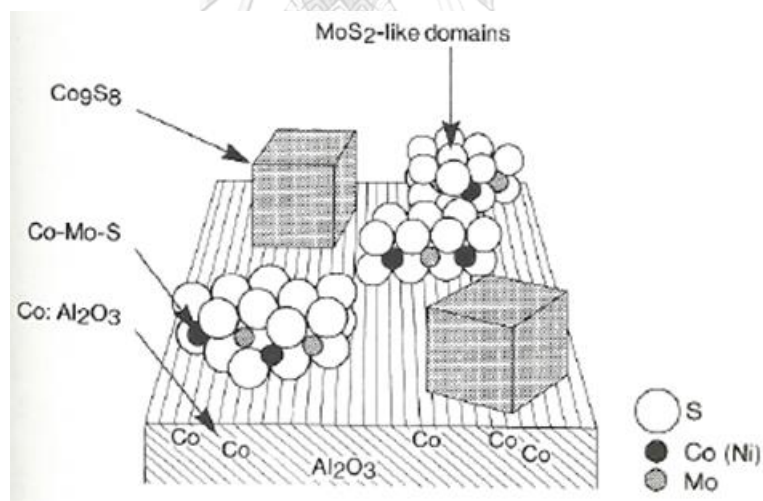
Figure 3.2   Schematic view of the different phased present in a typical alumina-
              supported CoMo catalyst.

CoMo catalysts are excellent for hydrodesulfurization and give relatively low hydrogen consumption when compared to NiMo catalyst. The purposes of using NiMo are often preferred for treating unsaturated feeds, hydrodenitrogenation (HDN), and

heteroatom removal. The NiW catalyst provides the highest activity for aromatic hydrogenation, and slight hydrocracking at low hydrogen partial pressure, but their use is limited due to the higher cost [25].

As mentioned before, different hydrotreating catalyst promoters provide disparate product selectivity and characteristics. Over the same catalyst support type, alumina, renewable diesel from CoMo catalyst shift the product distillation curve toward lower boiling point, while NiMo catalyst provide narrow range of boiling point as shown in **Figure 3.3**. Hydrocracking of C-C bond was claimed as resulting from the cobalt for the catalyst promoter. However, the conversion of triglyceride was lower in the case of CoMo (**Figure 3.4**. The product selectivity to naphtha and kerosene was also in correlated with the simulated product boiling range [19].
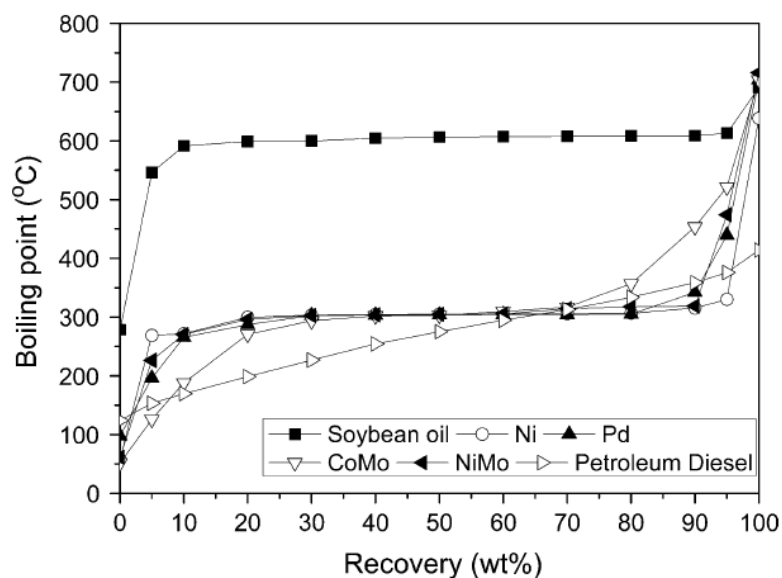
Figure 3.3   Simulated distillation curves of hydrotreated products of various

catalysts. The catalyst/oil weight ratio was 0.088 in batch type. Feed:

Soybean oil, 400 $^{\circ}$C. 9.2 MPa.
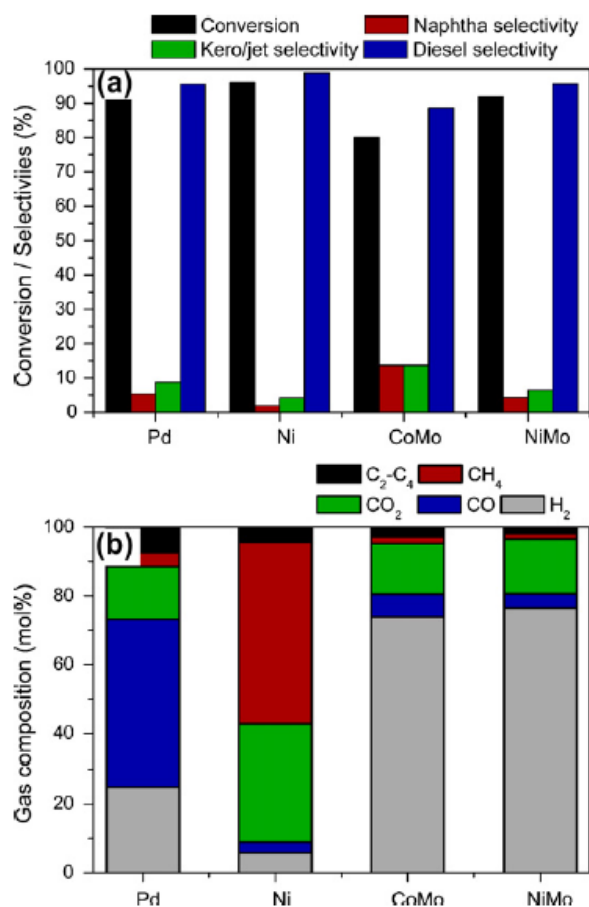
Figure 3.4　　(a) Effects of catalysts on conversion and selectivity and (b) Effects of
catalysts on the dry gas composition. The catalyst/oil weight ratio was
0.088 in batch type. Feed: Soybean oil, 400 ^{o}C. 9.2 MPa.

Since the catalyst selection plays an important role on the whole vegetable oil
hydrotreating process. The world leader in catalysis and surface science companies put
much effort to design this type of catalyst. For example, Haldor Topsoe has been
initiated the process to produce aviation fuel from triglyceride. The specialty catalyst for
biofuel hydroconverison had an aim to allow complete conversion of oxygenates and
control exothermic reaction with long cycle length together with BRIM^{TM} technology. The
catalyst series was TK-335, 337, 339, 341, and 351, but the composition and surface
characteristics was not yet disclosed due to proprietary of the invention [38].

Gamma-alumina is the most of the mesoporous material used as the support for hydrotreating catalyst. The acidity of the gamma-alumina support attributes c-c scission resulting in more cracking to lower components. Tiwari et al. found that the diesel range product yield was significantly lower in the case of NiW/Si-Al (high acidity) than NiMo/Al$_2$O$_3$ (moderate acidity) with soybean oil – gas oil mixture, while kerosene range product yield was in the opposite [39]. Consequently, in order to produce renewable diesel with improved cold properties, one should modifies the acidity of the catalyst support. The ratio and structure of silica-alumina has also been selected to vary support acidity depending on the application/product needs [18]. The porosity of the catalyst support is another important factor on the hydrotreating catalyst activity. The large and bulky triglyceride molecule requires larger pore size catalyst such as alumina to overcome diffusion limitation. Tiwari et al. suggested that the mesoporous of alumina in the study was three times larger than the largest triglyceride dimension. Their results was not only providing better diffusion of reactants and products, but also reducing catalyst deactivated by pore blockage, coking, and waxy product intermediates [39].

In this study, the commercial CoMo/Al$_2$O$_3$ (KF-757-1.3E) will be used. The existing CoMo catalyst has already been processing ultra-low sulfur diesel for two year. The catalyst has preliminary tested to be able to handle hydrotreatment of vegetable oil and fatty acid mixture.

3.3   Hydrodeoxygenation conditions

Even though the hydroprocessing technology has been widely studied and commercialized for almost 60 years, the optimal conditions and cost effectiveness on the production of green diesel by varying process conditions has been still an interesting issue. It plays an important role on hydrogen consumption, uncertain catalyst stability, product distribution and product quality. Various studies have been focusing on

both standalone triglyceride hydrotreatment as well as co-processing with petroleum gas-oil. **Table 3.2** summarizes examples of feedstock used in the process, catalyst type used, temperature, pressure, and other process conditions. In this study, the co-processing of triglyceride and/or fatty acids with gas oil will be focused.

Table 3.2   Example of feedstocks, reactor types, catalysts, and reaction conditions

Feedstocks	Reactor type	Temp. (°C)	Pressure (MPa)	Catalysts	Space time velocity	Refs.
Palm oil + Gas oil 0, 2.5, 5, 10 wt%	Trickle-bed	310-350	3.35	Commercial $CoMo/Al_2O_3$(sulphided)	0.7-1.4 h^{-1}	[1]
Sunflower oil + Vacuum gas oil (HDT/non-HDT) 30/70 and 10/90	Trickle-bed	350	13.5	Commercial hydroteating catalyst	1.5	[40]
Sunflower oil + Vacuum gas oil (HDT/non-HDT) 30/70 and 10/90	Single fixed-bed reactor	350	0-15	- Commercial mild hydrocracking catalyst - Commercial severe hydrocracking catalyst	1.5	[41]
Waste soybean oil + gas oil (10,25,40,100%)	Fixed bed	340-380	5.0	NiW/Al_2O_3, $NiMo/Al_2O_3$ (Sulphided)	2, 4 h^{-1}	[39]
Crude palm oil + Straight-run gas oil	Fixed bed	350	1.5-9.0	$NiMo/Al_2O_3$ (Haldor Topsoe 217) (Sulphided)	2.0 h^{-1}	[24]
Sunflower oil + Gas oil	Trickle bed	340-360	6.0-8.0	Sulfided Metal / Al_2O_3	1-3 h^{-1}	[42]
Rapeseed Oil	Fixed bed	250-350	0.7-7.0	Sulfided CoMo/OMA	1.5	[43]

Table 3.2 Example of feedstocks, reactor types, catalysts, and reaction conditions

(continued)

Feedstocks	Reactor type	Temp. (^{o}C)	Pressure (MPa)	Catalysts	Space time velocity	Refs.
5,10 wt% Palm oil in gas oil (5000 ppmS)	Trickle bed	330-365	3.3	Commercial CoMo/ Al$_2$O$_3$	0.85-1.4	[5]
Methyl heptanoate add H$_2$S and H$_2$O	Continuous flow reactor	250	1.5	Sulfided NiMo/ Al$_2$O$_3$, CoMo/ Al$_2$O$_3$	3 h Run	[44]
Sunflower oil + Straight Run gas oil (20:80, 40:60)	Fixed bed	330	6.0	NiO(3%)-MoO3(12%)/ Al$_2$O$_3$ + (0,15,30 wt%) zeolite BETA	2.0	[45]
Rapeseed Oil + Gas oil	Continuous flow reactor	320-380	6-8	NiMo/ Al$_2$O$_3$	1.0	[46]
Sunflower oil + Gas oil	Tubular reactor	300-380	4-8	NiMo/ Al$_2$O$_3$ /P	0.75-3.0	[47]
Rapeseed Oil	Fixed bed	350	3.5	Sulfided CoMo/ Al$_2$O$_3$	2	[48]
Waste Cooking Oil	Fixed bed	350	5.0	NiMo/Al$_2$O$_3$, NiW/ Al$_2$O$_3$, CoMo/ Al$_2$O$_3$	2.8	[49]
Soybean Oil	Batch reactor	400	9.2	Sulfided NiMo, CoMo/ Al$_2$O$_3$, Ni/SiO$_2$, Pd/ Al$_2$O$_3$, Ru/ Al$_2$O$_3$	28.1 g cat	[21]
Rapeseed Oil	Fixed bed tubular reactor	350	3.5	Sulfided CoMo/ Al$_2$O$_3$	2	[48]

3.3.1 Reaction Temperature

A key parameter for catalyst effectiveness, catalyst lifetime, and product distribution is reaction temperature. According to **Table 3.2**, average temperature for co-processing of vegetable oil and petroleum intermediate was about 340-350 $^{\circ}$C. Higher temperature up to 350 $^{\circ}$C was an optimal temperature with maximum yield of hydrocracking of vacuum gas oil and vegetable oil approximately 70/30 v/v [26].

The reaction temperature has a potential impact on product selectivity and physical properties of products. Boiling range of hydrocarbon products from hydrotreating of sunflower oil with vacuum gas oil resulted in shifting to lower range at higher temperature [50]. It was evidence that the conversion on oxygen removal increased with increasing temperature, but the selectivity of light fraction, naphtha and kerosene, doubled with increasing temperature from 350 to 390 $^{\circ}$C as shown in **Figure 3.5**. Hydrocracking of deoxygenated products was then claimed as responsible on further step at higher temperature. In related to product selectivity, the product density was decreased with increasing reactor temperature [41]. The other indication was the measurement of triglyceride concentration and oxygen concentration in the product stream at different temperature as shown in **Figure 3.6**. The result depicted significance increasing in the rate of oxygen disappearance with increasing temperature. The results were also empirically predicted to pseudo-first order kinetics [51].
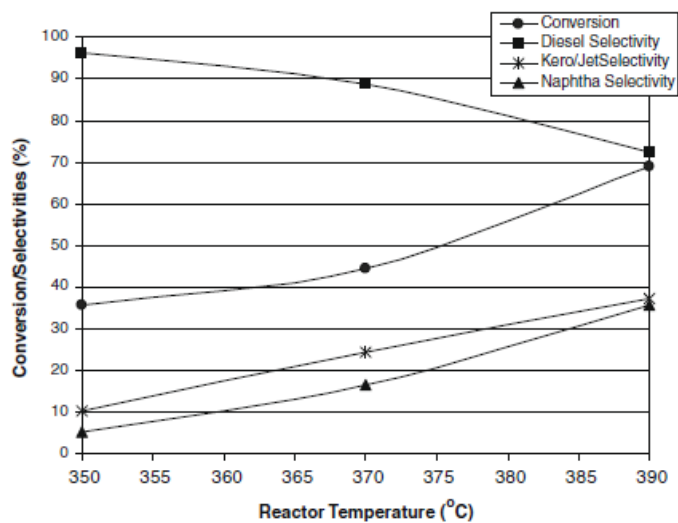
Figure 3.5   Effect of reactor temperature on conversion, and product selectivity[41].
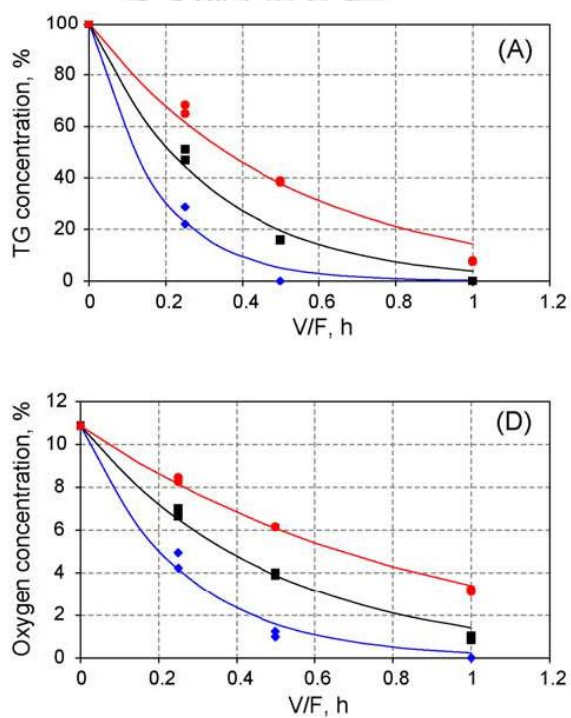
Figure 3.6   The change in concentration of triglycerides (A) and oxygen (D) as a

function of contact time for NiMo/Al$_2$O$_3$ catalysts at three temperatures

(◆ 280 $^{\circ}$C, ■ 270 $^{\circ}$C, ● 260 $^{\circ}$C). Solid points = experimental data,

solid lines = concentrations based on the pseudo-first-order kinetics

approximation of experimental data [51].

Hydrodeoxygenation, decarbonylation, and decarboxylation pathway were also susceptible to reaction temperature. The indicator for assessing decarbonylation and decarboxylation over hydrodeoxygenation was the ratio of n-alkane with odd number of carbon atoms to even number of carbon atoms. Generally, the ratio could be calculated from the amount of n-C$_{17}$/n-C$_{18}$, n-C$_{15}$/n-C$_{16}$, and n-C$_{(15+17)}$/n-C$_{(16+18)}$. The selectivity of decarbonylation and decarboxylation was increased with increasing temperature as shown in **Figure 3.7** during co-processing of 6.5 vol% of rapeseed oil with atmospheric gas oil at 30-55 barg under NiMo/Al$_2$O$_3$, LHSV 1 h^{-1}. Hydrodeoxygenation with large consumption of hydrogen was obviously found to be favorable at relatively high temperature. Substantial carbon monoxide and propylene were largely produced at temperature above 340 $^{\circ}$C [52].
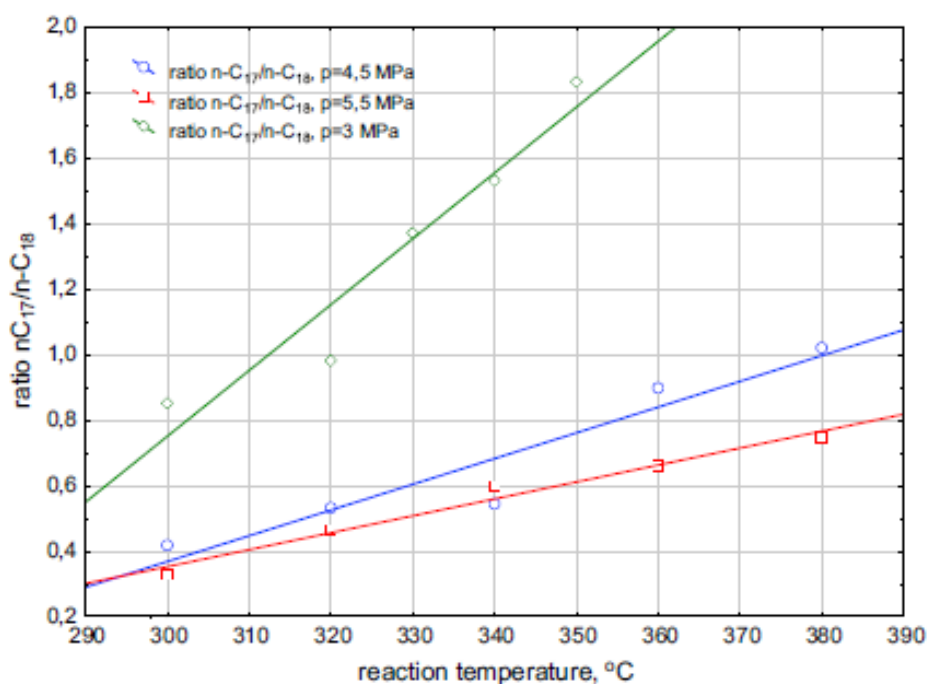
Figure 3.7   Hydroconversion of rapeseed oil. Temperature dependence of n-C17/n-C18 ratio [52].

3.2.2 Reaction Pressure

In general, the lowest pressure in hydroprocessing of diesel as well as triglycerides was about 15 barg. Below this point, there might not have enough hydrogen dissolved in liquid stagnant and diffused to the catalyst surface. Since active sites require hydrogen molecules to be dissociated to hydrogen atoms before reacting with reactant, free fatty acid, alcohol, glyceride, etc. Thus, it is necessary to have enough partial pressure of hydrogen in the reactor [53, 54].

Reaction pressure has an effect on product distribution, catalyst lifetime and stability, rate of reaction, and reaction pathway selectivity. A study from Sankaranatayanan et al. showed that slightly lower conversion was observed at low pressure run when sunflower oil was blended and converted over sulfided $NiMo/Al_2O_3$ as shown in **Figure 3.8 (A**. Lower partial pressure of hydrogen might result in more side reactions. The formation of naphthenic and aromatics at low partial pressure was 4 times higher than that at higher pressure condition. Hydrodeoxgenation was proven to be more favorable at higher pressure than decarbonylation and decarboxylation as shown in **Figure 3.8 (B)** as the ratio of n-C18/n-C17 increased with increasing pressure [45]. Not only hydrogen pressure, but also hydrogen to feed ratio can result in the same manner. Higher hydrogen to feed ratio increased hydrogen consumption and supported hydrodeoxygenation route rather than decarboxylation and decarbonylation as shown in **Figure 3.9** [24].
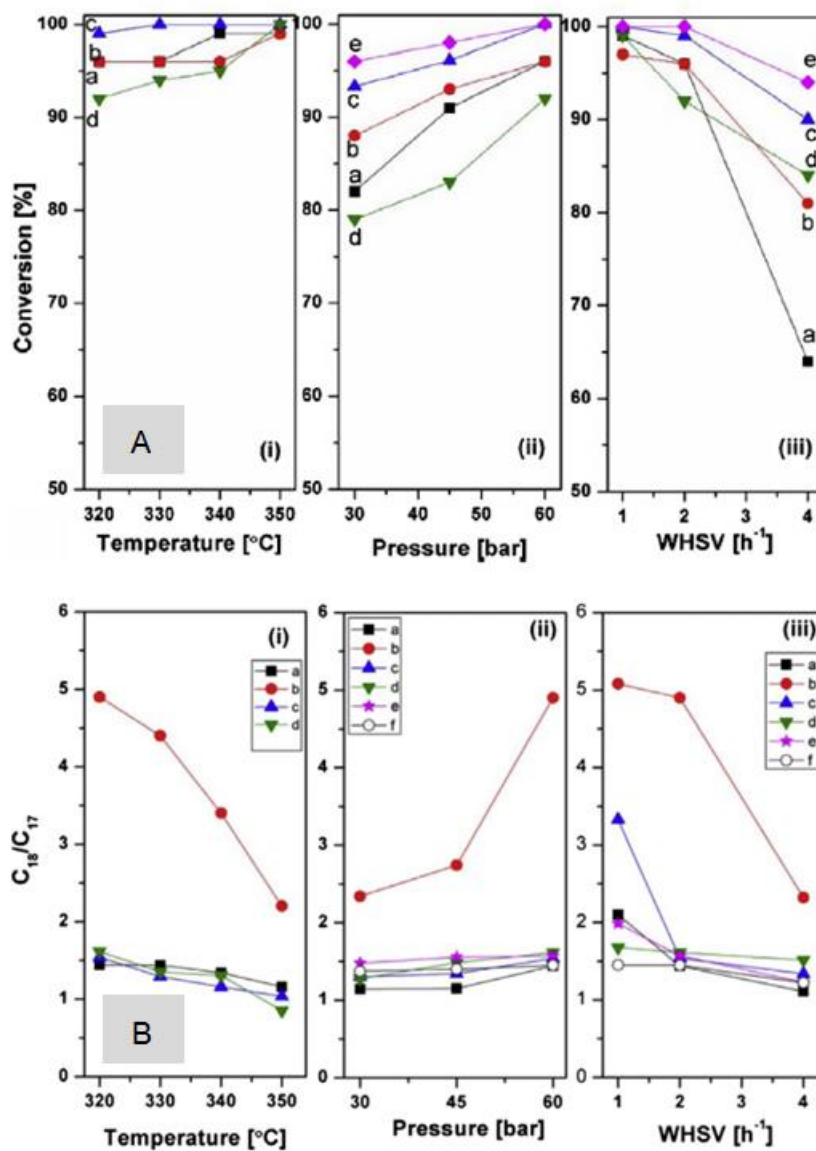
Figure 3.8   The influence of process parameters on conversion of oil/fatty acid (A), and n-C18/n-C17 ratios (B) in various oil/fatty acid-diesel blends.

Conditions: (i) 60 bars, WHSV (h^{-1}), (ii) 320 $^{\circ}$C, WHSV (h^{-1}), (iii) 60 barg, 320 $^{\circ}$C, H_2/feed (v/v), 500 STP for all runs; data based on single experiment] (a) 20% oil–diesel blend; Ni–Mo–Al, (b) 20% oil–diesel blend, Ni–Mo–15BEA, (c) 20% oil–diesel blend, Ni–Mo–30BEA, (d) 40% oil–diesel blend, Ni–Mo–30BEA, (e) 20% oil (+10% oleic acid)–diesel blend, Ni–Mo–30BEA [45].
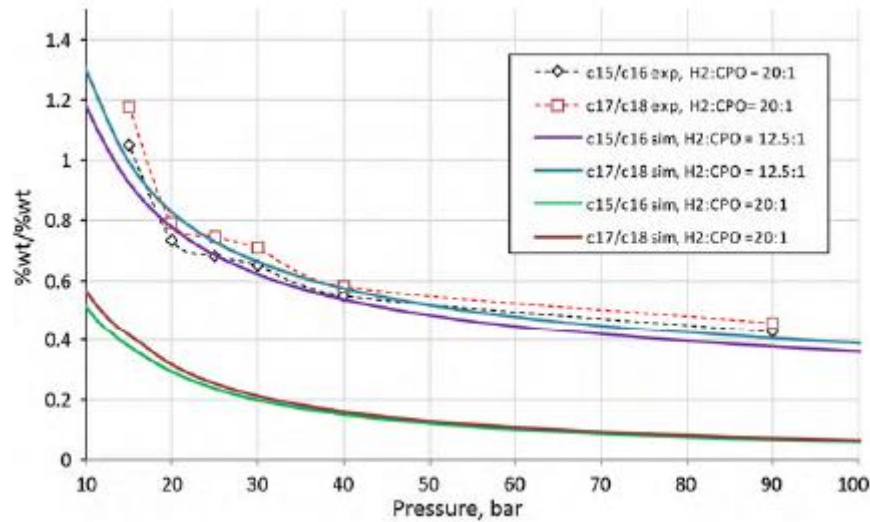
Figure 3.9   Equilibrium and experimental C_{15}/C_{16}, C_{17}/C_{18} profiles at 350 $^\circ$C as a

function of reactor pressure [24].

3.2.3   Space Velocity

It is necessary to reach conversion of at least 80-90% to convert triglyceride to

hydrocarbons. From many studies, liquid hourly space velocity (LHSV) of 1.0 or lower is

more favorable. However, to increase LHSV at any experiment, one could determine the

rate and conversion over catalyst bed and loading. Hancsok et al. varied the effect of

LHSV on the conversion of rapeseed oil under different hydrotreating catalyst as shown

in **Figure 3.10**. According to the results, the yield of paraffin increased with lower LHSV

due to longer contact time of feed to the catalysts. Also, at higher LHSV, the yield and

conversion was decreased as a result of insufficient contact time [18].
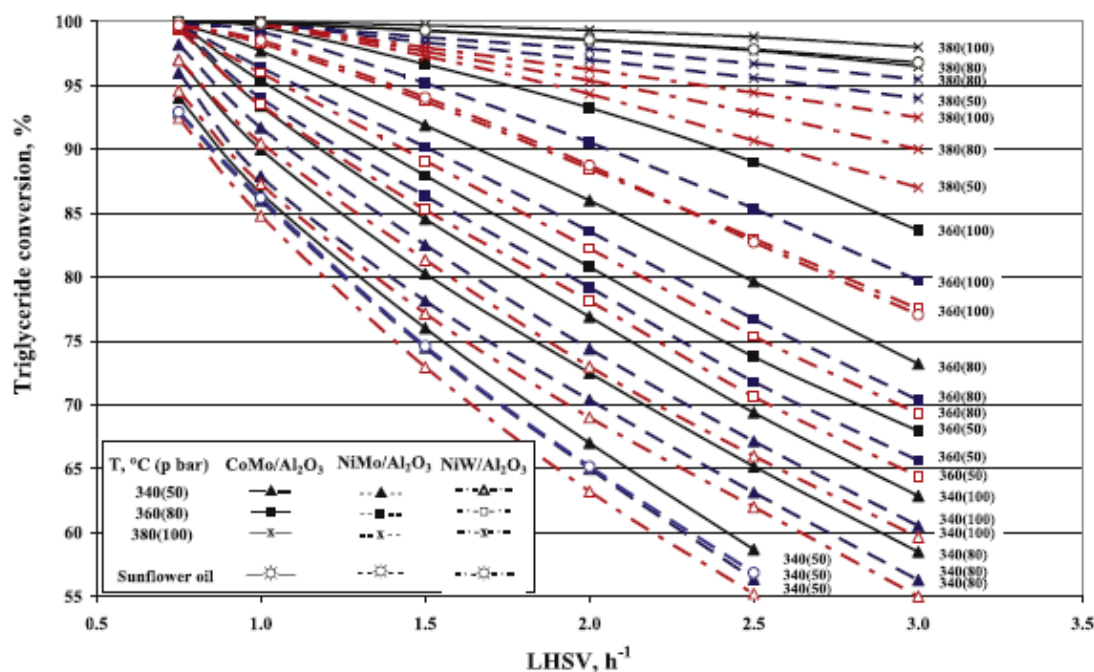
Figure 3.10   Conversion of the triglycerides as a function of LHSV at different
temperatures and pressures (feedstock: rapeseed oil; H_2/HC: 450
Nm^3/m^3) [18].

According to **Table 3.2**, many studied focused on the use of sulfide NiMo,
CoMo, and NiW on γ-Al_2O_3 by both commercial and laboratory-scale synthesis. These
results showed positive on deoxygenation reactions. The product qualities were
reported and providing very high quality renewable diesel, e.g. higher cetane number,
and lower sulfur containing. Consequently, in this study, commercial hydrotreating
CoMo/γ-Al_2O_3 (KF-757 1.3E) will be tested with feed mixture of PFAD and petroleum gas
oil. Currently, this catalyst is able to desulfurize petroleum gas oil containing 450 ppmw
of sulfur to below to 50 ppmw in the product stream.

3.4   Usage of non-edible fats and oils as feedstock

The usage of non-edible feedstock had lately interested as the food crop
competitiveness and the world's starving problems in the last decades. Waste vegetable

oil, or so called used cooking oil had been extensively studied in both standalone and co-processing with gas oil.

3.5   The effect of vegetable oil during HDS of gas oil

Instead of standalone hydrotreating unit on pure vegetable oil, the co-processing of vegetable oil with crude-oil based refinery fraction in the existing hydrotreating unit and utilities can reduce the investment need, and improve catalyst stability. This co-hydroprocessing was explored as another potential technology for biofuels production [40].

It has been claimed that sulfur in feed can maintain the catalyst activity during hydrotreatment of triglyceride. Over conventional hydrotreating catalyst, the active phase during deoxygenation was proven to be the sulfided state on the sulfided catalyst surface. Senol et al. suggested that the presence of high molecular weight from oxygen-containing molecules and the replacement of sulphided active surface with oxygen were causes of the catalyst deactivation [44]. Donnis et al. also suggested the solution to overcome this problem by co-processing vegetable oils with sulfur containing feed in conventional hydrotreating facilities since there were no conventional hydrotreating catalyst that can handle pure vegetable oil [55]. His research group has been found that gradual leaching of sulfur from active surface by oxygen containing molecules caused gradual deactivation in hydrodeoxygenation and hydrodesulfurization activities [42].

The fraction of vegetable oil derivatives in petroleum gas oil will be studied in the present work. The mixing ratio should be in consideration to meet diesel fuel specification. This will be described later in the objective work. In previous study, Templis et al. has been studied the co-processing of palm oil with gas oil up to 10 wt% under CoMo/Al$_2$O$_3$ catalyst. They observed that hydrodesulfurization rate was decreased with the addition of vegetable oil up to 5 wt%, but there was no affect when the

vegetable oil was mixed at further than 5 wt% [1, 5]. It has also been suggested that hydrodesulfurization catalyst could handle deoxygenation reaction of vegetable oil whist deactivation still remained but only at an acceptable level. A long-term performance of catalyst was appeared to reach steady-state after 300 hours in operation when co-processing 10 wt% cotton seed oil with desulfurized petroleum diesel at 320 $^\circ$C, 30 barg, together with partial pressure of H_2S = 1 vol% [56]. The addition of sulfur containing compound was proven to improve conventional hydrotreating catalyst activity. Bezergianni et al. also found that the addition of dimethyl-disulfide (DMDS) to the feedstocks containing hydrotreated-gas oil – vegetable oil improve percentage oxygen removal higher than non-hydrotreated-gas oil – vegetable oil. The decomposition of DMDS was found to be positive on increasing deoxygenation rate [40].

3.6   The effect of impurities

Co-processing mixture of renewable feed with petroleum intermediates had been recently widely studied. In the standalone unit, without addition of sulfur component, the deactivation of catalyst was a main problem because the deoxygenation of oxygen-containing molecules can cause leaching of sulfur from the catalyst surface [39]. Kubicka et al. suggested that different type of renewable feedstock impacted the different rate of gradual deterioration of catalyst activity as shown in **Figure 3.11**.
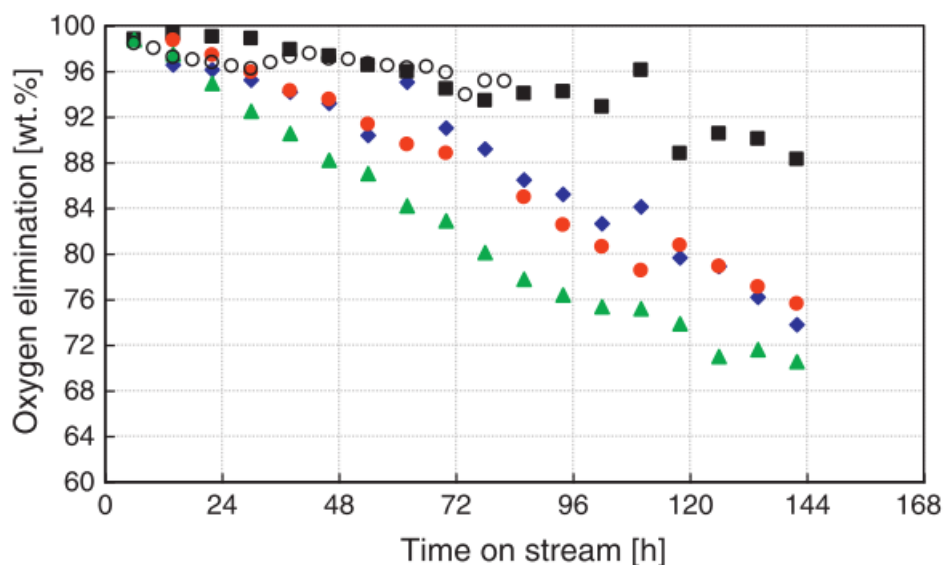
Figure 3.11 Deoxygenation of rapeseed oil obtained from different stage of its processing as a function of time-on-stream:

● RRO – refined rapeseed oil (food grade), (■) PRO – primary refined rapeseed oil (after degumming, without bleaching and des- odoration), (◆) NRO – neat rapeseed oil (oil before degumming), (▲)WRO – waste rapeseed oil, (○) oleic acid [39].

Further study the effect proved that the cause of the deactivation was due to natural impurities of feed. Alkali, phosphate, and imbalance between cation and anion were all claimed to affect deactivation [48]. Palm oil products were also studied over sulfide NiMo/ Al_2O_3 catalyst. The presence of phospholipid gum in palm oil deteriorated conversion as it acted catalysts for oligomerization and polymerization to form high molecular weight oligomers deposited on the surface of the catalyst [31, 57].

CHAPTER FOUR
MATERIAL AND METHODS

4.1 Reactor and reactor setup

The experiment has been conducted in three reaction systems, e.g. pilot-scale unit, laboratory-scale unit, and modified laboratory-scale unit.

4.1.1 Pilot-scale unit

The hydrodesulfurization unit at Verasuwan Co.,Ltd, depicted in **Figure 4.1**, has a design capacity of 100,000 liter of light gas oil feed / h considering as a pilot-scale unit when compared with complex oil refineries. The unit had been operated for 8 months since the fresh catalyst was reloaded with a commercial hydrotreating unit. Sulfur removal efficiency of the catalyst as hydrodesulfurization had been achieved to ultra-low sulfur diesel containing sulfur less than 50 ppm by mass. Prior to the experiment, the process was operated at steady-state operating conditions for at least 36 h. Then, the feed tank was switched from sulfur-containing LGO to the renewable mixture at 2.7 m^3/h (0.75 h^{-1} of LHSV). The feed stream was preheated with reactor effluent in order to recover heat prior to mix with hydrogen-rich gas stream. The mixture of gas and liquid feed was then heated up to desired reaction temperature by direct-fired heater, and charged to the reactor from top to bottom. After the reaction, the effluent was then exchanged with feed liquid and separated the gas phase so as to scrubbing off hydrogensulfide and re-entering the reactor by a gas compressor. Liquid phase was separated at the bottom of the horizontal separator, decanted, and flowed to the stripping unit. At this stream, the liquid was sampled to analyze the qualification of the reaction, in this case, desulfurization.
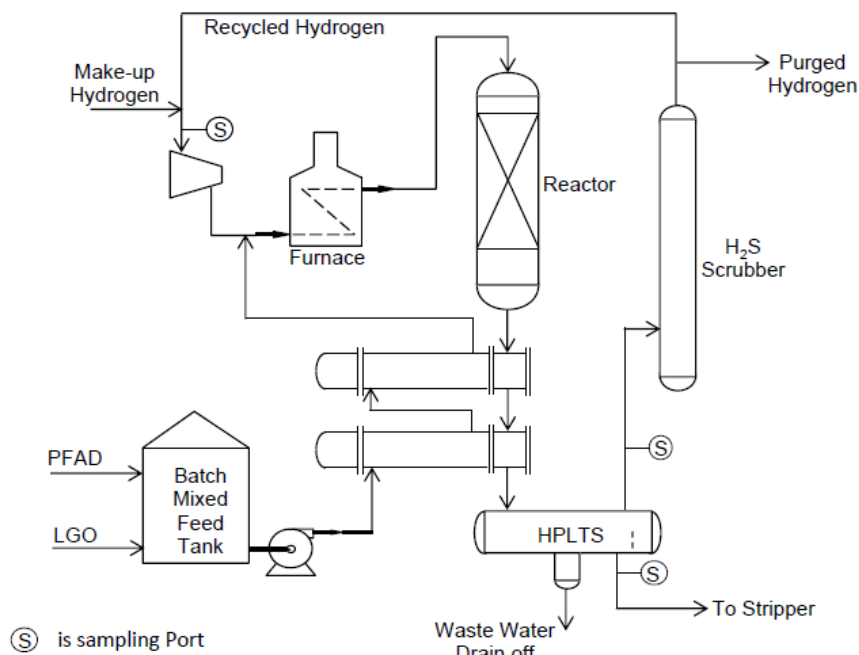
Figure 4.1 Simplified process scheme of hydrotreating unit developed by Verasuwan Co., Ltd., Thailand.

Process parameters of the unit such as reactor temperature and pressure were continuously measured and recorded with thermocouples and precise pressure transmitter. At the reactor, each thermocouple was installed in four layers, top, and bottom pressure were also measured. Hydrogen consumption was detected by corriolis flow meter at make-up stream of 99.5 wt% hydrogen as cubic meter at standard state. The liquid product at every hour was collected for 3 liters at the high pressure gas-liquid separator (HPLT). The condition of the reaction during co-processing PFAD in LGO was as followed.

Feed	0, 5, 8, 12, 25 wt% PFAD (75 wt% minimum of FFA) with non-hydrotreated gas oil (300-500 ppmw Sulfur)
Temperature	Feed inlet temperature = 280-285 $^{\circ}$C
Pressure	Maximum outlet pressure = 26 barg

Catalyst   3.6 m^3 with KF-757-1.3E, Albermarle-Nippon Ketjenfine

$(CoMo/Al_2O_3)$

Reactor type   Single fixed-bed reactor (assumed <u>adiabatic reactor)</u>

Reactor dimension   1 m in internal diameter

6 m in height with

4.6 m in height of the catalyst bed

Reactor design Maximum temperature   = 380 ^{o}C

Maximum pressure   = 60   barg

Flow scheme   Downward co-current flow with uniform distribution

H_2 Flow rate   Max at 1000 SCFM (ft^3/min at standard state)

4.1.2 Laboratory-scale reactor

The reaction was conducted in a laboratory scale fixed-bed tubular reactor, and the process diagram was shown in <u>Figure 4.2</u>. The reactor was a 316L stainless steel tube, 1/2 inch of outer diameter, and 50 cm of total length. A type-K thermocouple with 1/16 inch of diameter inserted from the bottom using a bored through connector to the middle of the catalyst bed. The catalyst bed was loaded between two packs of glass wool and between two stacks of glass beads, respectively. Height of the catalyst bed was approximately 4 centimeters that can be assumed to be a trickle-bed flow scheme with a uniform temperature distribution. The reactor temperature was controlled by a temperature controller with a solid-state driving 3 sets of 3000 watts heating element. The feed pump were preheated at 80 ^{o}C by a silicone heating element at the outer wall of the syringe pump, Teledyne ISCO 500D, and the feed was injected to the reactor at 0.2 ml/min (12 ml/h, 10 g/h). The feed injection line was a stainless steel tube with 1/8 inch in diameter, and traced with electrical silicone heater to prevent solidification. Also, the end of the feed tube was heated to 200 ^{o}C with electrical preheater before entering

top of the reactor. The reactor effluent was naturally cooled down to room temperature with bared tube of a ¼ inch OD of stainless steel tube with 60 cm long before flowing to a back pressure regulating valve. The valve was capable of steadily holding the system pressure, and the effluent flow rate was controlled by gas and liquid flow rate.
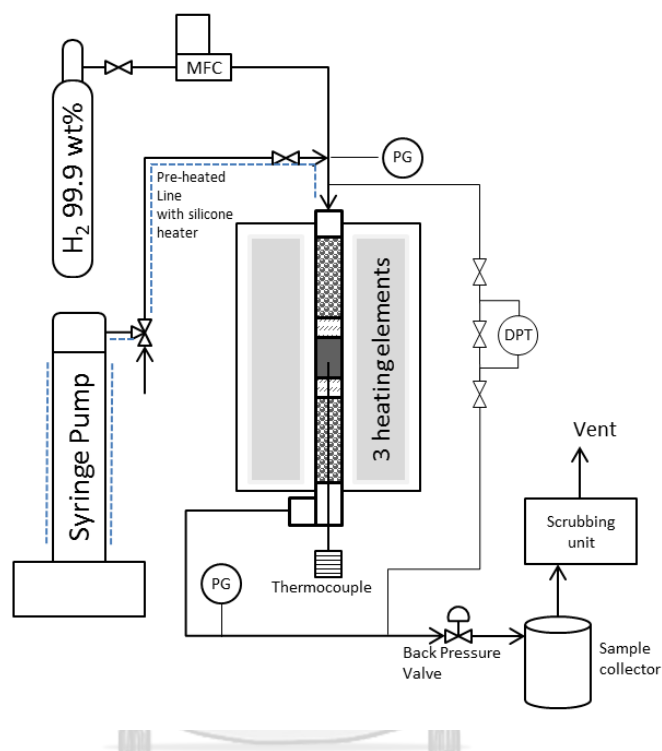
Figure 4.2   Simplified process scheme and equipment of the laboratory-scale isothermal reactor. (PG = pressure gauge, DPT = differential pressure transmitter, MFC = mass flow controller)

Hydrogen gas 99.9 wt% was fed co-currently with liquid feed from top to bottom of the reactor and it was controlled the flow rate by mass flow controller (MFC) at 630 NL/L (126 ml/min at standard temperature and pressure). Feed inlet pressure was controlled at 25 – 25.5 barg. Two pressure gauges, and high resolution differential pressure transmitter ("Azbil" model GTX31D) were installed at the inlet and outlet of the reactor. The liquid samples were collected at the outlet of the back pressure valve, while the gas phase was scrubbed before it was vented off to atmosphere.

4.1.3 Modified laboratory-scale reactor

In order to investigate the cause of the polymerization of unsaturated fatty acid chain in model feedstock, the modification of the laboratory-scale reactor was introduced. Increasing feed temperature at moderate heat transfer rate must be achieved by heat transfer from higher temperature air or combusted air to reactor wall, thin film of liquid, and bulk of liquid. At thin film with conduction might be resulted in too high temperature to initiate polymerization led to polymerized material that block catalyst pores.

The modified experiment was a splitting of isothermal reactor to a heating section and an adiabatic section as depicted to **Figure 4.3**. The heating zone was capable of increasing the temperature of mixtures to 275 $^{\circ}$C with 3 heating elements. The adiabatic tubular reactor was installed at the outlet of the heating zone, and insulated with 3 inches of high density rock wool with 15 centimeter height. Prior to the experiment, heat loss of the adiabatic section was only 2 $^{\circ}$C when the system was experimented with n-octadecane at 275 $^{\circ}$C. Thermocouple #1 was connected to the temperature controller, and thermocouple #2 had two elements with 4 centimeter between each. Two differential pressure transmitters were installed at each section, separately. The catalyst in the adiabatic zone was similarly in-situ pre-sulfided as in **Figure 4.2** by moving the tubular reactor to the heating zone. The size of the reactor was thoroughly the same, but three tee-joints were additionally installed between the heating and adiabatic section so as to install the thermocouple #1 and the fittings for both differential pressures.
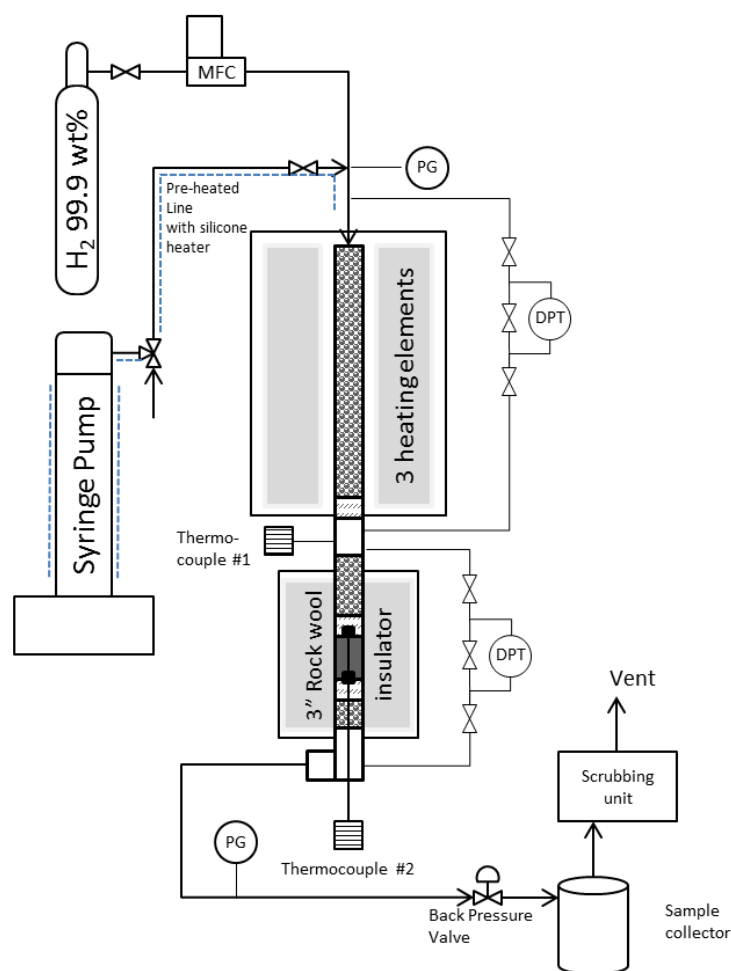
Figure 4.3 Modified process scheme and equipment. Thermocouple #1 equipped with temperature controller, and thermocouple #2 has 2 elements. (PG = pressure gauge, DPT = differential pressure transmitter, MFC = mass flow controller)

4.2 Catalyst and catalyst composition

The catalyst was a commercial hydrotreating catalyst, $CoMo/Al_2O_3$ with 1.3 mm in diameter, and 4-8 mm in length in cylindrical shape. Prior to the catalyst loading, it was crushed and sieved between 0.8 to 2 mm in diameter in order to obtain the trickled-bed flow scheme. Types of metal loading onto the catalyst were analyzed by an energy-dispersive X-ray spectroscopy as shown in **Table 4.1**. The amount of cobalt was 1.7 wt%, and that of molybdenum was 11 wt%. An incorporation of phosphorous about 3 wt% into cobalt-molybdenum active metals was observed. The addition of phosphorus

benefits desulfurization activity as a second promoter or a modifier of the catalyst acidity [58, 59].

Table 4.1 The elemental composition of catalyst by energy-dispersive X-ray spectroscopy

	Element (%wt)					
	C	O	Al	P	Co	Mo
Spectrum 1	2.73	53.65	27.73	3.32	1.70	10.86
Spectrum 2	2.91	53.61	25.97	3.28	2.10	12.13
Spectrum 3	2.73	54.20	26.95	3.00	1.87	11.28
Spectrum 4	3.68	55.57	26.38	2.89	1.54	9.94
Spectrum 5	3.08	56.27	25.77	2.97	1.50	10.41
Average	3.03	54.66	26.56	3.09	1.74	10.92
S.D.	0.39	1.20	0.79	0.19	0.25	0.84

4.3   Feed preparation
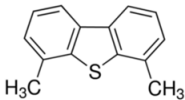
Feed and model feed specification and origin was listed in **Table 4.2**. The comparison of the pilot-scale feed and model feed was shown in **Table 4.3**.

N-octadecane (n-C18) had been used as model light gas oil so as to avoid the amount of poly-aromatics hydrocarbons and high refractory sulfur components. Moreover, n-C18 has normal boiling point near LGO. Sulfur components in light gas oil are generally naturally occurred containing various type of sulfur, so a known sulfur component with moderate to high refractory was introduced. In this study, 4,6-dimethyl-dibenzothiophene (4,6-DMDBT) represented amount of sulfur in LGO. Preliminary result experiment observed moderate to high conversion of desulfurization of 4,6-DMDBT over the experimental conditions and catalyst. Finally, palm fatty acid distillate (PFAD) might be containing impurities such as sodium, phosphorus, and phospholipid gum as it is a commercial specification. The use of palmitic in this study was to eliminate those impurities and study an intrinsic properties of fatty acids on various effects.

Table 4.2   Specification and origin for chemicals used in the study.

Chemical	Specification	Origin
Palm fatty acid distillate	84.5 wt%	Oleen Co.,Ltd
Light gas oil	Sulfur 484 ppmW	Verasuwan Co.,Ltd
Palmitic acid	99 wt%	Siam Absolute Co.,Ltd
Refined bleached and deodorized palm oil (RBDPO)	FFA < 0.1 wt%	Oleen Co.,Ltd
n-octadecane (n-C18)	99 wt%	Sigma Aldrich
4,6- Dimethyl dibenzothiophene	99.99 wt%	Sigma Aldrich
Nickel on sodium silicate	Unknown	Johnson Metthey
Commercial hydrotreating catalyst	$CoMo/Al_2O_3$	Nippon Ketjenfine

Table 4.3   Comparison of pilot-scale feed and lab-scale feed (model)

Pilot-scale feed	Light gas oil (Diesel with natural sulfur)	Natural sulfur In LGO	Commercial Palm fatty acid distillate (PFAD) 0, 5, 8, 12, 25 wt%
Lab-scale feed	n-Octadecane	4,6-Dimethyl dibenzo thiophene 180 ppm	Palmitic acid (PA) 0, 5, 10, 20 wt%

PFAD in LGO

The preparation of PFAD in LGO was experimented in pilot-scale unit. PFAD from Oleen Oil Public Company Limited (Thailand) was prepared as a renewable feedstock. PFAD and LGO at 5, 8, 12, and 25 wt% underwent batchwise mixing in 15,000 L jacketed tank with steam coiled heating tube maintaining at 60-75 °C. The feed

mixtures were agitated for 6 h in 15,000 L tank with steam coiled heating tube, and then transferred to the feed tank (50,000 L). The mixture was sampled and analyzed the amount of FFAs at different levels to ensure a complete mixing. In order to prevent solidification and obtain uniformity of the feeds, the feed tank was always heated at 60 $^{\circ}$C during the experiment.

Model of PFAD with 4,6-DMDBT in n-C18

A commercial grade palmitic acid 99.9 wt.% was used representing half of PFAD. N-octadecane 99 wt.% as a model LGO was obtained from Sigma-Aldrich (Germany). The model sulfur component in LGO was 4,6-dimethyl-dibenzothiophene (4,6-DMDBT) 99.99 wt.% was also obtained from Sigmal-Aldrich (Germany). Palmitic acid was melted and pre-mixed with n-octadecane at 5, 10, and 20 wt% and heated at 50 $^{\circ}$C for complete dissolution. 4,6-DMDBT was then slightly added to the mixture to obtain 178-183 ppmw of total sulfur. The amount of palmitic acid was analyzed by the titrimetric method using 0.1 N of NaOH solutions for exact amount.

Double bond hydrogenation as feed pretreatment

Pretreatment of RBDPO and PFAD was conducted in a batchwise reactor at 150 $^{\circ}$C, 6.5 barg, W/F = 2 g catalyst/100 g oil, and under hydrogen pressure over commercial nickel on synthetic silicates. According to **Table 4.4**, result of iodine value confirmed that the degree of double bond was almost completely reduced for hydrogenated RBDPO and PFAD, while amount of fatty acid content and other impurities were similar.

Table 4.4   Composition and Properties of feeds and hydrogenated feed mixtures

Feed	Abbreviate	Fatty acid content (wt%)	Iodine Value (g/100g)	Water Content (ppm)	Sodium (mg/kg)	Phosphorus (mg/kg)
Palmitic acid	PA	99.13	< 2	147	2.7	< 0.5
Refined Bleached and Deodorized Palm oil (RBDPO)[a]	PO	0.22	47.56	869	3.2	0.64
Hydrogenated RBDPO	HPO	0.37	1.15	744	3.1	0.41
90% Palmitic acid + 10% RBDPO	90PA + 10PO	89.80	4.71	202	N.D.	N.D.
90% Palmitic acid + 10% H-RBDPO	90PA + 10HPO	91.64	1.74	191	N.D.	N.D.
Palm Fatty Acid Distillate (PFAD)	PFAD	89.44	42.85	1254	4.2	< 0.5
Hydrogenated PFAD	H-PFAD	92.54	0.78	1157	3.9	< 0.5

(a) no addition of anti-oxidants for commercial product
N.D. = Not determined

4.4   Analysis and Measurement

The oxygen removal activity and sulfur removal activity was determined by un-reacted free fatty acid and sulfur component containing in products. Conversion will be calculated as following.

4.4.1   Free fatty acid content

All samples were decanted, and only the non-polar liquid phase was analyzed following AOCS 5a-40 (the free fatty acids existing in the sample). The amount of free fatty acids is assumed to be 1:1 of oleic acid (MW 282.46) to palmitic acid (MW 256.42). The average molecular weight of PFAD was 269.44 g/mol, while the molecular weight of palmitic acid at 256.42 g/mol was used in the model study.

4.4.2   Sulfur containing compound

Determination of sulfur component in feeds and products was analyzed by using a LABX3000 x-ray fluorescence (XRF) analyzer (Oxford Instrument Company Ltd., Osney Mead, Oxford) and following ASTM D4294. Prior to the analysis, the sample was decanted and then filtered by filter paper No. 1. In the case of high water content, water was decanted prior to filtering with filter paper. For the determination of palmitic acid in n-C18, the total sulfur content in both products and feeds were pre-heated at 45 $^{\circ}$C for preventing solidification of palmitic acid

4.4.3 Boiling range of the product

The analysis will follow standard test method for distillation of petroleum products at atmospheric pressure (ASTM D86). The sample was decanted to separate water phase, if it formed. The sample size was 100 ml.

4.4.4 Water content

Water content in hydrocarbon product was analyzed by Karl Fisher (Metrohm KF-752). The water fraction settling down to the bottom is firstly decanted out, and it was assumed that some water fraction in oil was at equilibrium.

4.4.5 Distribution of hydrocarbon product

The liquid hydrocarbon was analyzed using GC Shimadzu 2010 equipped with a flame ionization detector. HP-INNOWAX, 30 m, 0.25 μm was installed for determining linear-long chain hydrocarbons. The amount of individual hydrocarbon chain was analyzed under calibration with response factor relative to methyl octanoate as internal standard.

4.4.6 Hydrogen Consumption

Hydrogen consumption was measured by Coriolis gas flow meter from the make-up stream of hydrogen. The total system loss of hydrogen is about 0.3 Nm^3/h of hydrogen, but the purge rate was controlled manually. In this study, the purge gas line was closed during the co-processing, so the actual consumption could be a good representative figure. The measured unit is at gas standard state (0 $^{\circ}$C, 1 atm) in cubic meter per hour, Nm^3/h.

CHAPTER FIVE

RESULTS AND DISCUSSION

5.1   Deoxygenation of PFAD over commercial catalyst (Preliminary experiment)

Deoxygenation of PFAD over sulfided commercial $CoMo/Al_2O_3$ catalyst, Nippon Ketjenfine KF-757-1.3E in the laboratory-scale reactor could be achieved at 320 ^{o}C, 30 barg (435 psig), LHSV = 2.0 h^{-1}, and H_2/oil = 630 NL/L. The feed rate of PFAD was 12 ml/min. The hydrogenated product was colorless liquid hydrocarbons with 4-7 vol% of hazy water phase at the bottom of sample collector.

Analysis of the distillation range of hydrogenated PFAD (H-PFAD) was determined as shown in **Figure 5.1** in comparison with fatty acid chain containing in PFAD. Very narrow distribution of the boiling range was observed between 280 to 300 ^{o}C, representing the presence of normal alkane ranging from n-C14 to n-C20 according to the boiling range of normal paraffin hydrocarbons shown in **Table 5.1**. Determination of hydrocarbon chain length by gas chromatography was also investigated. It was clearly observed that PFAD can be converted to long chain hydrocarbon via theoretical suggested reaction pathway, hydrodeoxygenation, decarbonylation, and decarboxylation due to the presence of both even and odd number of carbon. Some hydrocracking reaction was also observed as the presence of light fraction smaller than n-C14. Less than a few percentages of heavy fractions were observed. This was undesired pathway due to a polymerization of esters, acid, and alcohol to longer molecules.
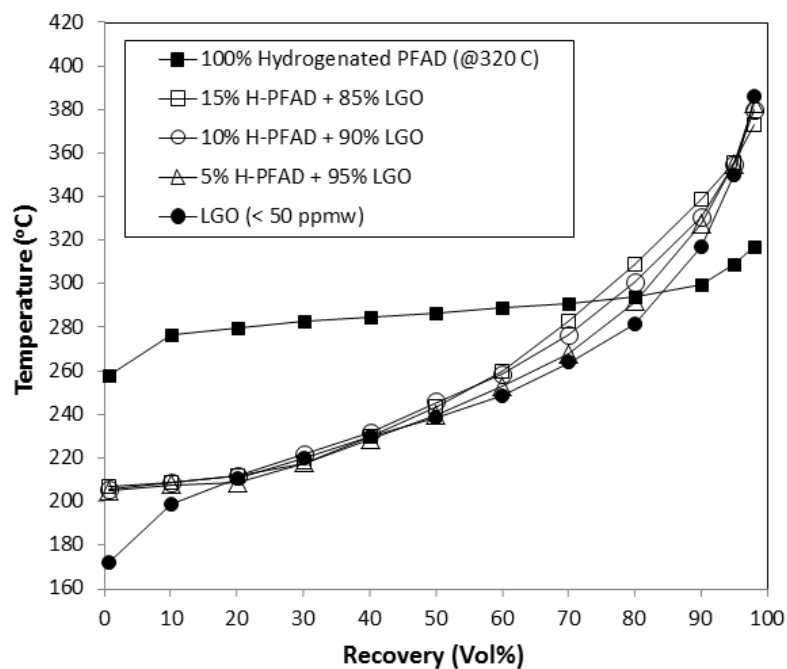
Figure 5.1   Distillation curves following ASTM D86 of different product mixtures of hydrogenated PFAD high sulfur diesel (520 ppmw) over CoMo/Al$_2$O$_3$ (KF-757) catalysts, LHSV = 2.0 hr^{-1}, T=320 $^{\circ}$C, P=30 barg (435 psig), H$_2$/PFAD = 630 NL/L with hydrotreated light gas oil.

Table 5.1 Normal Boiling of normal alkane

Number of Carbon	Boiling Point (°C)
n-C6	69
n-C7	98
n-C8	126
n-C9	151
n-C10	174
n-C11	196
n-C12	216
n-C13	234
n-C14	254
n-C15	270
n-C16	287
n-C17	303
n-C18	317
n-C19	333
n-C20	343

The sample of H-PFAD was collected every 6 h for 48 h. The boiling range of each sample was not significantly different from the initial sample at the first 6 h. The whole sample was then mixed with hydrogenated light gas oil (LGO) containing sulfur less than 50 ppmw. According to **Figure 5.1**, an addition of the H-PFAD to hydrotreated LGO resulted in changes of boiling range of the product mixture ranging from 40 vol% to 90 vol% recovery. The boiling range was increased while the product density was decreased. Heavy components from hydrogenated PFAD as higher molecular weight than n-C18 slightly lowered the final boiling point at 95 vol%. Due to the lower density but higher 50 vol% boiling range, cetane index of products was impressively improved that it could be claimed as a cetane improver for diesel fuel. However, final boiling point and density of the product must be cautioned for higher fraction of H-PFAD. The former can cause smoke and sooths at the tail pipe, and the latter can affect the performance of fuel pump due to lower density and viscosity. As the lower density and viscosity might resulted in damaging fuel pumping system, an addition of fuel lubricity improver additive was suggested by an additive supplier in Thailand, White Group Co., ltd.

5.2   Co-processing of PFAD with light gas oil

The preliminary results (5.1) showed that a mixture of hydrogenated PFAD with LGO could produce fungible renewable automotive diesel that followed the European diesel fuels standard EN590. Co-processing of PFAD with non-hydrotreated light gas oil to produced drop-in renewable fuel that could be interchangeable and compatible with conventional diesel was then suggested in this step. Due to the fact that the current hydroprocessing technology, catalysts, and the availability of large amount of hydrogen for hydroprocessing of vegetable oil, hydrodesulfurization units can be promptly capable of converting a mixture of vegetable oil and petroleum derived diesel to renewable one [9, 41].

The experiment was achieved in a pilot-scaled reactor operated at a moderate condition as shown the schematic diagram drawn in **Figure 4.1**. This unit was an existing hydrodesulfurization unit at Verasuwan Co.,Ltd. (Thailand) Firstly, the purpose of this unit was to eliminate sulfur compounds in LGO from 1000 ppmw to lower than 50 ppmw of sulfur. Implementation of PFAD in LGO was varied from 0, 5, 8, 12, and 25 wt% at maximum. The constricted amount was due to the following. (1) The theoretical calculation of hydrogen consumption was 300 m^3/h, while the maximum hydrogen making-up rate was 350 m^3/h. (2) The onset of solidification of PFAD in 25 wt% PFAD in LGO was observed at temperature of 48 $^{\circ}$C.

The reactor was 1 m in diameter and 6 m in height. Since March 2011, the reactor was loaded with commercial CoMo/Al_2O_3 hydrotreating catalyst with the amount of 3.6 m^3 as a single-bed catalyst. It was neither hydrogen nor fresh feed quenching streams between the catalyst beds. The insulation was 6 inches of high density rock wool and the outer layer was covered by aluminum sheet, so the reactor can be considered as a near adiabatic condition. A back pressure regulator was set to maintain the system pressure from 25.5 to 26.0 barg. Pressure change for all experiment was not observed. The reactor inlet temperature was controlled by a direct-fired heater with a fuel oil burner in the range of 280–285 $^{\circ}$C. Liquid hourly space velocity (LHSV) was fixed at 0.75 h^{-1}, while the liquid feed flow rate was 2.7 m^3/h.

5.2.1 Feeds and products

PFAD contained 84.5 wt% of free fatty acids (FFAs) and a mixture of glycerol esters with the distribution of fatty acid chain shown in **Table 5.2**. The distribution of fatty acid chain of PFAD was determined by converting PFAD to a mixture of fatty acid methyl esters (FAME) using 1.5 wt% sulfuric acid as catalyst with 9:1 molar ratio of methanol to

PFAD for 36 h of the reaction time at 68 $^{\circ}$C. Total conversion of 98.7 wt% was achieved as it could be assumed as the actual distribution of fatty acid chain.

Table 5.2 Fatty acid composition of PFAD (FFAs 84.5 wt%) and the amount of hydrogen required for double-bond hydrogenation and complete hydrodeoxygenation.

Fatty acid	Structure	Formula	MW	Composition (wt%)	Required H$_2$ (mol H$_2$/mol FFAs)	
					Double bond Hydrogenation	HDO
Lauric acid	C12:0	$C_{12}H_{24}O_2$	200.3	1.3	0.000	0.051
Myristic acid	C14:0	$C_{14}H_{28}O_2$	228.4	1.4	0.000	0.049
Palmitic acid	C16:0	$C_{16}H_{32}O_2$	256.4	46.7	0.000	1.460
Steric acid	C18:0	$C_{18}H_{36}O_2$	284.5	4.4	0.000	0.123
Oleic acid	C18:1	$C_{18}H_{34}O_2$	282.5	36.5	0.347	1.037
Linoleic acid	C18:2	$C_{18}H_{32}O_2$	280.4	9.2	0.177	0.264
Linolenic acid	C18:3	$C_{18}H_{30}O_2$	278.4	0.4	0.012	0.012
Arachidic acid	C20:0	$C_{20}H_{40}O_2$	312.5	0.2	0.000	0.005
Total				100.0	0.535[a]	3.000[b]

Average molecular weight of total free fatty acid in PFAD = 268.5 g/mol

[a,b] Double bond hydrogenation and hydrodeoxygentation of FFAs in PFAD require 3.535 mol H$_2$/mol FFAs

A mixture of PFAD at 12 and 25 wt% with non-hydrotreated LGO was prepared. The distillation range of both feeds was analyzed and shown in **Figure 5.2**. It was observed that an increasing of distillation temperature was increased with fraction of PFAD, especially, at 90 vol% recovery. The limitation of 90 vol% recovery was aim to control soot and CO for the engine emission. Higher values can also increase maintenance requirements, and tremendously increase fuel density [60]. The cetane index of feed calculated by 50 vol% recovery and fluid density was also observed as decreasing with amount of PFAD. As a result, a mixture of raw PFAD to LGO was certainly not following the diesel specification EN 590. The mixture was then required to be treated with hydroprocessing resulting in the hydrotreated products shown in **Figure 5.2(B)**. Not only the distillation range, the feed mixture was also not following other diesel specification, cetane index, density, acid value, and viscosity. The upgrading of those properties by hydroprocessing aimed to meet diesel specification so as to be compatible with diesel engine.
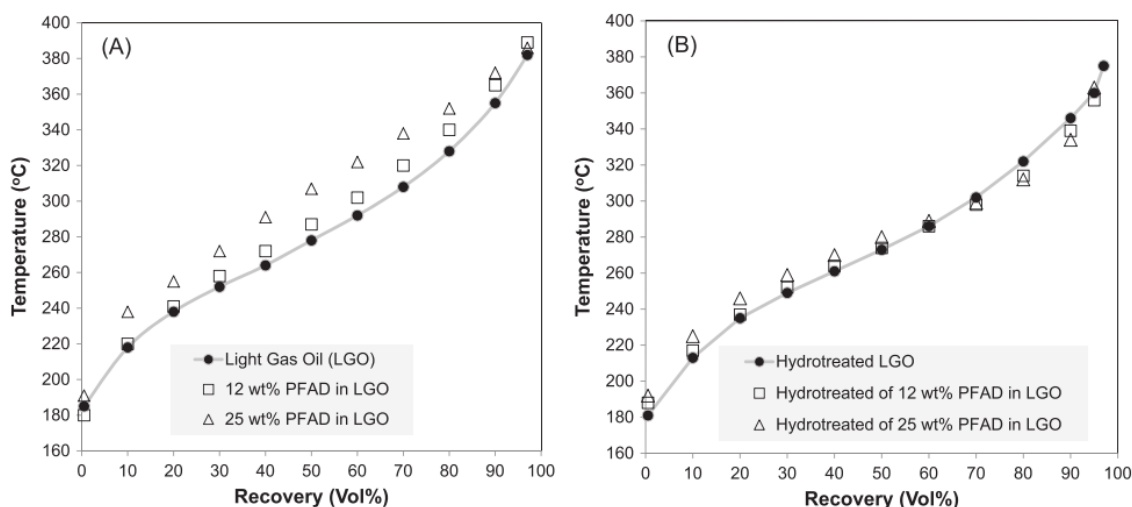
Figure 5.2 The distillation range following ASTM D86 for the feed mixtures (A) and the hydroprocessed products (B) of 12 wt% and 25 wt% PFAD in LGO.

5.2.2 Effect of PFAD in the feedstock on reactor temperature

The objective of this result was a safety issue raised by the operation team of the company. Since the designed reactor condition was only 380 $^{\circ}$C and 60 barg, any changes of the operation that exceeded the mechanical limitation must be the first priority to be concerned. Consequently, the experiment at 8 wt% PFAD was an initial trial. It was observed that amount of PFAD in LGO largely affected the reactor temperature. Significant increase in the reactor outlet temperature at the bottom was observed as much as 60 $^{\circ}$C. Each case of PFAD faction was shown in **Figure 5.3**. Higher amount of PFAD affected the larger difference of the reactor temperature (top-bottom). It must be noted that the operation was only hold to 12 h so as to limit any catalyst deactivation or any other effect on hydrodesulfurization activities as the main objective of this commercial catalyst. Generally, the hydroprocessing of LGO is an exothermic process that there was a heat effect due to the composition of LGO. In this case, LGO contained 2.2 wt% olefinic, and 6.6 wt% aromatics hydrocarbons. Hydrogenation of both olefinic and aromatics is largely exothermic reactions, however, after deducting heat loss of the reactor wall, only 5-7 $^{\circ}$C was surged. When the initiation of PFAD for only 5

wt%,12 $^{\circ}$C of the reactor bottom temperature was increased within 4 h of time on stream. Tremendous increase in the reactor bottom temperature was largest in the case of 25 wt% of PFAD in LGO and this almost reached the reactor designed temperature. The increase in the reactor temperature was not a linear function with the amount of PFAD. For higher amount of PFAD in LGO, quenching stream of hydrogen or fresh feed should be introduced. The modification of the reactor by splitting to a series configuration might also reduce risk of mechanical failure due to the heat effect.
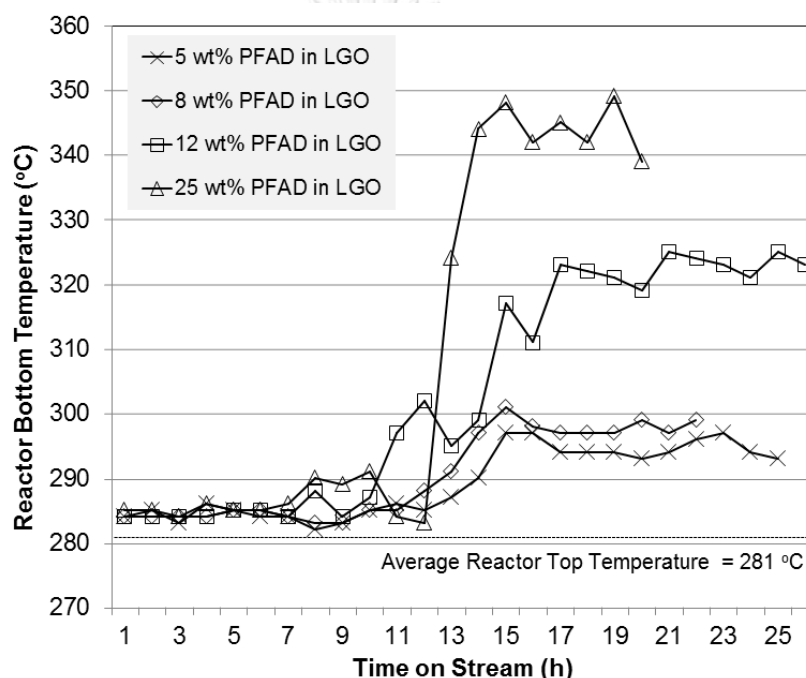
Figure 5.3   Temperature at the bottom of the reactor as a function of time on stream corresponding to the amount of PFAD in LGO.

Overall enthalpy of the hydroconversion of the feed mixture was a cause of the potential heat effect from PFAD than LGO. Various reactions involving a series of consecutive steps, side reaction, and inevitable double bond hydrogenation were suggested by many researches. The hydroconversion of triglyceride and FFAs begins with hydrogenation of double bond of fatty acid chain (1), followed by decomposition of triglyceride to FFAs and propylene (2) which was then hydrogenated to propane (7).

Deoxygenation of FFAs occurred via three different routes, hydrodeoxygenation (4), decarbonylation (5), and decarboxylation (6). The reaction routes based on oleic acid and steric acid including enthalpy of each step was the following.

- Saturation of oleic triglyceride (only double-bond hydrogenation)

$$C_{57}H_{104}O_6 + 3H_2 \rightarrow C_{57}H_{110}O_6 \qquad \Delta H = -303 \text{ kJ/mol} \qquad (1)$$

- Cleavage of fully-hydrogenated oleic triglyceride to three steric acids

$$C_{57}H_{110}O_6 + 2H_2 \rightarrow 3\ C_{17}H_{35}COOH + CH_2=CH-CH_3 \quad \Delta H = +251 \text{ kJ/mol} \qquad (2)$$
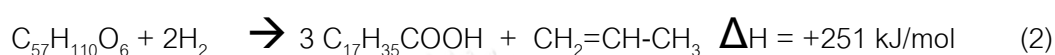
- Hydrogenation of oleic acid to stearic acid

$$C_{17}H_{33}COOH + H_2 \rightarrow C_{17}H_{35}COOH \qquad \Delta H = -91.7 \text{ kJ/mol} \qquad (3)$$

- Hydrodeoxygenation of stearic acid

$$C_{17}H_{35}COOH + 3H_2 \rightarrow C_{18}H_{38} + 2H_2O \qquad \Delta H = -129.6 \text{ kJ/mol} \qquad (4)$$
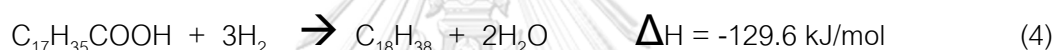
- Decarbonylation of stearic acid

$$C_{17}H_{35}COOH + H_2 \rightarrow C_{17}H_{36} + CO + H_2O \quad \Delta H = +20.2 \text{ kJ/mol} \qquad (5)$$
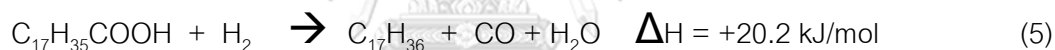
- Decarboxylation of stearic acid

$$C_{17}H_{35}COOH + H_2 \rightarrow C_{17}H_{38} + CO_2 \qquad \Delta H = -129.6 \text{ kJ/mol} \qquad (6)$$

- Propylene Hydrogenation to propane

$$CH_2=CH-CH_3 + H_2 \rightarrow C_3H_8 \qquad \Delta H = -125.1 \text{ kJ/mol} \qquad (7)$$

- Water Gas Shift (WGS)

$$CO + H_2O \rightarrow CO_2 + H_2 \qquad \Delta H = 43.7 \text{ kJ/mol} \qquad (8)$$

- Reversed Water Gas Shift (r-WGS)

$$CO_2 + H_2 \rightarrow CO + H_2O \qquad \Delta H = -43.7 \text{ kJ/mol} \qquad (9)$$

- CO - methanation

$$CO + 3H_2 \rightarrow CH_4 + H_2O \qquad \Delta H = -216.4 \text{ kJ/mol} \qquad (10)$$

- CO_2 - methanation

$$CO_2 + 4H_2 \rightarrow CH_4 + 2H_2O \qquad \Delta H = -177.2 \text{ kJ/mol} \qquad (11)$$

The endothermic effect (positive enthalpy) from the cleavage of triglyceride can be another factor to reduce heat effect due to exothermic reactions. In other words, the overall heat effect from fats and oils derivative comprising of high FFAs might have higher heat effect than that comprising of low FFAs. For instance, the enthalpy from hydroconversion of oleic triglyceride to steric acid and propane is -200.3 kJ/kg, while that of converting oleic acid to stearic acid is -332.9 kJ/kg. Although, low FFAs of feed was preferred for safety issue, but the hydrogen consumption for propylene hydrogenation and cleavage of triglyceride must be taken into consideration.

Another cause of heat effect was the hydrogenation of double bond of fatty acid chain as well as propylene hydrogenation. This effect could be reduced by screening the feeds that comprise of higher saturated fatty acid composition than unsaturated one, e.g. raw coconut oil, tall oil. However, saturated fats and oils composition was not naturally occurred and these types of feed are valuable and require an extra addition of hydrogenation process.

Methanation of CO and CO_2 was thermodynamically inevitable. Both reactions are highly exothermic and favorable with the presence of hydrogen pressure. Methanation reaction was claimed to cause local overheating into the catalyst bed as the decarbonylation and decarboxylation potentially provide CO and CO_2. Jeczmionek et al. claimed that decarbonylation and decarboxylation potentially provided large total heat effect on the catalyst bed due to the methanation reaction. The heat effect from steric acid decarboxylation/decarbonylation and the sequential reactions of CO (r-WGS and methanation) was approximately 1.4 times higher than that from hydrodeoxygenation to n-C18 [61]. Both decarboxylation and decarbonylation was not only affected het effect, but also hydrogen consumption according to methanation.

Consequently, the overall deoxygenation was preferred to be selective to hydrodeoxygenation rather than decarboxylation and decarbonylation.

5.2.3   Desulfurization and deoxygenation activities

Desulfurization and deoxygenation activity was defined by the conversion of sulfur in organic forms, and disappearance of FFAs content, respectively. Sulfur and FFAs content in the feeds and the products at 6 h after switching from processing LGO to co-processing PFAD in LGO are shown in **Table** 5.3. It should be noted that FFAs content in the liquid product was increased with the change of color into brown and severely to black with acrid smell.

Table 5.3 Deoxygenation and desulfurization activity

PFAD in LGO (wt%)	*Removal of Oxygen*			*Removal of Sulfur*		
	FFAs in Feed (wt%)	FFAs in Product (wt%)	**Deoxygenation Conversion (%)**	S in Feed (ppmw)	S in Product (ppmw)	**Desulfurization Conversion (%)**
0	0.01	0.008	-	545	34	93.8
5	4.87	0.076	98.4	504	36	92.9
8	7.91	0.130	98.4	495	37	92.5
12	11.89	0.175	98.5	463	36	92.2
25	24.78	0.094	99.6	347	28	91.9

The presence of PFAD in LGO slightly reduced desulfurization rate. The conversion of desulfurization for 5-25 wt% of PFAD slightly decreased with an increasing amount of PFAD. The result was conforming to the scaled-up reactor and the kinetic study by Templis et al. [5]. An addition of palm oil up to 5 wt% in gas oil under CoMo/Al$_2$O$_3$ decreased the desulfurization rate, but a slight effect on the rate was observed with the mixture contained crude palm oil above 5 wt% but not exceeding 10 wt% [1]. However, in another case, higher amount of sunflower oil up to 30% in heavy LGO was not significantly affected hydrodesulfurization rate [3].

Another reasonable explanation of the slightly changes of desulfurization and deoxygenation was the reaction condition where high space time velocity occurred.

Longer contact time of the reaction resulted in near complete conversion of both desulfurization and deoxygenation. The increase in deoxygenation conversion was probably due to the increase in reaction temperature at bottom of the reactor. The decrease in desulfurization was not exactly concluded. Low refractory sulfur component might be totally desulfurized, while high refractory one might not be eliminated due to the limitation of the catalyst performance even at higher temperature.

According to **Table 5.3**, high conversion of deoxygenation over varied PFAD in LGO in all cases was observed. Left over tri-glyceride was completely converted, since there was no trace amount of mono-glyceride and di-glyceride in the products quantified by GC-FID. Deoxygenation conversion was not significantly increase when increasing PFAD from 12 to 25 wt%. The very high deoxygenation conversion can be described by the dramatic increase in reactor bottom temperature. According to Fig. 5.7, FFAs content in the products was largely dropped when the reaction temperature at the bottom of the reactor reach 350 $^{\circ}$C where deoxygenation conversion was at the highest in the case of 25 wt% PFAD, the reaction temperature due to amount of PFAD in LGO slightly affected to the deoxygenation conversion at utmost high conversion.

5.2.4 Analysis of gaseous product

Gaseous product was sampled from a high pressure low temperature separator (HPLTS). Since hydrogen was a raw material for hydroconversion, other gaseous products, e.g. CO, CO_2, CH_4, and C_2H_6 was only qualified by GC-TCD equipped with zeolite 3A and 13X. The hydrogen purity in the gas stream separated from HPLTS was detected by TCD instrument. Lacking of hydrogen was observed as low as 72 vol% in the case of 25 wt% of PFAD in LGO, while a normal operation kept hydrogen purity at 93-97 vol% all the time. Since the exiting pilot-scale unit did not have pressure swing adsorption to remove other gaseous product, purging of hydrogen-lean gas and

making-up the system pressure with 99.5% hydrogen were achieved in the experiment. The lowest hydrogen purity was allowed at least 70 vol% so as to minimize catalyst deactivation and coking.

5.2.5   Analysis of Liquid product

Hydrogenated products was sampled by a sampling bomb cylinder at the inlet nozzle of HPLTS, depressurized and drained off to beaker. The liquid phase comprised on both hydrocarbon and water phase. Large amount of water was also observed at the bootleg of HPLTS, and it was drained off every hour. The formation of water was an evidence of the deoxygenation. Liquid hydrocarbon phase was clear and green to yellowish in color, while water phase was hazy with small white particulates in the case of 5 and 8 wt% PFAD, but it was clear and colorless in the case of 12 and 25 wt% of PFAD. Physical appearance of water phase might be related to reaction temperature that higher amount of PFAD resulted in larger heat effect and higher reaction temperature. Similar observation by Pavel et al. showed that white-waxy solid in oil phase at low reaction temperature (260-280 ^{o}C), was disappeared when the reaction temperature higher than 300 ^{o}C [62]. Dissolution of FFAs in water could be responsible for haziness. The amount of FFAs in water was 0.7-1.2 wt% in hazy water phase, but less than 0.3 wt% in the colorless water. The presence of hazy water phase could indicate the unconverted FFAs which can be partially soluble in water. Several studies demonstrated the adverse effect of water onto sulfide catalyst during hydroprocessing of vegetable oil [25, 44]. Destabilization and specific area of the catalyst support affected the stability of sulfide form by water molecule [63, 64]. Toba et al. also found a leaching of sulfur during hydrodeoxygenation of waste cooling oil by sulfided catalyst. The sulfur content in the oil products increased with the reaction time [49].

The physical properties of liquid hydrocarbon were depicted in **Table 5.4**, and the distillation range of the products following ASTM D86 was plotted in **Figure 5.2 (B)**. Cetane index of products was increased with increasing amount of PFAD, while product density was decreased in vice versa. Free fatty acid content and neutralization number indicated the left over fatty acid in products as well as corrosiveness of products. These were on the diesel specification EN590. Sulfur content was also lower than 50 ppmw following EURO IV EN590. The addition of linear alkane from hydrogenated PFAD benefited the quality of diesel fuel as increasing cetane number. In commercial point of view, the addition of hydrogenated PFAD could also be considered as commercial additives for improving cetane and reducing greenhouse gas emission [65]. In this study, cetane index was obtained by calculation based on petro diesel from crude oil depending on diesel density at $60^{o}F$ and 50 vol% recovery data by ASTM D86. This method is only applicable to fuels from petroleum, but not applied to the diesel containing additives, synthesized and pure paraffinic hydrocarbons. Consequently, the true cetane should be determined by ignition quality, known as cetane number, by using engine method (ISO 5165) than using cetane index [66].

Table 5.4   Physical properties and n-paraffin distribution in products

Parameter	PFAD in LGO				
	0 wt%	5 wt%	8 wt%	12 wt%	25 wt%
Cetane index	59.3	61.6	62.9	63.8	67.9
Density @ 15°C, g/ml	0.818	0.813	0.810	0.808	0.801
Free Fatty Acids Content	0.008	0.076	0.130	0.175	0.094
Neutralisation Number, mg KOH/g	0.06	0.05	0.07	0.09	0.08
Sulfur, ppmw	34	36	37	36	28
n-Paraffins Content, wt%					
< n-C14	15.91	14.91	13.53	12.39	11.10
n-C15	3.75	3.92	4.14	4.26	5.66
n-C16	2.76	3.65	4.60	6.40	8.22
n-C17	2.05	2.31	2.73	3.27	4.74
n-C18	1.38	3.12	4.60	5.86	6.90
> n-C19	3.90	4.02	4.06	4.25	3.97
TOTAL n-paraffin, wt%	29.74	31.93	33.66	36.44	40.60
(n-C16 + n-C18) / (n-C15 + n-C17)	0.71	1.09	1.34	1.63	1.45
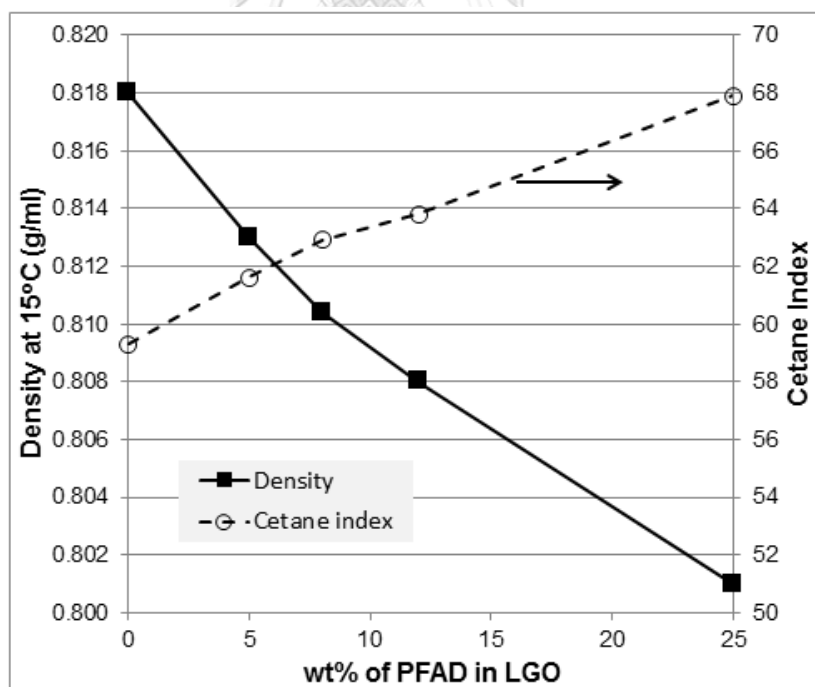
Figure 5.4   Cetane index and density of the liquid products as a function of PFAD in LGO.

According to **Figure** 5.4, the linearly reduction of bulk density of products with increasing PFAD in LGO was observed. Normal alkane ranging from n-C15 to n-C18 has the density ranging from 0.77-0.78 g/ml which is lower than that of diesel (0.818 g/ml). The lower density would result in lower fluid viscosity and lubricity for engine use. However, the advantage was the flexibility and more economic saving that refineries can maximize diesel production by fractionating heavier boiling point cut range. Converting more residue oil to gas oil pool and co-processing those with PFAD to meet the required density of diesel specification (0.81-0.84 g/ml) was preferred together with improving cetane number.

The presence of hydrogenated PFAD as hydrocarbon slightly increased the boiling point ranging from 180 to 300 $^{\circ}$C, but lowering the boiling point ranging above 300 $^{\circ}$C. The contribution of n-C15 to n-C18 shifted the ASTM D 86 curves especially increasing of the initial boiling of the product at 7 $^{\circ}$C and 9 $^{\circ}$C for 12 wt% and 25 wt% of PFAD in LGO, respectively. However, the boiling point range at 95 vol% recovery in the case of 12 wt% and 25 wt% PFAD should be lower but were slightly increased to 360 and 363 $^{\circ}$C, respectively. Heavy components due to undesired reaction, for instance, esterification of acid and alcohol to esters was responsible for the increase in boiling point at 95 vol% recovery. The presence of mainly n-C15 to n-C18 was confirmed by GC-FID results. Each of the n-paraffin (wt%) in products versus the number of carbon atoms corresponding to the amount of PFAD in LGO were plotted in **Figure 5.5**. The resulting product is not limited to n-C15 to n-C18, but the smaller hydrocarbons (< n-C14) were also observed. Hydrocracking reaction contributed the presence of lower n-paraffin which is more favorable at higher temperature. According to **Table 5.5 and Figure 5.5**, the amount of total n-paraffin was not linearly increased at higher PFAD amount. Due the higher temperature of the reactor and the presence of hydrocracking,

isomerization and hydrocracking were inevitable and concomitant reactions at the studied conditions.
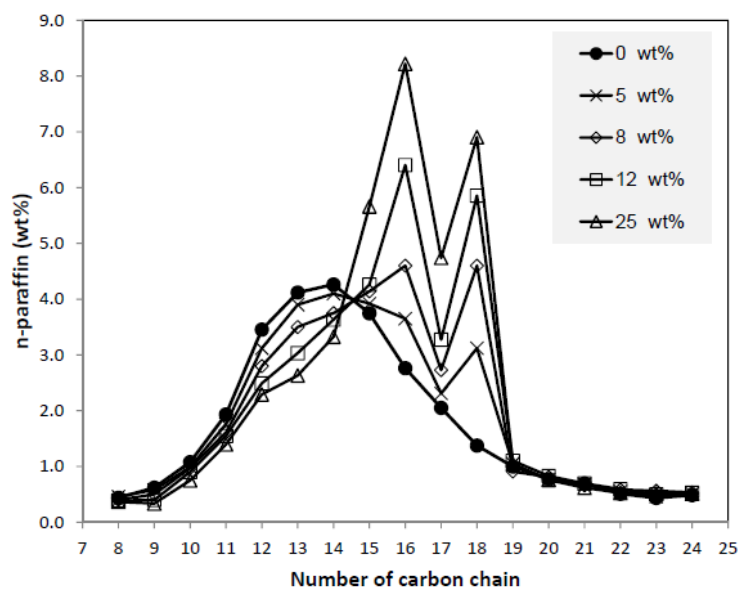
Figure 5.5   Total amount of n-paraffin (wt%) versus the number of carbon atoms corresponding to the amount of PFAD in LGO
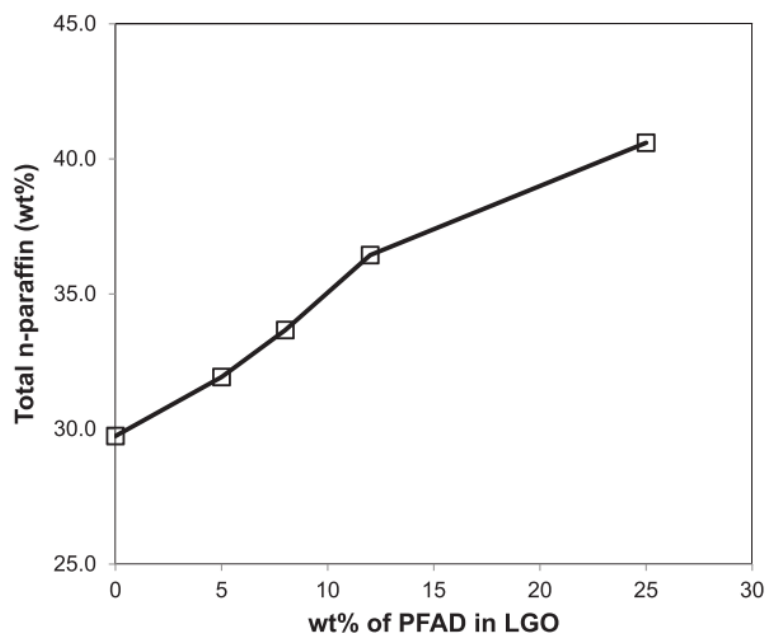
Figure 5.6   Total n-paraffin (wt%) in the hydrotreated product determined by GC-FID as a function of PFAD.

Figure 5.7 depicted that selectivity of hydrodeoxygenation over decarbonylation /decarboxylation by using ration of of even to odd number of hydrocarbon, (n-C16 + n-C18) over (n-C15 + n-C17). The ratio indicated a preferred pathway of one over another [39]. It was clearly observed that the selectivity toward hydrodeoxygenation increased with increasing PFAD fraction to 12 wt%, but decreased after exceeding 12 wt% PFAD. Previous studies on hydroprocessing of vegetable oil reported that the cause of the selectivity was depending on feeds, reaction pressure, reaction temperature, and different types of catalyst used [27]. In this case, the major factor was temperature due to the heat effect described earlier. The temperature rise at the reactor bottom temperature rendered the selectivity toward decarbonylation and decarboxylation. Both pathway cannot be distinguished due to the equilibrium between CO, CO_2, H_2, and H_2O as water gas shift reaction and reversed water gas shift reaction. Qualification of CO and CO_2 was able to determine but the methanation of CO and CO_2 were inevitable that resulted in a difficult analysis.
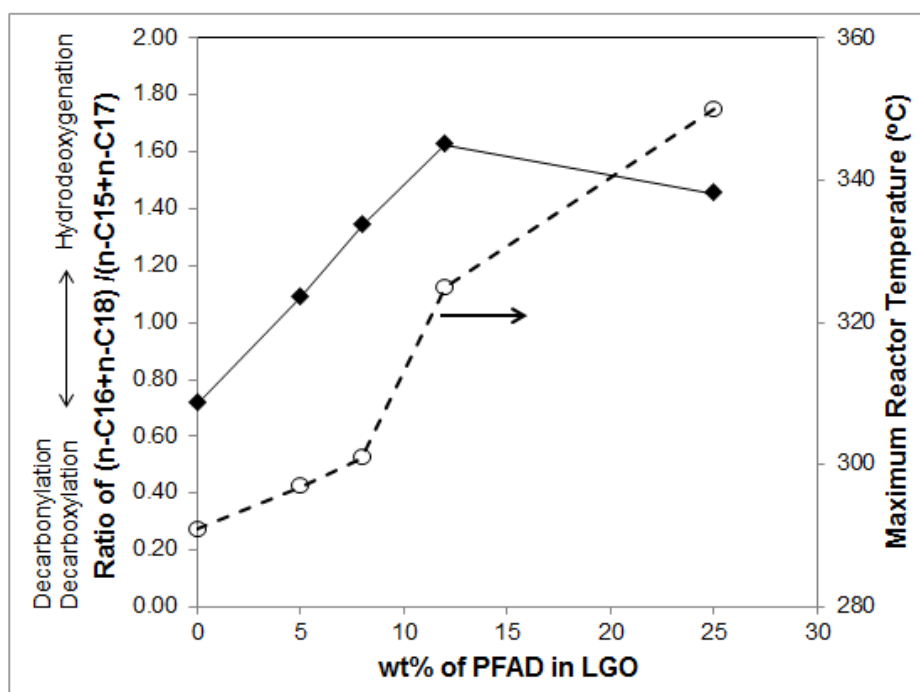
Figure 5.7   The ratio of (n-C16 + n-C18) over (n-C15 + n-C17) and the average reactor bottom temperature as a function of PFAD in LGO

5.2.6 Hydrogen consumption

Actual amount of hydrogen consumption have not yet been studied in academic research level. The amount and cost of hydrogen was an importance factor to make a decision for a process feasibility study in hydroprocessing of fats and oils derivatives. It should be noted many studies have been performed in oil refining section since hydrogen is a by-product from refineries. Thus, other sources of hydrogen production are more expensive. A standalone process without cheap hydrogen source could not be feasible for investment.

Hydrogen consumption during co-processing was recorded by an existing coriolis flow meter (Endress+Hauser). The system pressure was maintained by making up fresh hydrogen stream at the suction drum of the compressor at 12 barg, while the purged hydrogen-lean stream controlled hydrogen purity at least 70 vol%. **Figure 5.8** showed the amount of total hydrogen consumption based on the volumetric make-up

rate to the process under an influence of PFAD fraction in the feed mixtures. The consumption trend was a linear relationship with the amount of PFAD that could be extrapolated to obtain the consumption of only PFAD. Surprisingly, by extrapolation, PFAD require 344 Nm^3/m^3 to hydrogenate and deoxygenate to normal alkane at least 98 % conversion, while only 300 Nm^3/m^3 was theoretically enough to converting PFAD to normal alkane via totally hydrodeoxygenation and deoxygenation. The theoretical consumption could be comparable to the calculated consumption by Guzman et.al [24]. An extra 44 Nm^3/m^3 could be due to (1) inevitable reactions, e.g. methanation, water gas shift, and (2) the purged gas stream for maintaining hydrogen purity in the hydrodesufurization unit to at least 70 vol% in the returned gas stream before it was recompressed to the reactor. Egeberg et al. suggested that the additional of hydrogen amount might be varied between 20-35 Nm^3/m^3 due to the CO-methanation[24, 37].

จุฬาลงกรณ์มหาวิทยาลัย

CHULALONGKORN UNIVERSITY
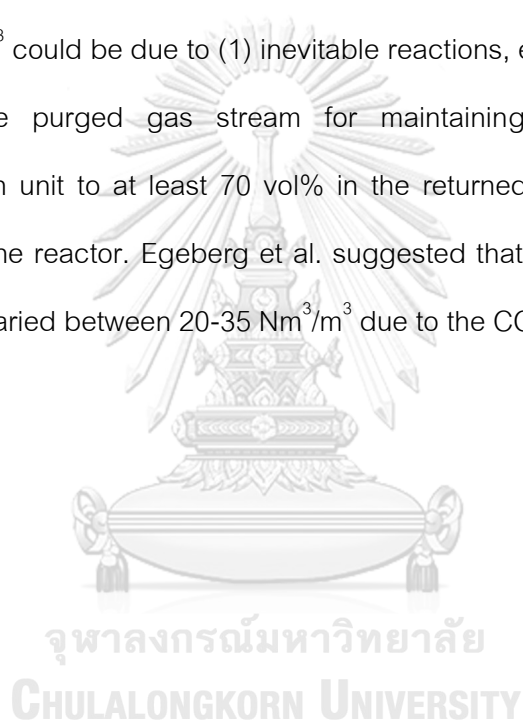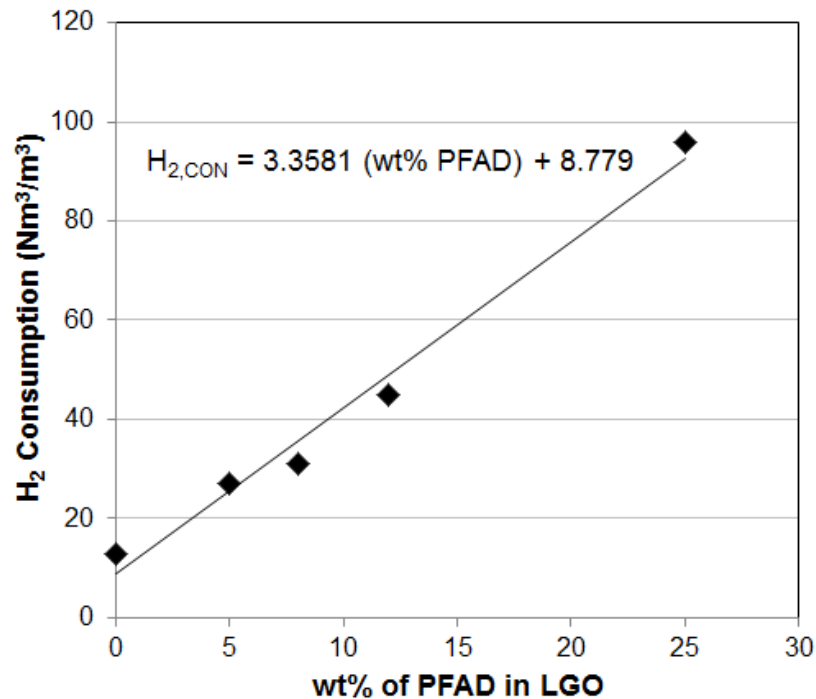
Figure 5.8   Average Hydrogen Consumption (Nm^3/m^3) as a function of PFAD in LGO

By Theoretical Calculation: H_2 consumption for 100% PFAD = 300 Nm^3/m^3

By extrapolated in experiment: H_2 consumption for 100% PFAD = 344 Nm^3/m^3

H_2 consumption for 100% LGO = 14.3 Nm^3/m^3

In economic point of view, hydrogen consumption for PFAD was about 24 times higher than that of hydrotreating of LGO (14.3 Nm^3/m^3). According to a recorded cost of hydrogen by Verasuwan Co.,ltd, 26 Baht/m^3 at STP was charged. The calculation of the hydrogen cost for only deoxygenation of PFAD was as following.

Cost of H_2 per m^3 of PFAD   = 344 Nm^3/h x 26 Baht/Nm^3 = 8,944 Baht/Nm^3 of PFAD

Cost of H_2 per m^3 of hydrotreating 25 wt% PFAD in LGO   = 97 Nm^3/h x 26 Baht/Nm^3

= 2,522 Baht/Nm^3 of feed

Price on May 31, 2018: Ex-refinery diesel = 19 Baht/liter, Hydrogen = 26 Baht/Nm^3

PFAD = 15 Baht/kg (13.5 Baht/liter)

The cost PFAD including cost of hydrogen was exceed ex-refinery price of diesel. Competitiveness between environmental-friendly fuel versus incentive price should be supported by the government of that country. If the government did not subsidize the fuel price and reduce tax, the hydroprocessing PFAD with LGO could be not be feasible at all.

According to **Table 5.2**, hydrogen consumption for double hydrogenation of fatty acid chain was taken into account of 15 % (0.53 / 3.53) of total amount of the theoretical consumption. This amount was a key factor for predicting economics of co-processing PFAD in LGO in hydrotreating unit. Thus, it could be concluded that higher saturated fatty acid feed was favorable as it could minimize hydrogen consumption and heat effect. An optimization of double bond, and heat effect should be considered. Heat effect also resulted in the favor of decarbonylation and decarboxylation over hydrodeoxygenation, higher hydrogen consumption, but providing better cold properties, and deoxygenation conversion. Consequently, a trade-off between product quality, hydrogen consumption, process safety, and gas purification cost should be carefully studied prior to an investment in renewable diesel production.

5.3 Model study of PFAD with model light gas oil

Previous studies (5.1 and 5.2) had been already proved that the production of renewable diesel by the co-processing of PFAD with LGO in pilot-scale hydrotreating unit over commercial catalyst and moderate hydrotreating conditions was achievable. Consequently, an expectation of co-processing for longer time on stream was a final expectation with safety, cost effectiveness, and economical feasible. As a result, several issues had been raised by an operation team working with the pilot unit as following.

- The deactivation of the catalyst at this operating condition over prolonging time on stream e.g. up to 10 days should be depicted since the catalyst deactivation and renewal would be costly for an investment.

- High conversion of both deoxygenation and desulfurization was already observed at 285 $^{\circ}$C and above. The reaction at lower temperature should be illustrated as it could be occurred during starting up and shutting down the hydrotreating unit, as well as the catalyst locating near the reactor wall where heat loss occurred.

- Lowering reaction temperature might not be possible to achieve enough activities and/or resulting in faster catalyst deactivation.

- What would be the desulfurization activities during deoxygenation of PFAD?

- Importance of hydrogen sulfide or sulfur in light gas oil. What would be the effect of lean-sulfur-containing feedstock.

- Pressure drop of the reactor was fairly observed as increasing with PFAD in pilot-scale unit, and the fired heater. The pressure drop might not be increases due to time and reactor size, but in a smaller scale, and prolonging time.

- How to reactivate the deactivated catalyst? Could the pre-sulfiding step be applied to reactivate the catalyst? Which condition was suitable and the amount sulfur.

- Quenching of feed or hydrogen might reduce heat effect and kept the co-processing safely.

A model study for PFAD in LGO over commercial CoMo/Al$_2$O$_3$ was then suggested. Palmitic acid 99 wt%, refined bleached and deodorized palm oil (RBDPO), 4,6-dimethyl-dibenzothiophene (4,6-DMDBT), and n-octadecane (n-C18) were prepared

as model PFAD in sulfur-containing LGO. The reaction was conducted in a laboratory-scale reactor, ½ inch reactor, isothermal controlled reaction at 275 $^{\circ}$C, 25 barg, liquid hourly space velocity = 1.7 h^{-1}, and hydrogen to oil = 630 NL/L. The catalyst used in this study was a commercial CoMo/Al$_2$O$_3$.

5.4.1 Effect of reaction temperature on both activities

At first, the reaction temperature was controlled at 300 $^{\circ}$C. A complete conversion of both deoxygenation of palmitic acid and desulfurization of 4,6-DMDBT was observed as shown in **Figure 5.9**. At lower reaction temperature, the extent of the analysis in the activity changes could be clearly observed. The reaction temperature was conducted at 275 $^{\circ}$C which was about 10 $^{\circ}$C lower than the inlet temperature of the pilot-scale experiment (285 $^{\circ}$C). It could be implied that at deoxygenation of PFAD in pilot-scale was already reached complete conversion at the only half of the catalyst bed. The rest of the catalyst bed in the pilot-scale reactor was not responsible for deoxygenation. Reduction of temperature can imply that the decrease of the reaction temperature had negative impact on desulfurization of 4,6-DMDBT than deoxygenation of palmitic acid.
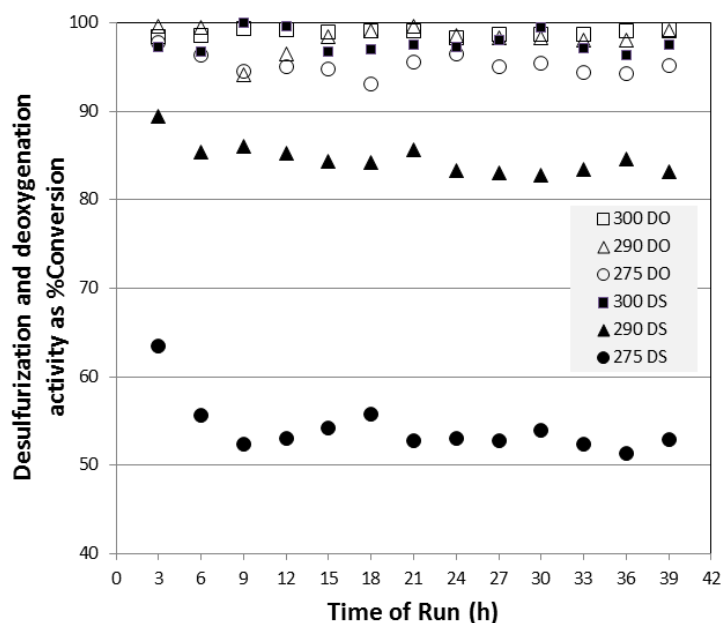
Figure 5.9   Desulfurization of 4,6-DMDBT and deoxygenation of 10 wt% palmitic acid at different temperature, 25 barg, LHSV = 1.7 h^{-1}, and H$_2$ to oil = 630 NL/L.

5.4.2 Effect of palmitic acid

Palmitic acid was selected as a model compound representing commercial PFAD which containing large amount of palmitic acid up to 45-50 wt%, according to **Figure 5.10**. The presence of palmitic acid from 0, 5, and 10 wt% in a mixture 180 ppmw of 4,6-DMDBT in n-C18 decreased desulfurization of 4,6-DMDBT. The negative effect of palmitic acid on desulfurization was higher when increasing palmitic acid from 10 wt% to 20 wt%. The relationship of palmitic acid and decrease in desulfurization was not in a linear. Competitive adsorption of palmitic acid over 4,6-DMDBT could be suspected to be a cause of such reduction. The similar result was observed by Viljiva et al. during desulfurization of mercaptobenzene in CoMo/Al$_2$O$_3$, the strong adsorption of phenol molecule was reported to be a competitor [67]. However, the effect of palmitic acid on desulfurization was partially recoverable after discontinued feeding palmitic acid or reducing to 10 wt% at 144 and 180 h of time on stream. This result was comparable to the study by Templis et al. that desulfurization of gas oil-palm oil mixture was decreased

with up to 5% palm oil, but further change was not observed when increasing palm oil to 10% [1]. Water was also considered as an important factor responsible for the decrease in desulfurization. Significant water amount was clearly observed in products, and it was increased with increasing palmitic acid in model feed. Reversible effect could be from water which is a by-product from deoxygenation of palmitic acid via hydrodeoxygenation, decarbonylation, reverse water gas shift, and methanation. Water adsorption was considered as a weak inhibition, and a weak adsorption onto the sulfide phase of the CoMo catalyst [63, 64]. The strength of water adsorption decreased with increasing temperature.

Moreover, some studies observed the decrease in the desulfurization rate. This could be due to (1) the impurities in the feedstock itself, (2) the strong adsorption of oxygen-containing molecules or by-product from the side reactions to some catalyst active sites and blocking pores, and (3) gradual leaching of sulfur, metal oxidation, and metal leaching of active site [27, 37, 48, 68].
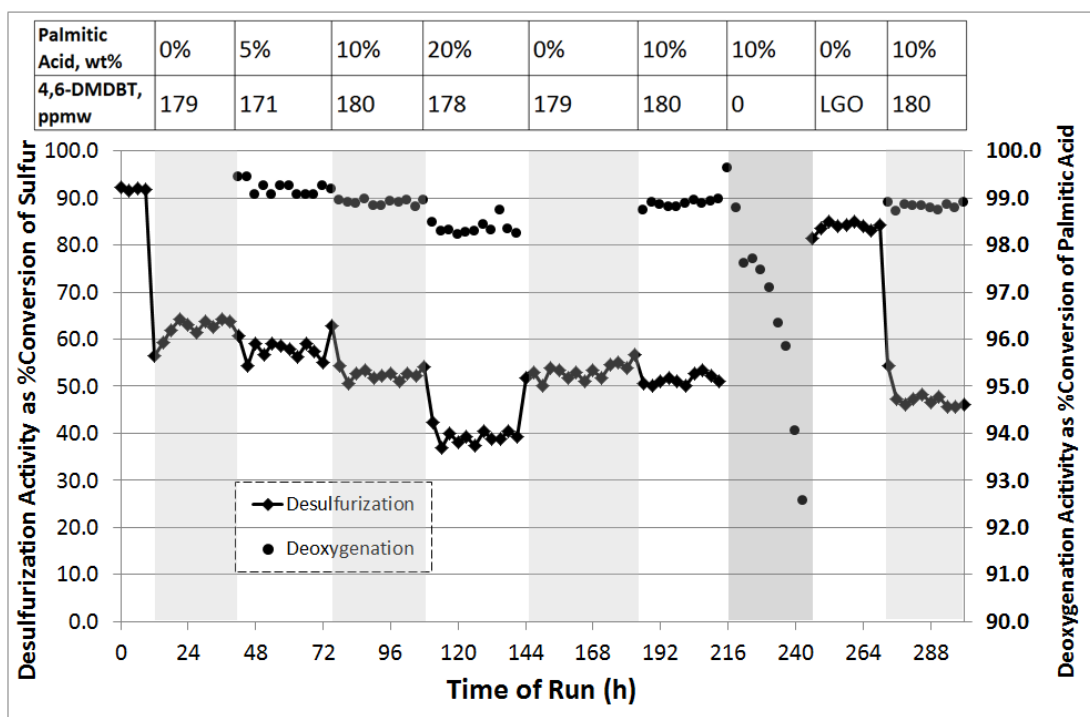
Figure 5.10   Desulfurization and deoxygenation activities in various fraction of palmitic acid while co-processing with 4,6-DMDBT and n-C18 as model sulfur-containing light gas oil.

5.4.3   Effect of 4,6-DMDBT

Deoxygenation of palmitic acid could be maintained by the presence of 4,6-DMDBT. Very slight deoxygenation of palmitic acid was observed at high conversion range (> 95%). According to **Figure 5.10**, the absence of 4,6-DMDBT at 216 h severely depressed palmitic deoxygenation within 24 h to 92% conversion. The sample at 230 h of time on stream was black, sticky, and free of any water droplet. Physically, this was totally different from those of previous conditions. Bright and clear with slight yellowish with some droplets of water was observed. Moreover, the pressure drop between feed inlet and outlet was recorded by a "Azbil" differential pressure transmitter shown in **Figure 4.2**. It was observed that the pressure raised 4 times (at 240 h) than normal operation which co-processing 4,6-DMDBT as evidence by **Figure 5.11**. The pressure drop was reached as much as 0.22 bar. The amount of FFAs was higher than 0.7 wt%

as palmitic acid, and quantification of heavier components was observed by gas chromatography technique. Black and sticky sample was collected at 254 h of time on stream. Due to the limitation of chromatography separation, it was unable to qualify the species of heavy products. It could be concluded that heavy components were free fatty acids, alcohols, and long chain esters from acids and alcohols [49, 68]. The reactor temperature was such low range (< 300 ^{o}C) that not enough to activate deoxygenation reaction, but stimulate alcohol-forming hydrogenation of carboxylic acids which then later reacted to form esters. The initiation of esterification to esters, and polymerization to ketones as side reaction could be occurred at lower temperature due to lower activation energy. The formation of by-products from the esterification and polymerization was so heavy that can block the catalyst pore, glass wool, and glass bead, resulting to an increase in the pressure drop across the reactor. Lacking of sulfur in the catalyst site could reduce a sulfide state on active site that was readily to deoxygenate palmitic acid than desulfurize 4,6-DMDBT. The presence of 4,6-DMDBT would then certainly stabilized deoxygenation activity of palmitic acid as the deoxygenation was recovered by the co-processing of sulfur-containing LGO and 4,6-DMDBT after 254 h of time on stream. The recovery of deoxygenation of palmitic acid was almost totally regained, but that of desulfurization was only partial. After the catalyst was reactivated by LGO, The product from 10% palmitic acid and 180 ppm of 4,6-DMDBT was clear, colorless, and containing a few droplets of water. The addition of sulfur in various forms, e.g. hydrogen sulfide (H$_2$S) in gas phase, dimethyl-disulfide (DMDS), and tetra-butyl-amine (TBA) assisted the readiness of the catalyst activity by preserving sulfided state on the catalyst surface during the reaction [41]. Pulsing and continuously fed DMDS to maintain rapeseed oil deoxygenation was studied by Kubicka et al. An addition of DMDS 0.5 wt% improved the catalyst stability by replenishing the depletion of sulfur from the catalyst active site, and the addition of DMDS by pulsing could partially restore deoxygenation

activity [48].

Palmitic Acid, wt%	0%	5%	10%	20%	0%	10%	10%	0%	10%
4,6-DMDBT, ppmw	179	171	180	178	179	180	0	LGO	180
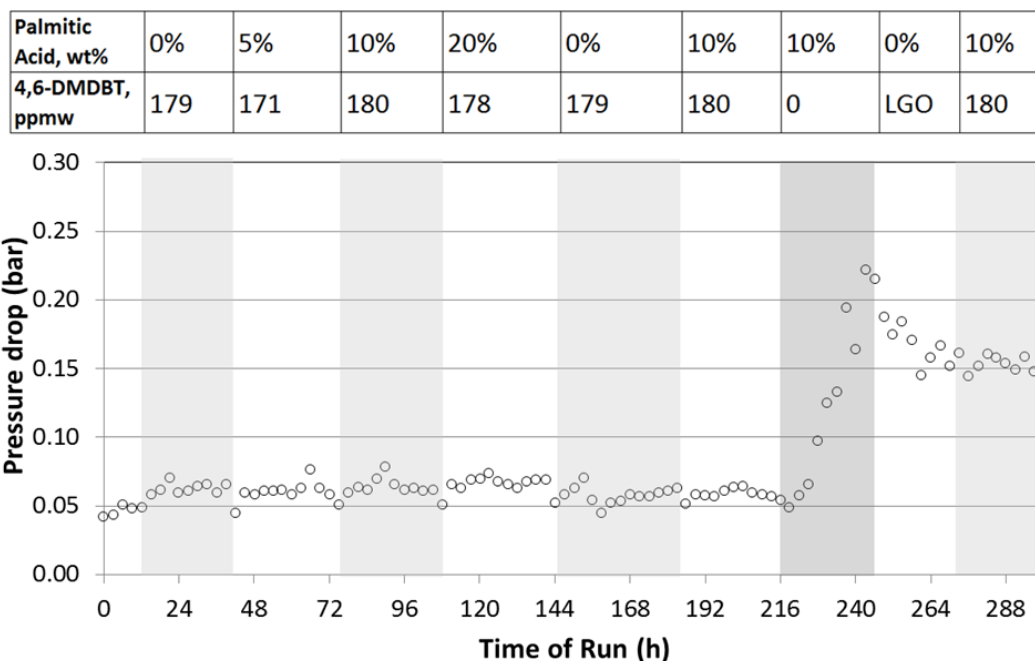
Figure 5.11   Pressure drop profile in various fraction of palmitic acid while co-processing with 4,6-DMDBT and n-C18 as model sulfur-containing light gas oil.

Processing of LGO could increase the deoxygenation after it was decreased due to lacking of sulfur. However, the reactor pressure drop was not reduced to normal. It was drop to only 0.15 bar and stable as shown in **Figure 5.11**. This must be taken into consideration for a safety of process pressure and maximum reactor pressure. The cause was those heavier products that were blocking catalyst porosity, a pack of glass wool, and a pack of glass beads underneath the catalyst bed. The blockage above the catalyst bed was not observed. These were evidenced during cleaning the reactor after the experiment. Significant amount of polymerized material trapped inside the stack of glass beads which was located underneath the pack of glass wool, and difficult to be pulled out.

The presence of sulfur as 4,6-DMDBT could answer the conditions which a revamping of the process would be implemented to improve the heat effect. A

quenching of reaction product by either fresh a hydrogen stream or renewable feed would result in low-sulfur reaction conditions. The hydrogen quenching stream was not only reduce heat effect but also making-up large hydrogen consumption so as to avoid hydrogen lacking due to deoxygenation and hydrogenation of PFAD. High refractory sulfur species containing in feed mixture, e.g. heavy gas oil, vacuum gas oil, etc. should be avoided as the desulfurization activity was actively effective at higher temperature (> 300 oC). Desulfurization of sulfur species would then result in stabilizing deoxygenation. . Significant amount of sulfur in feedstock should be considerable to maintain both catalyst activities. In this study, it was obviously found that at least 100 ppmw sulfur from desulfurized 4,6-DMDBT was enough to maintain the catalyst activity and 85% conversion of LGO containing 484 ppmw sulfur was adequate. Moreover, a starting up and a shutting down operation with lower reaction temperature with co-feeding mixture should be avoided since complete desulfurization of LGO might not enough to stabilize sulfided form of the catalyst.

5.4.4 Catalyst deactivation and reactivation

The catalyst was observed as slightly deactivated after 48 h of time on stream at 275 $^{\circ}$C, while, at higher temperature, the significant deactivation was initially observed over 120 h of time on str 8eam. The study of catalyst deactivation was renewed every experiment separately as shown in **Figure 5.12 (a) to (d)**. Deactivation of desulfurization was observed significantly over 200 h of time on stream, while the deactivation of palmitic deoxygenation was not shown due to the reduction at less than 5%. Desulfurization of 4,6-DMDBT could be recovered by the absence of palmitic acid, and the presence of low refractory sulfur-containing compound, in this case, dimethyl disulfide (DMDS), and LGO. The feedstock was switched to that of each cases (a) 2 wt% DMDS in n-C18 at the same reaction conditions, (b) light gas oil with 484 ppmw of

sulfur at the same conditions, (c) 2 wt% DMDS in n-C18 at 320 $^{\circ}$C, and (d) light gas oil with 484 ppmw of sulfur at 320 $^{\circ}$C. The co-processing of 2 wt% DMDS in model LGO could slightly improve catalytic desulfurization of 4,6-DMDBT, but largely improved when increasing reaction temperature up to 320 $^{\circ}$C, the same as pre-sulfiding condition. Slighly improvement of desulfurization was also observed when reactivation was done by processing LGO. Increasing of reactivation temperature was also benefit to the reactivation step as initial conversion of desulfurization of 4,6-DMDBT after reactivation by DMDS (c) and LGO (d) was comparable, but the deactivation profiles was clearly different. The reactivation by 2 wt% DMDS in n-octadecane provided the most effective among the others that almost 80% desulfurization conversion can be recovered. It can be concluded that type of sulfur-compounds were a key to the recovery of deactivated catalyst. Higher temperature provided better reactivation results due to the fact that high temperature supports the thermal decomposition of DMDS at S-S and C-S bonds to various radicals for sulfiding onto the catalyst surface [69]. To be more effective, DMDS injection might be the most effective among the other activation steps since DMDS is a commonly-used sulfiding agent for hydrotreating /hydrodesulfurization catalysts.
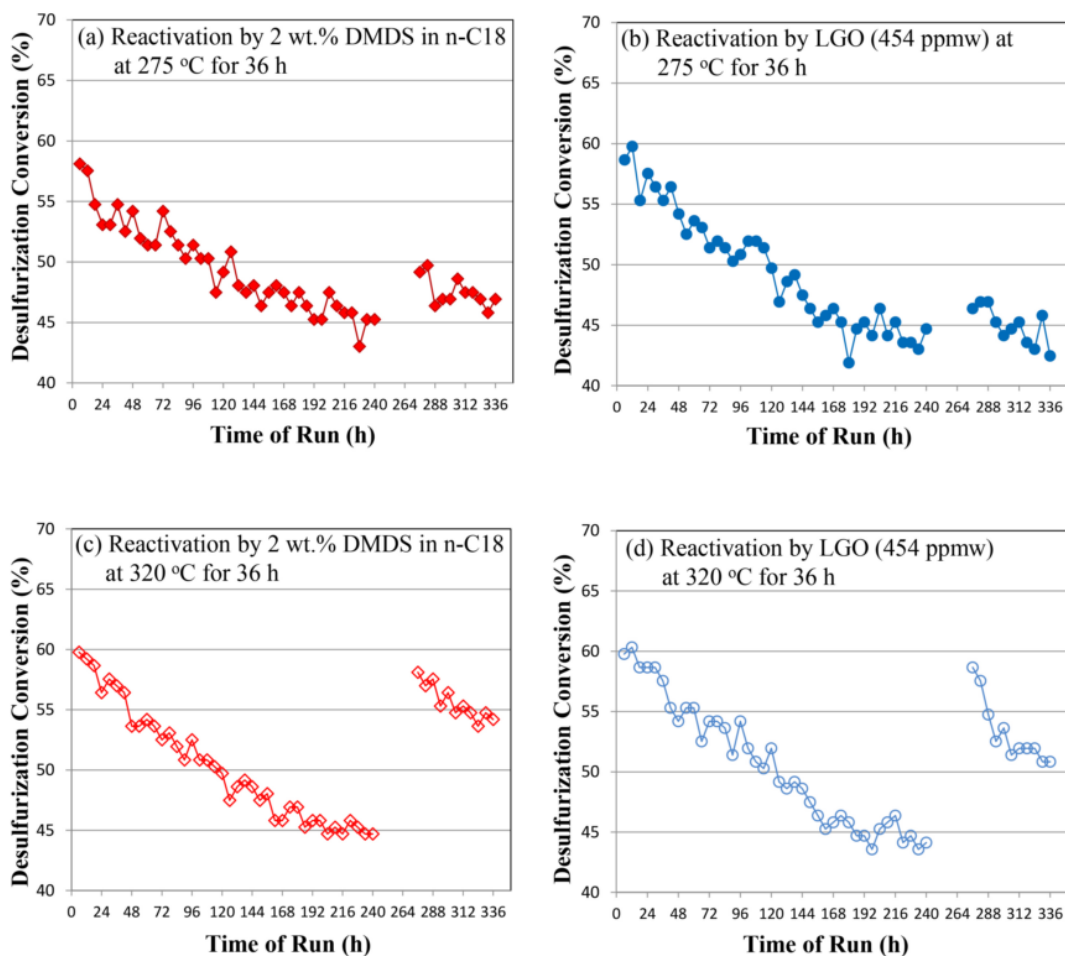
Figure 5.12 The catalyst deactivation profiles with different reactivation techniques of reactivation performing after 240 h.

5.4.5 Effect of pretreated feed by hydrogenation

Palmitic acid had already showed a detrimental impact on desulfurization of 4,6-DMDBT, while deoxygenation of palmitic acid was surprisingly stable at high conversion in the presence of 4,6-DMDBT at low temperature, 275 $^\circ$C. The cause of the catalyst deactivation has not been evidently investigated, and model study of palmitic acid might not dedicate enough for the studying of catalyst deactivation over prolonging time on stream. In this case, the model component was palmitic acid and a synthetic mixing of palmitic acid with refined bleached and deodorized palm oil (RBDPO) as model PFAD. The amount of 20 wt% of model PFAD in model LGO was experimented. Additional

pretreating feedstock was performed in this step. Hydrogenation of RBDPO and PFAD in batchwise for 6 h was to saturate double bond at fatty acid chain. The pretreating reaction was conducted at 150 $^{\circ}$C, 6.5 barg, W/F = 2.0 g of catalyst /100 g of oil, and under hydrogen pressure over commercial nickel on synthetic silicates as a carrier.

As shown in **Figure 5.13**, deoxygenation of palmitic acid was the least deactivated. A mixture of 90 wt% palmitic acid and 10 wt% refined bleached and deodorized palm oil (RBDPO) abbreviated as 90PA+10PO resulted in higher decreasing deoxygenation over prolonging time than co-processing with palmitic acid at the same conditions. The deoxygenation of 20 wt% PFAD provided the worst deactivation of deoxygenation. Moreover, palmitic acid and hydrogenated palm oil (90PA+10HPO) and hydrogenated PFAD (H-PFAD) resulted in less deactivation of deoxygenation over time on stream when compared to that of non-hydrogenated feed. According to **Table 5.5**, result of iodine value confirmed that the degree of double bond was almost completely reduced for hydrogenated RBDPO and PFAD, while amount of fatty acid content and other impurities were similar. Consequently, it could be depicted that deactivation of deoxygenation was certainly related to unsaturation of fatty acid in the model feeds.
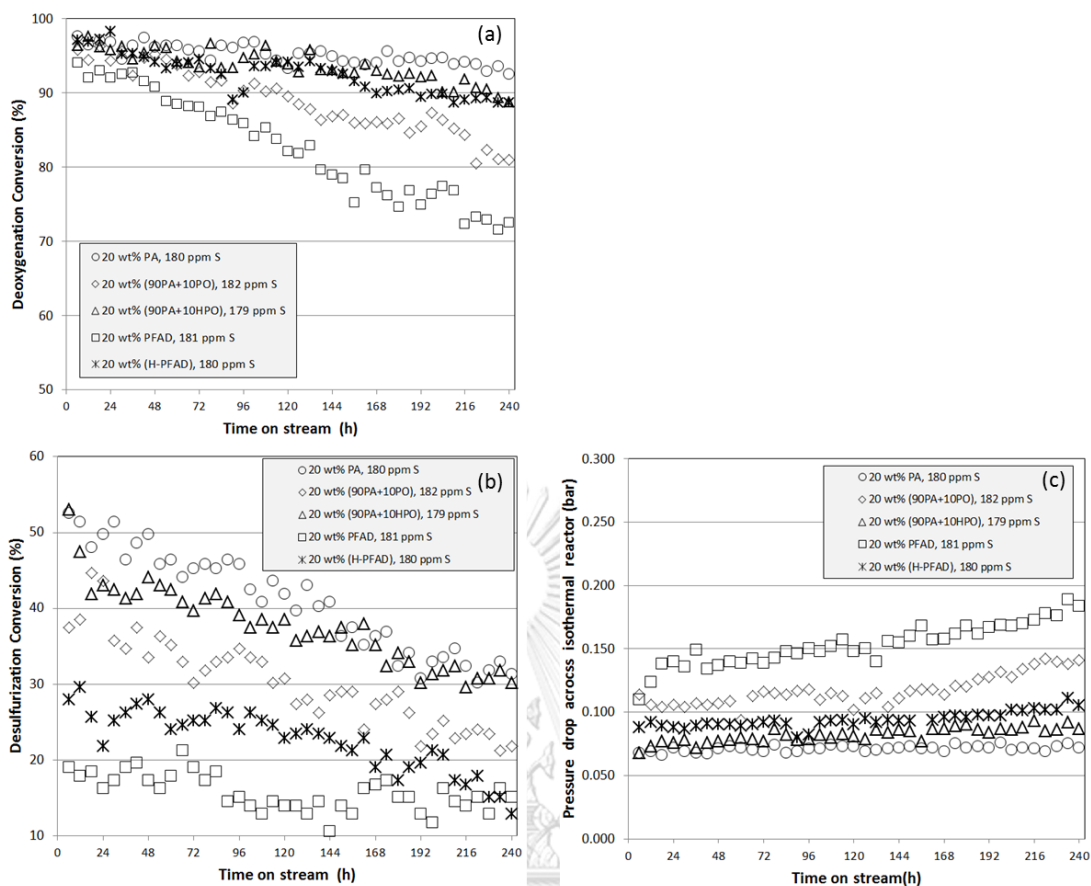
Figure 5.13 (a) Deoxygenation, (b) desulfurization, and (c) pressure drop various model feeds over isothermal reactor at 275 $^{\circ}$C, 25 barg, LHSV = 1.7 h^{-1}, and H$_2$ to oil = 630 NL/L.

○: 20 wt% of palmitic acid and 180 ppm of 4,6-DMDBT in n-C18;

◇: 20 wt% of a mixture of 90 wt% palmitic acid and 10 wt% RBDPO with 182 ppm of 4,6-DMDBT;

Δ: 20 wt% of a mixture of 90 wt% palmitic acid and 10 wt% hydrogenated RBDPO with 179 ppm of 4,6-DMDBT;

□: 20 wt% of palm fatty acid distillate with 181 ppm of 4,6-DMDBT;

✳: 20 wt% of hydrogenated palm fatty acid distillate with 180 ppm of 4,6-DMDBT;

Table 5.5 Composition and properties in feeds

Feed	Abbreviate	Fatty acid content (wt%)	Iodine Value (g/100g)	Water Content (ppm)	Sodium (mg/kg)	Phosphorus (mg/kg)
Palmitic acid	PA	99.13	< 2	147	2.7	< 0.5
Refined Bleached and Deodorized Palm oil (RBDPO)[a]	PO	0.22	47.56	869	3.2	0.64
Hydrogenated RBDPO	HPO	0.37	1.15	744	3.1	0.41
90% Palmitic acid + 10% RBDPO	90PA + 10PO	89.80	4.71	202	N.D.	N.D.
90% Palmitic acid + 10% H-RBDPO	90PA + 10HPO	91.64	1.74	191	N.D.	N.D.
Palm Fatty Acid Distillate (PFAD)	PFAD	89.44	42.85	1254	4.2	< 0.5
Hydrogenated PFAD	H-PFAD	92.54	0.78	1157	3.9	< 0.5

(a) no addition of anti-oxidants for commercial product
N.D. = Not determined

5.5.1 Effect of pretreatment on activity and pressure drop

Previous experiment (5.2.2) showed that heat effect expressively affected deoxygenation activity in co-processing of PFAD in LGO in pilot-scale unit, and the pretreatment of PFAD by hydrogenation can lower rate of deactivation of desulfurization of 4,6-DMDBT. In this step, the laboratory-scale reactor was modified as shown in **Figure 4.3**. The reactor was separated to heating section and adiabatic reaction section in order to observe the cause of the catalyst deactivation. Two differential pressure transmitters were installed to observed pressure drop across each section.

Increasing pressure drop was observed as shown in **Figure 5.13 (c)**. For 10 days, the increase in the pressure drop in the non-modified isothermal reactor was observed in the order PFAD > 90PA+10PO > H-PFAD > 90PA+10HPO > palmitic acid. Then, pre-treatment of the feedstock by complete hydrogenation of double bond (lower iodine value) was resulted in a plausible solution to minimize pressure surging for prolonging time on stream and improve catalyst deactivation. Slow to moderate deactivation of deoxygenation closer to ideal feed, palmitic acid, and hydrogenated feed resulted in higher activity of both deoxygenation and desulfurization 4,6-DMDBT. It could be suspected that the degree of unsaturation of fatty acid chain resulted in significant catalyst deactivation over prolonging time since deoxygenation of

unsaturated fatty acid can lead to catalyst coking [64]. An affirmation was found during cleaning up the reactor. Significant polymerized substances deposited on the top of the catalyst layer, and high pressure difference was observed in the case of PFAD and 90PA-10PO, while an increase in the reactor pressure drop was not significantly observed in the case of palmitic acid as shown in **Figure 5.13 (c)**. GC-FID result also showed a very little amount of heavy component in products from non-hydrogenated feeds than hydrogenated feeds.

The modification of the reactor by splitting the reactor and heating zone was performed in order to investigate the major cause of catalyst deactivation and pressure drop surging. The modified reactor also depicted the commercial hydrotreating /hydroprocessing reactors which are generally comprised of direct fired heaters to increase feed temperature before charging feed stream to an adiabatic reactor. The heating section was loaded with 1.0 mm glass beads to increase turbulence flow followed by a lightly-packed glass wool at the bottom. Adiabatic section was packed with the catalyst and other layer as the same as the isothermal reactor. By calculation, the retention of liquid feed in heating zone was about 15 min which is comparable to the commercial hydrotreating unit. The results of the pressure drop across heating and reaction sections were plotted over time on stream as shown in **Figure 5.14 (a), (b) and (c)**. Developing pressure drop across the heating section was obviously found increasing rather than that across adiabatic section. The heating section was maintained at 275 ^{o}C measured at the outlet stream. The increase in pressure drop across heating section supported that unsaturated fatty acid in non-hydrogenated feed can cause significant polymerization product even at low temperature, 275 ^{o}C, when the feed was subjected to heat at a certain time. Polymerized substance was found to be retained in heating section prior to adiabatic section. In addition, it was observed that the pressure

rises in the heating section was increased with increasing iodine value in feed in the order 90PA+10HPO, 90PA+10PO, and PFAD. Consequently, deoxygenation and desulfurization activity was significantly improved after splitting the reactor to two sections. The comparison of deoxygenation and desulfurization of 20 wt% palm derivatives in model LGO was shown in **Table 5.6**.

Table 5.6   Comparison of activity and reactor parameters at 204 h of time on stream

Feed	Palmitic acid	90PA+10PO	90PA+10HPO	PFAD	H-PFAD
SYMBOL in Fig.5, 6	O	◇	Δ	□	✳
Isothermal Reactor					
Deoxygenation (%)	94.8	86.3	89.9	77.4	89.9
Desulfurization (%)	33.5	25.1	31.8	16.2	20.7
ΔT (°C) [a]	-2.0	-1.7	-2.2	-1.6	-0.9
ΔP (bar) [b]	0.070	0.128	0.086	0.168	0.102
Color (ASTM D1500)	< 0.3	0.65	< 0.3	1.01	< 0.3
Carbon on Spent Cat	9.87	11.27	9.91	14.54	12.02
Adiabatic reactor					
Deoxygenation (%)	-	94.1	95.4	82.1	92.3
Desulfurization (%)	-	32.4	34.2	27.6	30.1
ΔT (°C) [a]	-	1.4	-1.2	3.2	-0.6
ΔP (bar) [b]	-	0.074	0.042	0.078	0.068
Color (ASTM D1500)		< 0.3	< 0.3	0.72	< 0.3
Carbon on Spent Cat. (wt%)		10.56	9.77	10.79	10.46

(a) ΔT = Tin-Tout

(b) ΔP = Pin-Pout

(c) determined after 240 h time of run
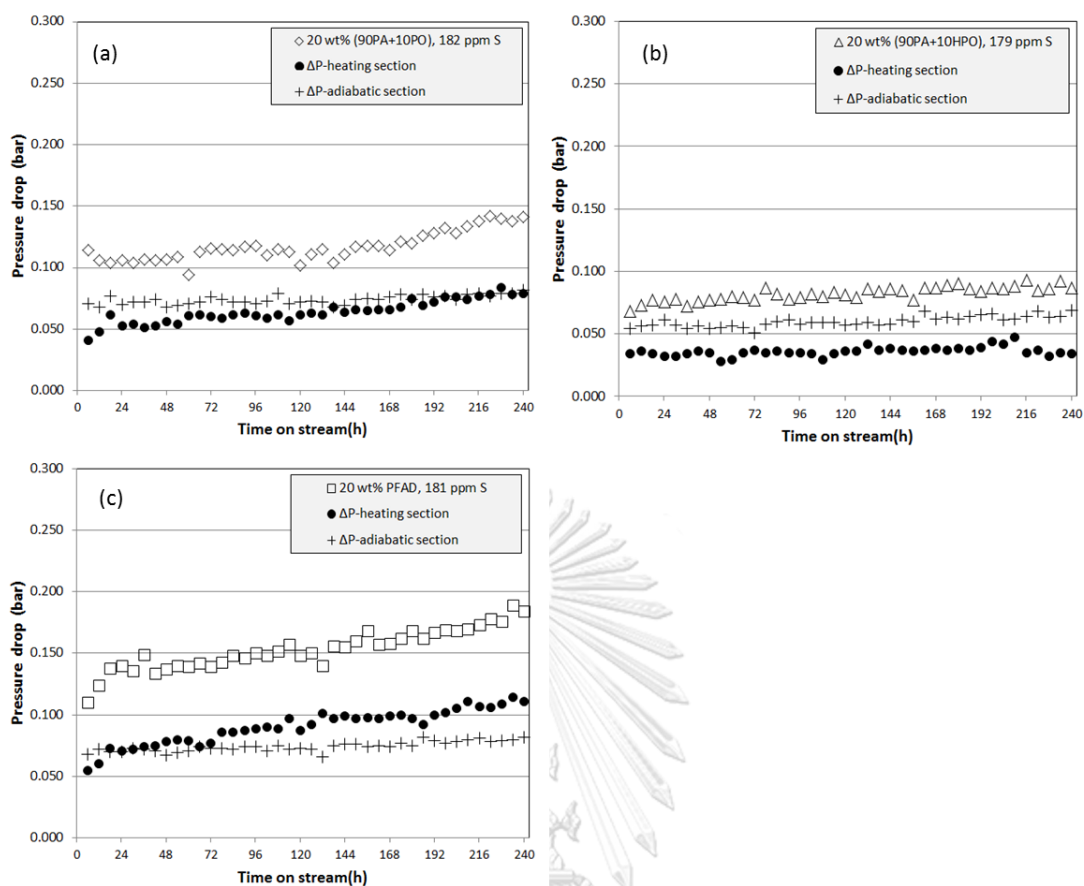
Figure 5.14   Comparison of pressure drop profile across the isothermal reactor versus that across heating section and adiabatic section of the modified reactor when processing

(a): ◇ 20 wt% of a mixture of 90 wt% palmitic acid and 10 wt% RBDPO with 182 ppm of 4,6-DMDBT;

(b): △ 20 wt% of a mixture of 90 wt% palmitic acid and 10 wt% hydrogenated RBDPO (HRBDPO) with 179 ppm of 4,6-DMDBT;

(c): □ 20 wt% of palm fatty acid distillate (PFAD) with 181 ppm of 4,6-DMDBT;

Lower catalyst deactivation was observed in the case of 90PA+10PO with a modification of the reactor that both activities were improved. The improvement of both activities was closer to that with ideal palmitic acid at the same time on stream. The color of products from adiabatic reactor was changed to brighter and clearer as an evidence of less formation of polymerized components. The effect of unsaturation degree on catalyst coking and deactivation was supported with the model study by Bartosz et al [70]. The cause of catalyst deactivation was mainly due to polymerization of unsaturated feed at certain time and temperature rather than in-situ decarboxylation of unsaturated fatty acid to form coking [71]. Moreover, carbon depositions on the catalysts were significantly lowered after feeding pretreated feed mixture. Consequently, the removal of the polymerized substance by separated the heating and the adiabatic reaction section reduced carbon deposition on to the spent catalysts resulting in declining of catalyst deactivation over prolonging time.
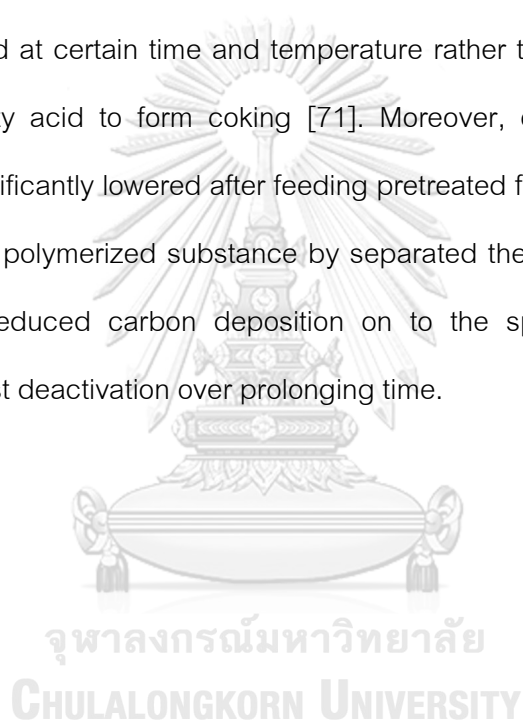
CHAPTER SIX

CONCLUSION

Co-processing of PFAD up to 25 wt% with sulfur-containing LGO in commercial hydrotreating unit can produce 'a drop-in' renewable diesel. The presence of PFAD affected the reaction temperature at the outlet of the pilot-scale reactor due to the heat effect including double bond hydrogenation, and CO/CO_2 methanation. By the studied reaction conditions in the pilot unit, desulfurization and deoxygenation activity were already sufficient to provide qualified renewable diesel following EN 590:2004 (Sulfur limited to 50 ppm, so called Euro 4). Contribution of total n-paraffin from PFAD at higher PFAD was observed as a result of hydrocracking and isomerization reaction of n-paraffin due to the increase in reaction temperature. Cetane index of the products was depending on the amount of PFAD in feed mixture and interestingly boosted as much as 67 at 25 wt% PFAD. This was due to the lower density of major hydrocarbon products, n-C15 to n-C18. The hydrogen consumption was shown a linear function of PFAD in LGO, but not depending on the reaction temperature. Extrapolation of the consumption observed large amount of hydrogen for hydroprocessing PFAD of 344 Nm^3/m^3, while only 300 Nm^3/m^3 was the theoretical amount according to the distribution of fatty acid chain in PFAD. The extra consumption might be from CO and CO_2 methanation, reverserd water gas shift reaction, and purged gas line to balance hydrogen purity.

In the model study, the presence of palmitic acid representing a major component in PFAD in model LGO adversely affected desulfurization of 4,6-DMDBT. Further impact was found when increasing palmitic acid from 10 to 20 wt%, while only slight decrease in desulfurization of 4,6-DMDBT was observed in the case of 0 to 10 wt% of palmitic acid. Deoxygenation of palmitic acid greatly affected desulfurization of 4,6-DMDBT than vice versa, and the deoxygenation activity was stable at near complete

conversion (> 95 wt%) at 275 $^{\circ}$C. The effect of palmitic acid to desulfurization of 4,6-DMDBT was reversible deterioration, while the presence of 4,6-DMDBT was benefit to stabilize deoxygenation of palmitic acid and the other palm oil derivatives. The cause of deactivation of deoxygenation and desulfurization was significantly observed due to the polymerization of unsaturated fatty acid chain in triglyceride at even low temperature. The pretreatment to lower polymerization of feed by hydrogenation of double bond delayed catalyst deactivation and reduced product color. In addition, the catalyst deactivation and the increasing pressure drop were due to the lacking of sulfur as 4,6-DMDBT which responsible to maintain sulfided state and maintain high deoxygenation activity. Significant desulfurization of 4,6-DMDBT was decreased after 10 days in the presence of palmitic acid. Then, the performance of the desulfurization could only be partially reactivated by processing 2 wt% DMDS in n-C18 at higher temperature up to 320 $^{\circ}$C. This was a favorable recovery and more practical than that with sulfur-containing LGO for commercial scale unit. The importance of the model study can elaborate as practical and foreseeing results for a refinery that is planning to utilize the existing hydrotreating unit to co-processing PFAD as a renewable feed

REFERENCES

1. Templis, C., et al., *Vegetable oil effect on gasoil HDS in their catalytic co-hydroprocessing.* Applied Catalysis B: Environmental, 2011. **104**(3-4): p. 324-329.

2. *Renewable Energy Technology Roadmap 20% by 2020. Report of the European Energy Council. November, 2008.*

3. Simakova, I., et al., *Decarboxylation of fatty acids over Pd supported on mesoporous carbon.* Catalysis Today, 2010. **150**(1-2): p. 28-31.

4. Barakos, N., S. Pasias, and N. Papayannakos, *Transesterification of triglycerides in high and low quality oil feeds over an HT2 hydrotalcite catalyst.* Bioresour Technol, 2008. **99**(11): p. 5037-42.

5. Vonortas, A., C. Templis, and N. Papayannakos, *Effect of Palm Oil Content on Deep Hydrodesulfurization of Gas Oil–Palm Oil Mixtures.* Energy & Fuels, 2012. **26**(6): p. 3856-3863.

6. KubiČková, I., et al., *Hydrocarbons for diesel fuel via decarboxylation of vegetable oils.* Catalysis Today, 2005. **106**(1-4): p. 197-200.

7. *Hydrocarbon Engineering.* 2007. **June**.

8. *Biodiesel and Other Renewable Diesel Fuels.* NREL, 2006(November).

9. Sotelo-Boyas, R., F. Trejo-Zarraga, and F.d. Jesus Hernandez-Loyo, *Hydroconversion of Triglycerides into Green Liquid Fuels.* 2012.

10. Holmgren, J., et al., *New developments in renewable fuels offer more choices - Vegetable oil-based diesel can offer better integration within crude-oil refineries for fuels blending.* Hydrocarbon Processing, September 2007.

11. Kalnes, T.N., et al., *Green diesel production by hydrorefining renewable feedstocks.* BIOFUELS TECHNOLOGY.

12. Bartholomew, C.H. and R.J. Farrauto, *Fundametal of Industrial Catalytic Processes.* WILEY-INTERSCIENCE, 2010.

13.   Topsøe, H., B.S. Clausen, and F.E. Massoth, *Kinetics and Mechanism of Model Compounds Reaction, Hydrotreating Catalysis Science and Technology.* 1996: p. 111-155.

14.   Chang, J.E.H., Y.K. Chang, and H.N. Chang, *Desulfurization of Dibenzothiophene and Diesel Oils by a Newly Isolated Gordona Strain , CYKS1.* Applied Environmental Microbiol, 1998. **64**(6): p. 2327-2331.

15.   Dharaskar, S.A., et al., *Extractive Deep Desulfurization of Liquid Fuels Using Lewis-Based Ionic Liquids.* Journal of Energy, 2013. **2013**: p. 1-4.

16.   Guan, Q. and W. Li, *The synthesis and evaluation of highly active Ni2P–MoS2 catalysts using the decomposition of hypophosphites.* Catalysis Science & Technology, 2012. **2**(11): p. 2356.

17.   Farrauto, R.J. and C. Bartholomew, *Introduction to Industrial Catalytic Processes* Chapman & Hall, London, UK, 1997.

18.   Hancsók, J., et al., *Production of bioparaffins by the catalytic hydrogenation of natural triglycerides.* Journal of Cleaner Production, 2012. **34**: p. 76-81.

19.   Veriansyah, B., et al., *Production of renewable diesel by hydroprocessing of soybean oil: Effect of catalysts.* Fuel, 2012. **94**: p. 578-585.

20.   Szukalska, E., *THE EFFECT OF TEMPERATURE DURING SOYBEAN OIL HYDROGENATION ON NICKEL CATALYST POISONING BY PHOSPHOLIPIDS.* POLISH JOURNAL OF FOOD AND NUTRITION SCIENCES, 2003. **12**(4): p. 19-23.

21.   *Kirk Othmer Encyclopedia of Chemical Technology, 2nd Edition.* 1964: p. 776-785.

22.   Chapman, G.W., F. Crops, and R.B. Russell, *Gas Chromatographic Determination of Free Fatty Acids in Vegetable Oils by a Modified Esterification Procedure.* 1979: p. 77-79.

23.   Palanisamy, S. and B.S. Gevert, *Study of non-catalytic thermal decomposition of triglyceride at hydroprocessing condition.* Applied Thermal Engineering, 2016. **107**: p. 301-310.

24.   Guzman, A., et al., *Hydroprocessing of crude palm oil at pilot plant scale.* Catalysis Today, 2010. **156**(1-2): p. 38-43.

25.   Laurent, E. and B. Delmon, *Study of the hydrodeoxygenation of Carbonyl Carboxylic acid and guaiacol group over sulphided CoMo Al2O3 and NiMo (II Influence of water ammonia and H2S.* Applied Catalysis A: General, 1994. **109**(93): p. 77-96.

26.   Huber, G.W., P. O'Connor, and A. Corma, *Processing biomass in conventional oil refineries: Production of high quality diesel by hydrotreating vegetable oils in heavy vacuum oil mixtures.* Applied Catalysis A: General, 2007. **329**: p. 120-129.

27.   Santillan-Jimenez, E. and M. Crocker, *Catalytic deoxygenation of fatty acids and their derivatives to hydrocarbon fuels via decarboxylation/decarbonylation.* Journal of Chemical Technology & Biotechnology, 2012. **87**(8): p. 1041-1050.

28.   Ismail, N.H., *Production of Cookies Using Palm Oil.* MPOB.

29.   Tunpaiboon, N., *BIODIESEL, Thailand Industry Outlook 2017-2019.* Krungsri Research, May 2017: p. 1-6.

30.   Termmahawong, W., *Oil palm production in Thailand - with a special focus on small scale producers.* JIRCAS.

31.   Kiatkittipong, W., et al., *Diesel-like hydrocarbon production from hydroprocessing of relevant refining palm oil.* Fuel Processing Technology, 2013. **116**: p. 16-26.

32.   da Silva, V.T. and L.A. Sousa, *Catalytic Upgrading of Fats and Vegetable Oils for the Production of Fuels.* 2013: p. 67-92.

33.   *Palm Fatty Acid Distillate (PFAD) in biofuels.* ZERO and Rainforest Foundation Norway, 2016: p. 1-5.

34.   Gusmão, J., et al., *Utilization of vegetable oils as an alternative source for diesel-type fuel: hydrocracking on reduced Ni/SiO2 and sulphided Ni-Mo/γ-Al2O3.* Catalysis Today, 1989. **5**: p. 533-544.

35.   *Tallow Pathway Description, NExBTL Renewable Diesel Singapore Plant.*

36. Mccormick, R. and T. Alleman, *Renewable Diesel Fuel, Renewable diesel goes by many names :.* 2016.

37. Egeberg, R.G., N.H. Michaelsen, and L. Skyum, *Novel hydrotreating technology for production of green diesel.* 2010: p. 21.

38. Harbor, N., *Hydrotreating of Triglycerides to make Aviation Biofuels Topsøe Group.* 2011.

39. Tiwari, R., et al., *Hydrotreating and hydrocracking catalysts for processing of waste soya-oil and refinery-oil mixtures.* Catalysis Communications, 2011. **12**(6): p. 559-562.

40. Lappas, A.A., S. Bezergianni, and I.A. Vasalos, *Production of biofuels via co-processing in conventional refining processes.* Catalysis Today, 2009. **145**(1-2): p. 55-62.

41. Bezergianni, S., A. Kalogianni, and I.A. Vasalos, *Hydrocracking of vacuum gas oil-vegetable oil mixtures for biofuels production.* Bioresour Technol, 2009. **100**(12): p. 3036-42.

42. Rár, M.K., et al., *INVESTIGATION OF THE HETEROGENEOUS CATALYTIC TRANSFORMATION OF VEGETABLE OIL / GAS OIL BLENDS.* Hungarian Journal of Industrial Chemistry, 2008. **36**(1-2): p. 71-76.

43. Kubička, D., P. Šimáček, and N. Žilková, *Transformation of Vegetable Oils into Hydrocarbons over Mesoporous-Alumina-Supported CoMo Catalysts.* Topics in Catalysis, 2008. **52**(1-2): p. 161-168.

44. Şenol, O.İ., T.R. Viljava, and A.O.I. Krause, *Hydrodeoxygenation of aliphatic esters on sulphided NiMo/γ-Al2O3 and CoMo/γ-Al2O3 catalyst: The effect of water.* Catalysis Today, 2005. **106**(1-4): p. 186-189.

45. Sankaranarayanan, T.M., et al., *Hydroprocessing of sunflower oil-gas oil blends over sulfided Ni-Mo-Al-zeolite beta composites.* Bioresour Technol, 2011. **102**(22): p. 10717-23.

46.   Tóth, C., P. Baladincz, and J. Hancsók, *Production of Biocomponent Containing Gas Oil with the Coprocessing of Vegetable Oil–Gas Oil Mixture.* Topics in Catalysis, 2011. **54**(16-18): p. 1084-1093.

47.   Tóth, C., et al., *Investigation of catalytic conversion of vegetable oil/gas oil mixture.* 2009(November 2014).

48.   KubiČka, D. and J. HoráČek, *Deactivation of HDS catalysts in deoxygenation of vegetable oils.* Applied Catalysis A: General, 2011. **394**(1-2): p. 9-17.

49.   Toba, M., et al., *Hydrodeoxygenation of waste vegetable oil over sulfide catalysts.* Catalysis Today, 2011. **164**(1): p. 533-537.

50.   Huber, G.W. and A. Corma, *Synergies between bio- and oil refineries for the production of fuels from biomass.* Angew Chem Int Ed Engl, 2007. **46**(38): p. 7184-201.

51.   KubiČka, D. and L. Kaluža, *Deoxygenation of vegetable oils over sulfided Ni, Mo and NiMo catalysts.* Applied Catalysis A: General, 2010. **372**(2): p. 199-208.

52.   Mikulec, J., et al., *Second generation diesel fuel from renewable sources.* Journal of Cleaner Production, 2010. **18**(9): p. 917-926.

53.   Hagen, J., *CHAPTER 5: Heterogeneous Catalysis: Fundamentals.* 2006: p. 99-222.

54.   Smejkal, Q., L. Smejkalova, and D. Kubicka, *Thermodynamic balance in reaction system of total vegetable oil hydrogenation.* Chemical Engineering Journal, 2008.

55.   Donnis, B., et al., *Hydroprocessing of Bio-Oils and Oxygenates to Hydrocarbons. Understanding the Reaction Routes.* Topics in Catalysis, 2009. **52**(3): p. 229-240.

56.   Sebos, I., et al., *Catalytic hydroprocessing of cottonseed oil in petroleum diesel mixtures for production of renewable diesel.* Fuel, 2009. **88**(1): p. 145-149.

57.   Klerk, A.d., *Oligomerization of 1-Hexene and 1-Octene over Solid Acid Catalysts.* Ind. Eng. Chem. Res., 2005: p. 3887-3893.

58.   R, H.-a., et al., *World ' s largest Science , Technology & Medicine Open Access book publisher Overview of Phosphorus Effect in Molybdenum-Based Hydrotreating Catalysts Supported on Ordered Mesoporous Siliceous Materials*

59.   R, I. and G. J, *Influence of Phosphorus on the Properties of Alumina-Based Hydrotreating Catalysts.* Advances in Catalysis, 2000(44): p. 417-503.

60.   Stuart, W., *Influence of cetane number , 90 % distillation temperature and aromatic content on HCCI combustion NRC Publications Archive (NPArC) Archives des publications du CNRC (NPArC) Influence of cetane number , 90 % distillation temperature and aromatic content on HCCI combustion Cosmin E .; Chippior , Wallace L .* 2010(May 2014).

61.   Jȩczmionek, Ł. and K. Porzycka-Semczuk, *Hydrodeoxygenation, decarboxylation and decarbonylation reactions while co-processing vegetable oils over NiMo hydrotreatment catalyst. Part II: Thermal effects – Experimental results.* Fuel, 2014. **128**: p. 296-301.

62.   Šimáček, P., et al., *Hydroprocessed rapeseed oil as a source of hydrocarbon-based biodiesel.* Fuel, 2009. **88**(3): p. 456-460.

63.   Badawi, M., et al., *Effect of water on the stability of Mo and CoMo hydrodeoxygenation catalysts: A combined experimental and DFT study.* Journal of Catalysis, 2011. **282**(1): p. 155-164.

64.   Laurent, E. and B. Delmon, *Influence of water in the deactivation of a sulfided NiMo -Al2O3 catalyst during hydrodeoxygenation.* 1994. **146**(1).

65.   Drive, H. and S. Sn, *THE EFFECT ON DIESEL ENGINE EMISSIONS WITH HIGH CETANE ADDITIVES FROM BIOMASS OILS.* 1980.

66.   Lapuerta, M., et al., *Key properties and blending strategies of hydrotreated vegetable oil as biofuel for diesel engines.* Fuel Processing Technology, 2011. **92**(12): p. 2406-2411.

67.   Viljava, T.-R., *FROM BIOMASS TO FUELS : HYDROTREATING OF OXYGEN-CONTAINING FEEDS ON A CoMo / Al 2 O 3.* 2001(11).

68.   Snåre, M., et al., *Heterogeneous Catalytic Deoxygenation of Stearic Acid for Production of Biodiesel.* Industrial & Engineering Chemistry Research, 2006. **45**(16): p. 5708-5715.

69.   Vandeputte, G. and G.B. Marin, *Theoretical Study of the Thermal Decomposition of Dimethyl Disulfide.* 2010: p. 10531-10549.

70.   Rozmysłowicz, B., *Deoxygenation of fatty acids for production of fuels and chemicals.* 2014.

71.   Yeh, T.M., *Hydrothermal Catalytic Deoxygenation of Fatty Acids and Upgrading Algae Biocrude by.* 2015.

APPENDIX

A.1 Calculation of theoretical hydrogen consumption

BASIS of CALCULATION					
TOTAL FEED RATE	892 kg/h				
Density of FEED	892 kg/m3				
Volumetric Feed Rate	1 m3				
Percentage of Free Fatty Acids	84.5 wt%				
Free Fatty Acids			**Palm Oil as Triglyceride**		
Free Fatty Acids	753.7	kg/h	Palm Oil as Triglyceride	138.3	kg/h
Average Molecular Weight	267.96	kg/kmol	Average Molecular Weight	829.9	kg/kmol
Free Fatty Acids	2.813	kmol/h	Palm Oil as Triglyceride	0.167	kmol/h
Hydrogen required to Sat. Double Bond	0.561	mol H2/mol FFA	Hydrogen required to Sat. Double Bond	1.68	mol H2/mol Palm Oil
			Hydrogen required decomposition to FFAs	3.00	mol H2/mol Palm Oil
REACTION					
Total Decarbonylation	0	mol H2/mol FFA	Total Decarbonylation	3	mol/mol Palm Oil
Total Decarboxylation	1	mol H2/mol FFA	Total Decarboxylation	6	mol/mol Palm Oil
Total Hydrodeoxygenation	3	mol H2/mol FFA	Total Hydrodeoxygenation	12	mol/mol Palm Oil
Hydrogen Consumption					
			Decomposition of Triglyceride	0.500	kmol/h
Saturation of Double bond	1.577	kmol/h	Saturation of Double bond	0.280	kmol/h
Total Decarbonylation	0.000	kmol/h	Total Decarbonylation	0.500	kmol/h
Total Decarboxylation	2.813	kmol/h	Total Decarboxylation	1.000	kmol/h
Total Hydrodeoxygenation	8.439	kmol/h	Total Hydrodeoxygenation	1.999	kmol/h
Hydrogen Consumption (1 Nm3 = 0.0422 kmol)					
			Hydrocarcking	11.84	
Saturation of Double bond	37.38	Nm^3/h	Saturation of Double bond	6.64	Nm^3/h
Total Decarbonylation	0.00	Nm^3/h	Total Decarbonylation	11.84	Nm^3/h
Total Decarboxylation	66.66	Nm^3/h	Total Decarboxylation	23.69	Nm^3/h
Total Hydrodeoxygenation	199.97	Nm^3/h	Total Hydrodeoxygenation	47.38	Nm^3/h
To Complete HDO Require	237.35	Nm3/h	To Complete HDO Require	65.86	Nm^3/h
Complete HDO of PFAD + Complete HDO of Triglyceride				303.21	Nm^3/h
Experiment				344.6	Nm^3/h

A.2 ABBREVIATIONS

Abbreviate	Definition
LGO	Light gas oil
PFAD	Palm fatty acid distillate
HDS	Hydrodesulfurization
FFAs	Free fatty acids
4,6-DMDBT	4,6-Dimethyl-dibenzo thiophene
PA	Palmitic acid
n-C18	Normal-octadecane
GC-FID	Gas chromatography equipped with flame ionized detector
LSHV	Liquid hourly space velocity
PO	Refined bleached and deodorized palm oil
HPO	Hydrogenated refined bleached and deodorized palm oil
H-PFAD	Hydrogenated palm fatty acid distillate

จุฬาลงกรณ์มหาวิทยาลัย

CHULALONGKORN UNIVERSITY

VITA

Mr. Sunya Boonyasuwat was born on 30 September, 1986 in Bangkok, Thailand. He received Bachelor of Science in Chemical Engineering from Chulalongkorn University with First Class Honors in 2008. With passionate in the biofuel and chemical reaction since bachelor degree, he fulfill his endeavor to achieve Master of Science in Chemical Engineering from the University of Oklahoma in 2011. The master degree was a topic of biofuel from biomass and waste plastic pyrolysis. Then, he continued in Doctoral of Engineering from the department of Chemical Engineering, Chulalongkorn University in June, 2012.